Meteorology Master's Thesis

A CRITICAL ASSESSMENT OF OCCLUDED FRONTS

Alessandro Chiariello

21.11.2006

Supervisor: Aulikki Lehkonen

Reviewers: Hannu Savijärvi, Aulikki Lehkonen

UNIVERSITY OF HELSINKI
DEPARTMENT OF PHYSICAL SCIENCES

PL 64 (Gustaf Hällströmin katu 2)
00014 University of Helsinki, FINLAND

HELSINKI UNIVERSITY

Faculty	Department
Faculty of Science	Department of Physical Sciences

Author
Alessandro Chiariello

Title
A critical study of occlusions

Subject
Meteorology

Level	Month and year	Number of pages
Master's Thesis	November 2006	98 pp

Abstract
The aim of this work was the assessment about the structure and use of the conceptual model of occlusion in operational weather forecasting.

In the beginning a survey has been made about the conceptual model of occlusion as introduced to operational forecasters in the Finnish Meteorological Institute (FMI). In the same context an overview has been performed about the use of the conceptual model in modern operational weather forecasting, especially in connection with the widespread use of numerical forecasts.
In order to evaluate the features of the occlusions in operational weather forecasting, all the occlusion processes occurring during year 2003 over Europe and Northern Atlantic area have been investigated using the conceptual model of occlusion and the methods suggested in the FMI. The investigation has yielded a classification of the occluded cyclones on the basis of the extent the conceptual model has fitted the description of the observed thermal structure.
The seasonal and geographical distribution of the classes has been inspected.

Some relevant cases belonging to different classes have been collected and analyzed in detail: in this deeper investigation tools and techniques, which are not routinely used in operational weather forecasting, have been adopted.

Both the statistical investigation of the occluded cyclones during year 2003 and the case studies have revealed that the traditional classification of the types of the occlusion on the basis of the thermal structure doesn't take into account the bigger variety of occlusion structures which can be observed. Moreover the conceptual model of occlusion has turned out to be often inadequate in describing well developed cyclones.

A deep and constructive revision of the conceptual model of occlusion is therefore suggested in light of the result obtained in this work. The revision should take into account both the progresses which are being made in building a theoretical footing for the occlusion process and the recent tools and meteorological quantities which are nowadays available.

Key Words
Occlusion, occluded front, type of occlusion, classical occlusion

Place of storage

Additional information
-

INDEX

1. INTRODUCTION

Conceptual models have been an important tool in the operational routines in the weather forecasting offices, because they give forecasters the means of understanding the essential processes taking place in the atmosphere and predicting their evolution in the near future.

The operational environment routines have undergone substantial modifications in the last decades: forecasts produced by numerical models have been rapidly spreading and getting more and more precise, which has resulted in the forecasters relying on the numerical outputs to a great extent. This trend has the recognized disadvantage that the forecasters may loose the know-how about the behavior of the atmosphere and any critical capacity of control on the numerical forecasts, which can indeed fail or be partly wrong.

On the other hand the observations, especially those related to remote sensing systems, are increasing in precision and coverage allowing the forecaster a deeper insight into the weather systems, which wasn't possible before.

In this continuously changing operational environment some of the traditional conceptual models have not been updated according to the new knowledge, and they are now facing the problem of being inadequate.

Among the conceptual models traditionally used in weather forecasting, the occlusion seems to be among those which suffer most of a missing revision and integration with modern tools and methodologies. In fact the occlusion has yielded animated debates and objections in the literature since it was first introduced: The underlying reason for its inadequateness in modern environment is the missing firm theoretical background.

In this work new emerging theoretical frameworks and approaches to the occlusion process are therefore mentioned and explored to bring out the efforts that have been made recently. At the same time an overview about the classical occlusion as it was originally created and about the main objections proposed through the years is offered: the reader can therefore better understand the direction and meaning of the most recent studies about occlusions.

The purpose of this work is to demonstrate, both from a quantitative and qualitative

point of view that the conceptual model of occlusion does need an urgent revision so that it could be properly and usefully used in operational forecasting.
In order to achieve these goals an extensive investigation of the cyclones occluding over the European continent and northern Atlantic Ocean will be pursued, using as criteria the structure of the occlusions as proposed in the synoptic guidelines for operational forecasters in the Finnish Meteorological Institute and aiming at defining the type of the classical occluded cyclones and looking for structures differing from the classical model.

The results of this investigation are meant to show how weak and imperfect the conceptual model of occlusion reveals to be when inspecting the structure and development of the observed well developed cyclones in a traditional manner.
The meaning of the work is not only to demonstrate that the occlusion ought to be completely revised and integrated with the results of recent studies, but also to propose the direction of possible studies in the future. In this context some case studies will be investigated in details in order to show the usefulness of relatively new methodologies, like for example the vertical cross sections, which were once used in the past but then abandoned.

2. OCCLUSION PROCESS IN THE PAST AND IN THE PRESENT

2.1 The origins

2.1.1 The occluded front in the Norwegian cyclone model

The occlusion has its roots in the so called Norwegian Cyclone Model (hereafter NCM), which is the first modern model for the life cycle of a cyclone and was created after the First World War at Bergen Geophysical Institute in Norway.

The occlusion process was first identified by Bergeron when studying a cyclone which occurred on November 18th 1919 (Schultz and Mass, 1993) and it was later included into the NCM by Bjerknes and Solberg (1922). The complete and detailed treatment of the polar theory underlying the NCM as it was originally proposed goes far beyond the purposes of this work: the interested reader is advised to go into the aforementioned studies of Bjerknes and Solberg.

According to their theory a wave forming in the preexisting knife-sharp temperature boundary between cold polar and warm mid-latitude air masses, known as the polar front, amplifies and leads to the formation of a surface low pressure and to a related warm sector. Due to the established cyclonic motion, the cold front moves counterclockwise around the low, so that at a certain stage it overtakes the slower advancing warm front. At the same time the shrinking warm sector is forced upwards, whereas the cold air spreads out along the ground: the occlusion process has begun (fig.2.1).

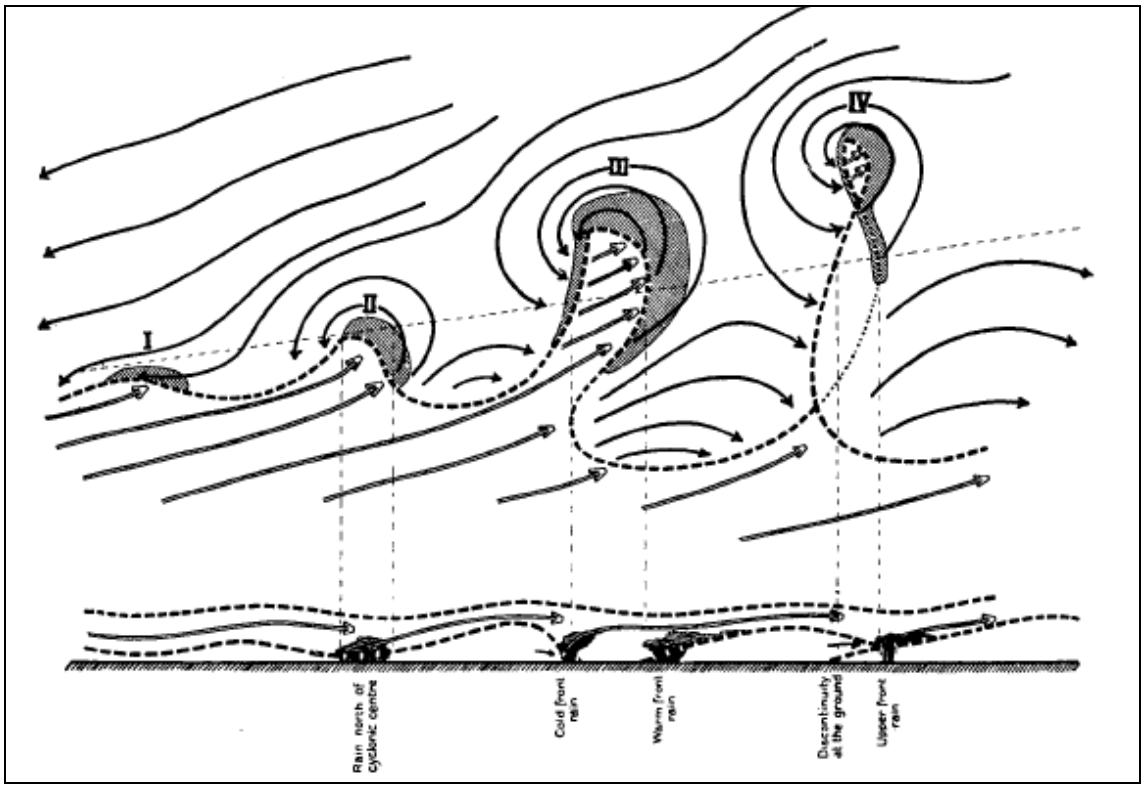

Figure 2.1. The life cycle of an extratropical cyclone according to the Norwegian model. Solid lines indicates streamlines and bold dashed lines frontal boundaries; light dashed lines refer to the cross section on the bottom (Bjerknes and Solberg, 1922).

Related to the occlusion process two main aspects were observed: the surface pressure minimum is detached from the peak of the warm sector and an occluded front forms along the surface where the two fronts meet, connecting the peak of the warm sector to the surface low pressure (fig. 2.1IV).

Bjerknes and Solberg (1922) discussed the vertical structure of the occlusion process. They first supposed an occluded vertical structure where no thermal boundary surface forms between the two wedges of cold air meeting each other at the occlusion of the cyclone, but claimed that usually there will be some difference in temperature between

the two, so that a boundary also remains after the occlusion. According to their conclusions the polar air from the rear of the depression is generally either warmer or colder than the polar air ahead of it, producing a warm or a cold occlusion, respectively. In warm occlusions the cold front would climb over the warm front: the occluded front, the frontal zone between the surface front and the leading edge of the lifted cold front has a forward slope (fig.2.2, left hand side). In case of cold-type occlusion the cold front thrusts itself forward under the warm front: the occluded front in this case slopes backward (fig.2.2, right hand side).

In the same study Bjerknes and Solberg suggest that in Europe cold-type occlusions should be more frequent in the warm time of the year, because the cold air coming directly from the ocean is likely to be colder than the cold air which has rested some time over the continent. In Europe the warm-type occlusion generally occurs in winter, when the cold but maritime air from the rear of the cyclone is not cold enough to undermine the still colder continental air in front of the cyclone.

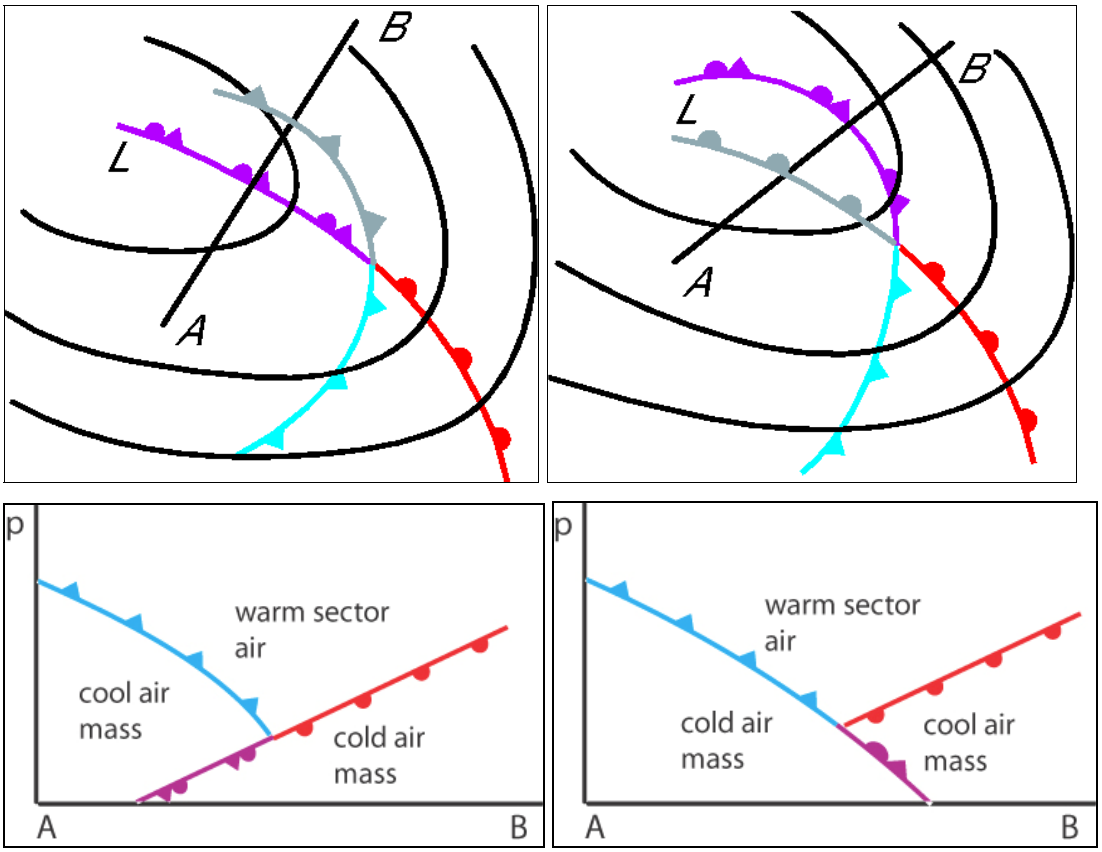

Figure 2.2. Schematic surface maps and relative vertical cross sections of a warm- and cold-type occlusion. The upper occluded front is colored in gray, otherwise other fronts are colored as conventionally on surface weather maps. Cross sections AB display in each case frontal boundaries and different air masses interacting in the occlusion process.

It is worth mentioning that NCM was initially formulated almost solely on the basis of ground observations mainly from the area reaching from Eastern Atlantic to Southern Scandinavia. Its vertical structure was mainly inferred from theoretical argumentation and only later partly validated by upper air observations (Friedman, 1989).
It will be never stressed enough that at the very base of NCM there is the interaction of two well distinct air masses over a quite homogeneous surface (Northern Atlantic) and under the influence of a prevailing westerly upper flow.

The NCM was immediately a great success not only for giving a theoretical explanation of mid-latitude cyclone development but also, and this was indeed the task in the very beginning, as a diagnostic and forecasting tool in operational meteorology.
Weather map analysis and forecasting have been based on the frontal cyclone model for long time. The positions of fronts give information about winds, temperature, clouds, and precipitation; moreover, the shape of a frontal cyclone is indicative of its stage of development and can thus give information about its future behaviour. The frontal cyclone model thus turned out to be an extremely useful tool in weather forecasting (Eliassen A., 1975)

2.2 Objections to the classical model

The NCM has been objected in several instances soon after its birth, the most debated aspect being the occlusion.
A review of the main objections to the classical occlusion can be found in Schultz and Mass (1993). In this work the focus is on those topics which have gained most appreciation from an operational point of view.

2.2.1 The conceptual model of trowal

According to Martin (1999) Crocker et al. (1947) noted that in occluded cyclones the crest of the thermal wave at successive heights in most of the cases slopes westward. Later Godson (1951) noted the same structure and extended it in a three-dimensional view defining the “sloping valley of tropical air”, region of high potential or equivalent potential temperature.
Further studies (Penner, 1955; Galloway, 1958, 1960) revealed that the characteristic

cloud and precipitation distribution associated with occluded front often occurred in the vicinity of a thermal ridge, as it was also observed in the previous studies. On the basis of these observations and studies scientists in the Canadian Meteorological Service concluded that the essential feature in warm-type occluded processes is the trough of warm air aloft, i.e. the trowal, lifted ahead of the upper cold front, and not the position of the occluded front on the surface as in the classical model (Martin, 1999).

These argumentations led to the creation of the conceptual model of trowal, that has been used so far in Canadian meteorological offices (fig. 2.3), for it bears a close correspondence with the weather on the surface associated with occlusions.

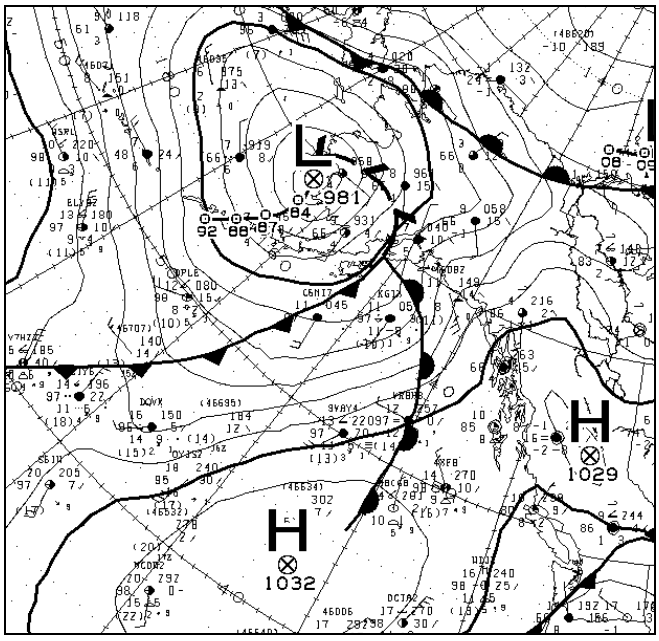

Figure 2.3. Surface weather chart and subjective frontal analysis, produced at the Canadian Weather Service, of a post-mature cyclone over Alaska and northeastern Pacific from 03.10.2006 18 UTC; note the use of conceptual model of trowal in the proximity of the low center (dashed lines).

Fig. 2.4 shows a modern revision of the conceptual model of trowal for a warm-type occlusion: the occluded front on the surface lies far behind the precipitation area on the ground, which, on the other hand, is better correlated to the position of the trowal aloft, i.e. the base of the warm-air trough aloft.

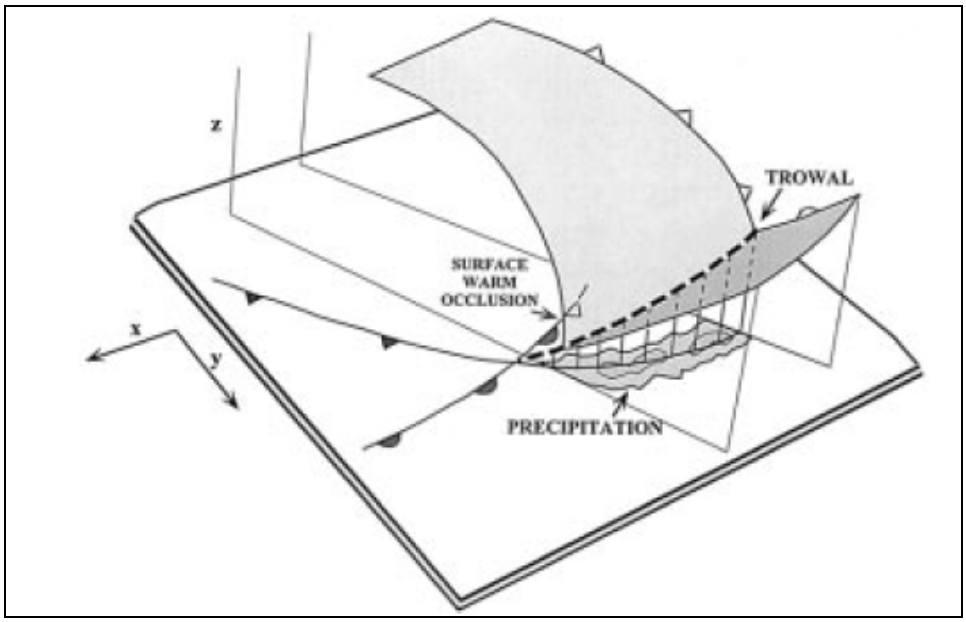

Figure 2.4. Schematic illustration of the trowal conceptual model. The dark (light) shaded surface represents the warm edge of the cold (warm) frontal zone. The bold dashed line at the 3-D sloping intersection of those two frontal zones lies at the base of the trough of warm air aloft – the trowal. The schematic precipitation in the occlude quadrant of the cyclone lies closer to the projection of the trowal to the surface than the position of the surface warm occluded front (Martin, 1999).

The studies performed about the structure of the trowal were generally missing any dynamical background, which is being offered only in the most recent studies (e.g. Martin, 1998b). As fig. 2.4 reveals, the trowal did not offer a new alternative structure to the post-mature stage of cyclones as described in the NCM, but it was a mere three-dimensional reinterpretation of the classical warm occlusion.

2.2.2 Non-classical features: the "instant" occlusions

Among the weather systems there are structures that look like occlusions, but are formed differently.

Anderson et al. (1969) identified a process resulting in an occluded-like structure which was called instant occlusion. According to their study a comma cloud associated with an upper geopotential anomaly approaches and merges with a frontal wave. The structure resulting from this process reminds the occlusion, with the essential difference that no frontal "catch up" has occurred.

The instant occlusion has been recognized and further studied in some other instances

(Locatelli et al., 1982; Mullen, 1983; Carleton, 1985; McGinnigle, 1988), in which slightly different interpretations or points of view have come out.
Browning and Hill (1985) even proposed a variant of instant occlusion process, which was called pseudo-occlusion: the main difference from the canonical instant occlusion was the formation of the comma and the polar wave cloud at the same time.

An accurate treatment of studies about the instant occlusion goes beyond the purposes of this work. In this work only an overview of the latest studies is given.
According to Zwatz-Meise and Hailzl (1983) the formation of the instant occlusion can be schematically identified in three main steps. In the so called pre-merging phase, there is a preexisting frontal boundary and an upper trough in the cold side of the front, stirred by a trough in upper and middle levels: between the two systems an area of shallow moist air can be usually observed (McGinnigle et al., 1985). The upper trough approaches the almost stationary polar front (fig. 2.5, left hand side).
During the second step, the merging phase, warm air advection in advance of the upper trough causes frontogenesis, which induces the formation of a thermal gradient on its northern side; in addition a wave within the cold front is enhanced, as shown in central part of fig. 2.5 (see also McGinnigle et al., 1985).

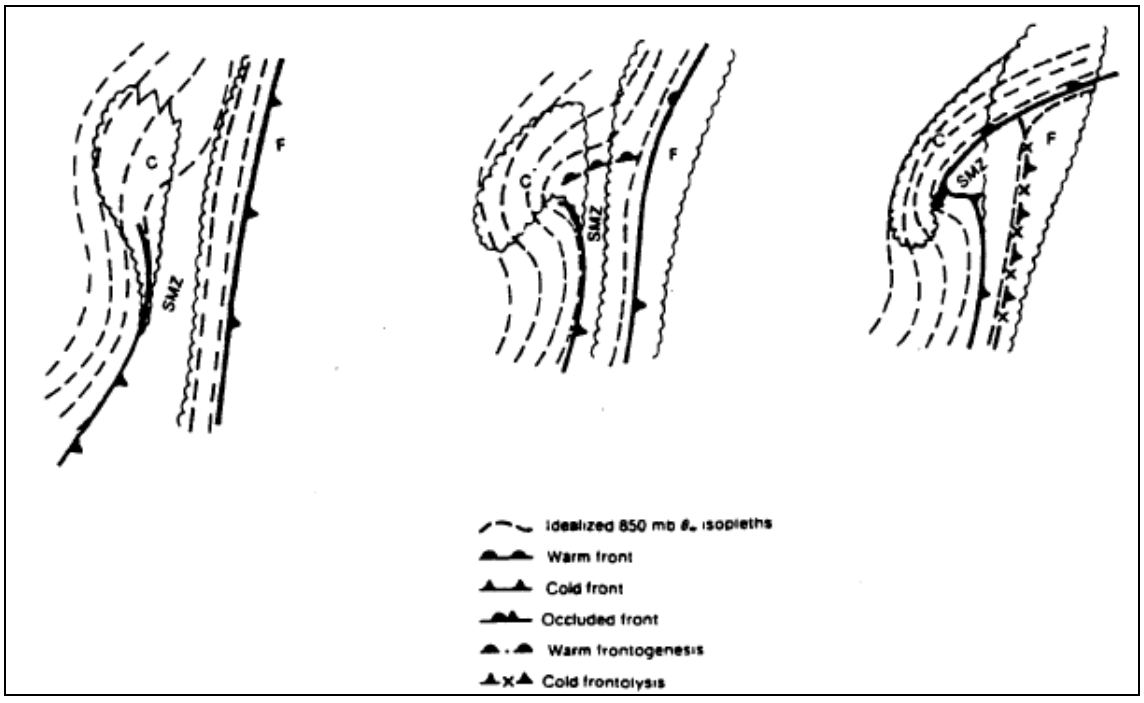

Figure 2.5. Life cycle of an instant occlusion after McGinnigle et al. (1985); C stands for the cold air mass cloud feature and F for the polar frontal cloud. SMZ indicates the shallow moist zone and stippling the upper cloudiness (Schultz and Mass, 1993).

The mature stage of the instant occlusion life cycle is characterized by the dissipation of the original cold front as the second frontal band becomes the primary cold front (McGinnigle et al., 1988). At this stage the cloud configuration is very similar to the one typical of classical occluded front.

2.2.4 The T-bone model for marine developments

Investigating both the data furnished by research field programs, which provided unique datasets within the evolution of extratropical marine cyclones, and related numerical studies, Shapiro and Keyser (1990) came up with many examples of a cyclone structural evolution substantially different form the classical conceptualization.
In their model, which is usually known as the T-bone model, the life cycle of a marine extratropical cyclone is schematically divided into four different stages. In the first stage the cyclone is characterized by an incipient continuous broad baroclinic zone (fig. 2.7I). In the second phase the cyclogenesis yields the separation of the cold front from the warm front in the vicinity of the cyclone center, a process called fracture, with the cold front advancing into the warm sector and perpendicular to the warm front (from here the name “T-bone”; at the same time a scale contraction of the discontinuous warm and cold frontal gradients occurs (fig. 2.7II). The midpoint of cyclogenesis is characterized by the frontal T-bone and bent-back warm front structure (fig. 2.7III). The mature fully developed cyclone exhibits the warm-core seclusion within the post-cold frontal polar air stream (fig. 2.7IV).

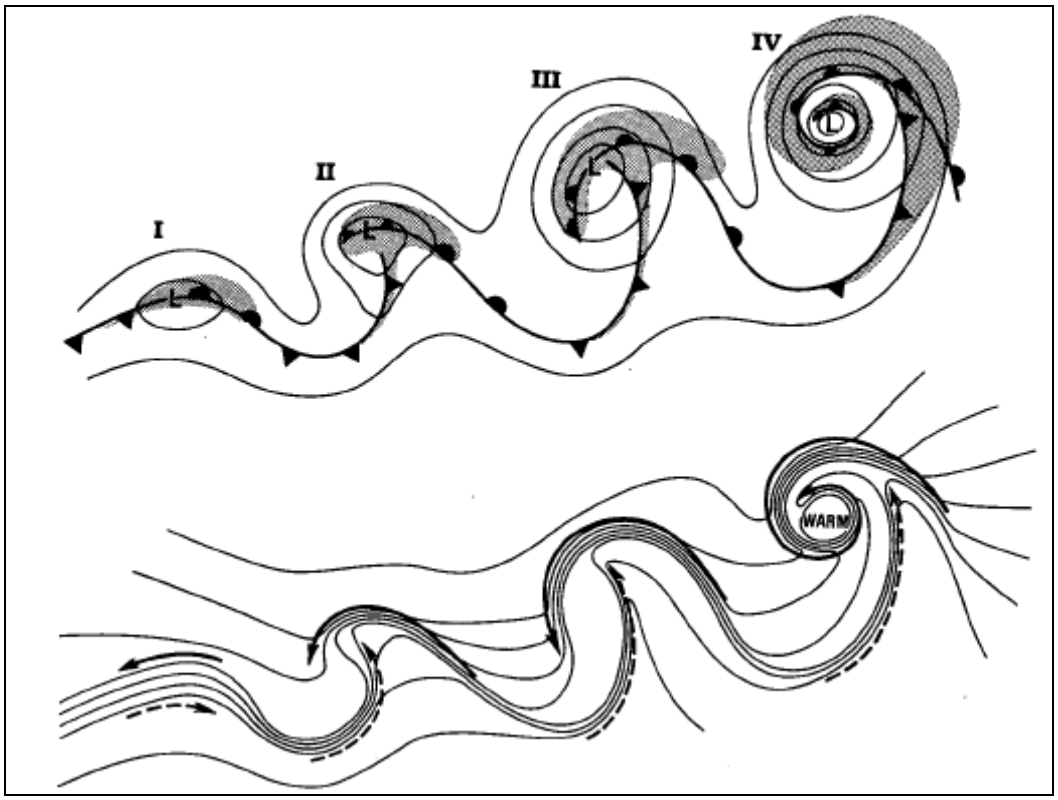

Figure 2.7. An alternative model for marine extratropical frontal cyclone: (I) incipient frontal cyclone; (II) frontal fracture; (III) bent-back warm front and frontal T-bone; (IV) warm-core seclusion. Upper: sea-level pressure, solid lines; front, bold lines; and cloud signature, shaded. Lower: temperature, solid lines; cold and warm air currents, solid and dashed arrows, respectively. (Shapiro and Keyser, 1990)

Neiman and Shapiro (1993) emphasize that the frontal-cyclone life cycle introduced by Shapiro and Keyser (1990) is not characteristic of all marine cyclogenetic events and has not been described for continental cyclones. Also Schultz and Mass (1993) mention that several numerical simulations of marine cyclogenesis have yielded structure exhibiting frontal fractures and warm seclusions (e.g. Kuo et al., 1991), but on the other side not all have produced such nonideal features (Kuo et al., 1992).

Neiman and Shapiro (1993) stress that the T-bone model should be considered as an alternative to, rather than a replacement of, the classical Norwegian frontal-cyclone occlusion life cycle, and that it is usually observed in connection with rapidly deepening lows, over the sea only.

2.3 Latest progresses

2.3.1 Stability rule for occlusion types

Stoelinga et al. (2002) have revised the classical concept of occlusion type and proposed an alternative procedure based on different assumptions for determining the type.

In the classical framework the occlusion's type is determined by the different thermal properties of the two cold air masses wrapping the warm sector and undergoing the occlusion process. In practice the type is assessed by comparing the horizontal temperature (or potential temperature) gradients of the two cold air masses on either side of the occluded front; as mentioned in section 2.1.1 a warm-type occluded front has a forward slope, while a cold-type is sloping backward.
On the basis of generally accepted notions and collected examples Stoelinga et al. (2002) proposed a simplified scheme of the cross section perpendicular to an occluded front (fig 2.8) according to which the occluded frontal surface is characterized by a first-order discontinuity of potential temperature field that separates broad zones of roughly uniform horizontal potential temperature gradient and static stability.

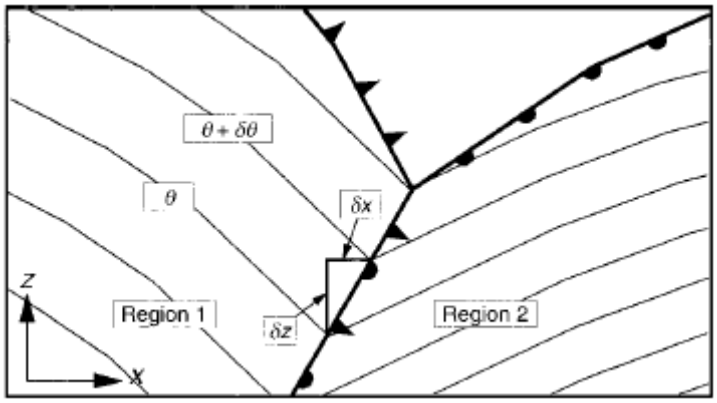

Figure 1.8 Schematic vertical cross section through an idealized occluded front, with potential temperature (solid contours) and frontal positions (Stoelinga et al., 2002).

The following relation between the inclination of the occluded front and the vertical and horizontal derivatives of the potential temperature along the front can be easily derived:

$$\left(\frac{dz}{dx}\right)_{front} = \frac{\left(\frac{\partial\Theta}{\partial x}\right)_1 - \left(\frac{\partial\Theta}{\partial x}\right)_2}{\left(\frac{\partial\Theta}{\partial z}\right)_2 - \left(\frac{\partial\Theta}{\partial z}\right)_1}, \qquad (1)$$

where Θ is the potential temperature and the indexes refers to the regions (air masses) in fig 2.8.

Because the occluded front is generally located along a maximum in potential temperature (e.g. Martin, 2006, p. 320) the numerator of the right side of (1) is positive regardless of the relative magnitude of the Θ horizontal gradients on both sides of the front. Therefore the sign of the slope of the occluded front is determined by the sign of the denominator, i.e. by the static stability contrast across the front, and not by the contrast in horizontal Θ gradient as claimed in the classical theory.

According to these considerations an occluded front slopes over the air mass that is statically more stable, which yields to a modified definition of occlusion types as follows:

- a cold occlusion results when the statically more stable air is behind the cold front. The cold front undercuts the warm front
- when the statically more stable air lies ahead of the warm front, a warm occlusion is formed in which the original cold front is forced aloft along the warm front surface.

It is important to highlight that the argumentation leading to this alternative definition of occlusion type addresses one specific aspect of the occlusion type definition, namely the relation between the slope of the front and the thermal structure of the air masses involved in the occlusion process.

According to Stoelinga et al. (2002) the type determined with the static stability rule may disagree with the one assessed by means of traditional methods. In the specific case shown in fig. 2.9 the traditional reasoning would yield to a cold type occlusion since the horizontal potential temperature gradient in the vicinity of the front is much higher within the cold air mass in the rear side of the occluded front than in the fore side. The static stability rule states instead that a warm type is in question and is thus able to correctly predict, in this case, the type of the occlusion according to the slope of the frontal surface.

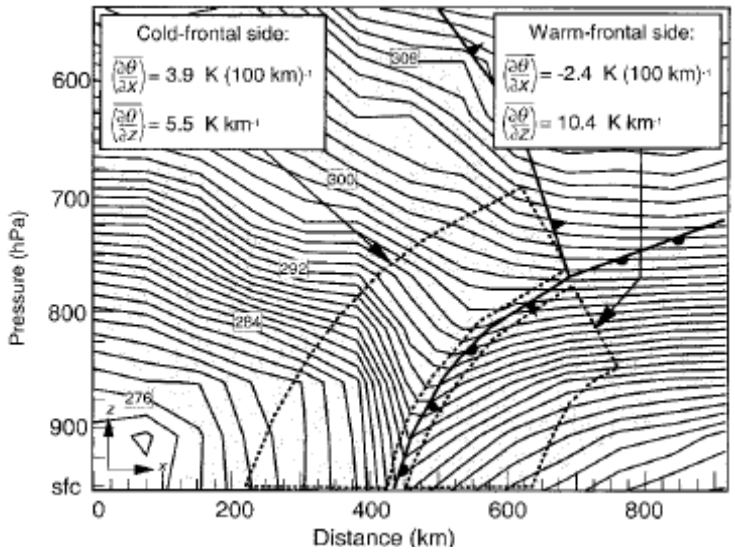

Figure 2.9. Vertical cross section through the occluded front in a model-simulated cyclone studied by Schultz and Mass (1993). Contoured field is potential temperature (interval 1 K). Values of horizontal vertical partial derivatives of potential temperature shown in the inset are mean values within the two regions enclosed by the dotted lines. (Stoelinga et al., 2002)

2.3.2 Occlusion formation within an emerging quasi-geostrophic theory framework

The occlusion process has traditionally been regarded as a mere frontal-scale process where the interaction between the faster advancing cold front and the warm front is responsible for inducing the formation of the typical warm thermal ridge and associated ascent in the occluded quadrant of mid-latitude cyclones.

Recent studies (Martin, 1999; Posselt and Martin, 2004) have been able to configure the occlusion process within the quasi-geostrophic (QG) theory, so that the occlusion has been given a dynamical background that has missed since it was created. In this new framework the occlusion is regarded more as a process stirred by synoptic-scale mechanisms.

At this point it is advisable to spend some words about the Q-vector, which is a meteorological quantity used in the following.

According to Martin (1999) the Q-vector represents an alternative form of the omega equation and has the characteristic of expressing the forcing of the vertical motion in terms of the divergence of a horizontal vector forcing field. In his work he expresses the Q-vector as (the original references of the Q-vector go back to Hoskins (1978)):

$$\vec{Q} = f_o \gamma \frac{d}{dt_g} \nabla_p \Theta , \qquad (2)$$

where $d/dt_g = \partial/\partial t + \overrightarrow{V_g} \cdot \nabla_p$ (the subscript g denotes geostrophic), Θ stands for equivalent potential temperature and f_o and γ are constants. As a result, the Q-vector contains information about both the rate of change of the magnitude of $\nabla_p \Theta$ and the rate of change of the direction of the vector $\nabla_p \Theta$.

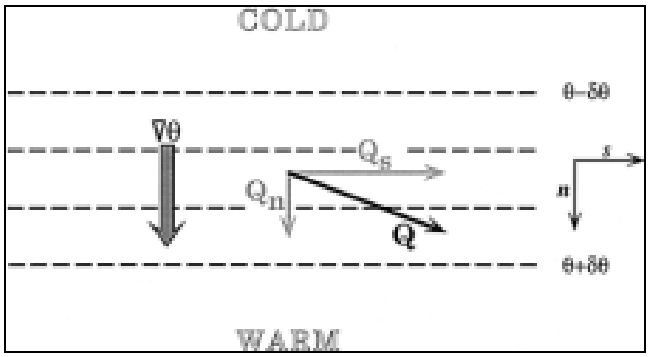

Figure 2.10. Schematic describing the natural coordinate partitioning of the Q-vector. Thick dashed lines are isentropes on an isobaric surface (Martin, 1999).

Considering a framework where the Q-vector is divided into the natural coordinate components in the direction across (Q_n) and along (Q_s) the isentropes (fig. 2.10), Martin (1999) has shown that Q_s plays a fundamental role in the formation of the warm thermal ridge and its associated ascent. The mathematical expressions for Q_n and Q_s are not shown: in the following we limit with offering the qualitative results of Martin's (1999) studies.

Figure 2.11(a) shows a straight baroclinic zone across which a convergence area of Q_s is located. This convergence is responsible for producing upward motions, as predicted by the QG omega equation, and for differentially rotating the potential temperature gradient on either side of the convergence axis (fig. 2.11(b)). This last mentioned process is not treated in detail in this context: the interested reader is forwarded to the extensive argumentation of Martin (1999).

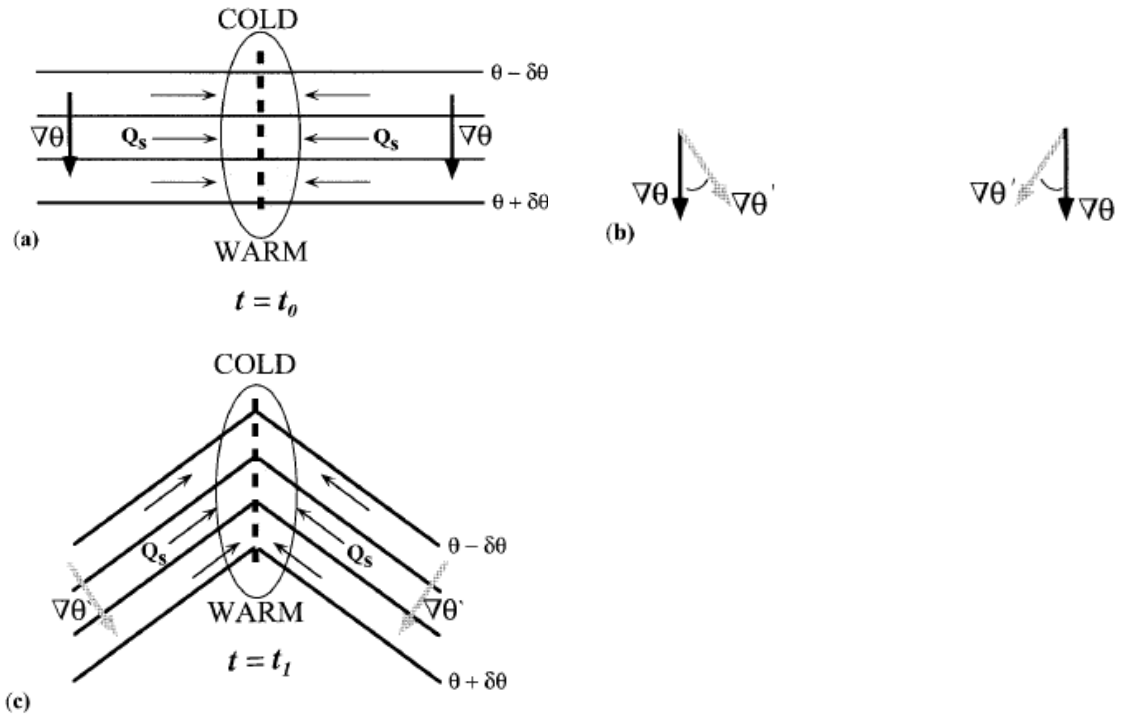

Figure 2.11. The effect of Q_s vector convergence on horizontal thermal structure. (a) Straight line isentropes (solid lines) in a field of Q_s vector convergence. The thick dashed line indicates the axis of maximum convergence. The direction of Θ-gradient is shown with black arrows. (b) Rotation of Θ-gradient implied by Q_s vectors. The thick black arrows denote the original direction of the Θ-gradient vector, while the gray arrows after the rotation implied by Q_s vectors. (c) Orientation of the baroclinic zone depicted in (a) after differential rotation of Θ-gradient on either side of the Q_s vector convergence maximum (Martin, 1999).

Because Q_s cannot affect the magnitude of the potential temperature gradient, the result is the formation of a thermal ridge and associated ascent as earlier mentioned (fig. 2.11(c)).

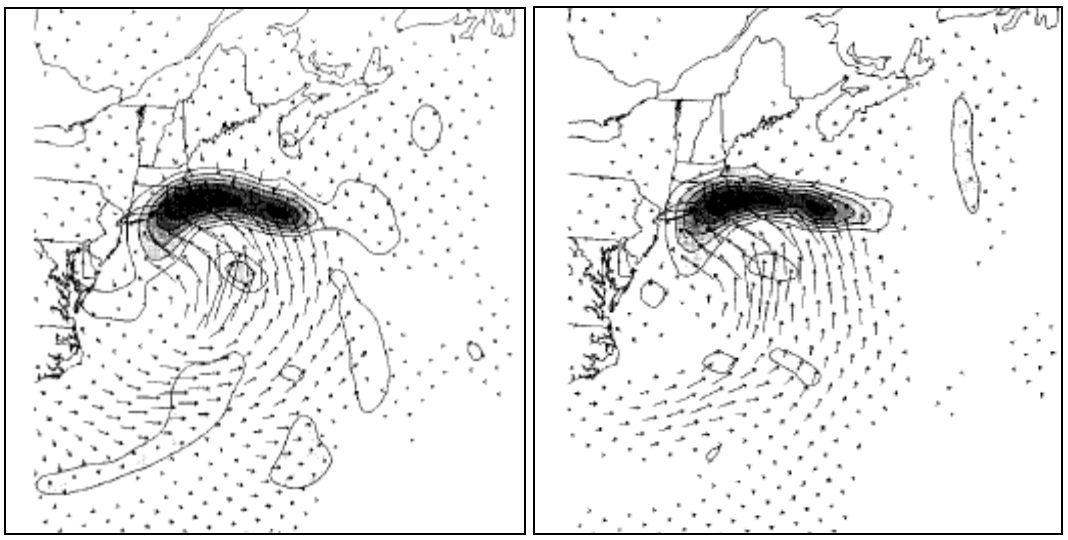

(a) **(b)**

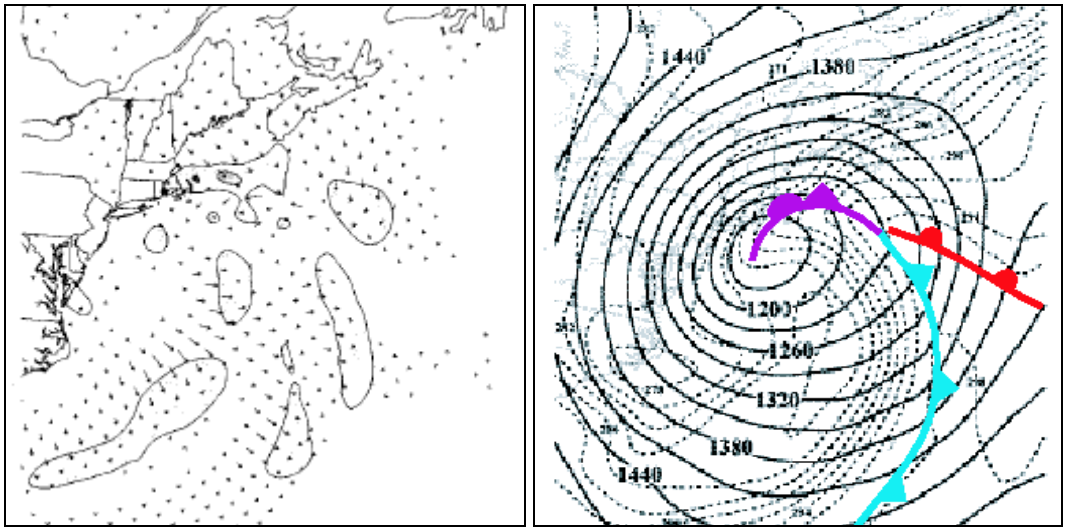

(c) **(d)**

Figure 2.12. (a) The 500-900 hPa averaged Q-vector and Q-vector convergence from an 18 h forecast valid at 06 UTC 1 April 1997. Q-vector convergence is contoured and shaded every $5x10^{16}$ m kg^{-1} s^{-1}. Thin dashed gray lines are 500-900 hPa column-averaged isentropes contoured every 3 K. (b) As in (a) except for Q_s vector. (c) As in (a) except for Q_n vector. (d) 850 hPa geopotential (solid lines) and potential temperature (dashed lines) fields (Martin, 1999). The subjective frontal analysis has been superimposed to (d) by the author of this work to allow the reader a better identification of the occluded quadrant mentioned in the text.

This process can be observed and verified in real weather situations. Fig. 2.12(a) shows the 500-900 hPa column averaged Q-vector forcing related to a mid-latitude cyclone over northeastern America in its post-mature stage (fig. 2.12(d)): the forcing exhibits its highest values in the occluded quadrant.

If we look at the natural components of the Q-vector, respectively Q_s (fig. 2.12(b)) and Q_n (fig. 2.12(c)), we find out that in the occluded quadrant the along-isentropic component plays a predominant role with respect to the cross-isentropic one.

The example in question puts in clear evidence the role of Q_s as the synoptic-scale dynamical mechanism responsible for producing the thermal ridge and the upward vertical motion in the occluded quadrant of post-mature cyclones.

2.3.3 Potential vorticity perspective of the occlusion

In several recent issues an alternative, but still equivalent, framework based on the knowledge of the spatial distribution of the potential vorticity (PV) has been adopted for the interpretation of the dynamical mechanisms underlying meteorological

developments.

Investigations portrayed by Martin (1998) within the PV framework have revealed a typical upper-tropospheric configuration related to occlusions, which has been termed “treble clef”. Fig. 2.13 shows the schematic appearance of the treble clef, which is characterized by a reservoir of high PV at low latitudes connected, by a thin filament of high PV values, to a high-PV reservoir at higher latitudes.

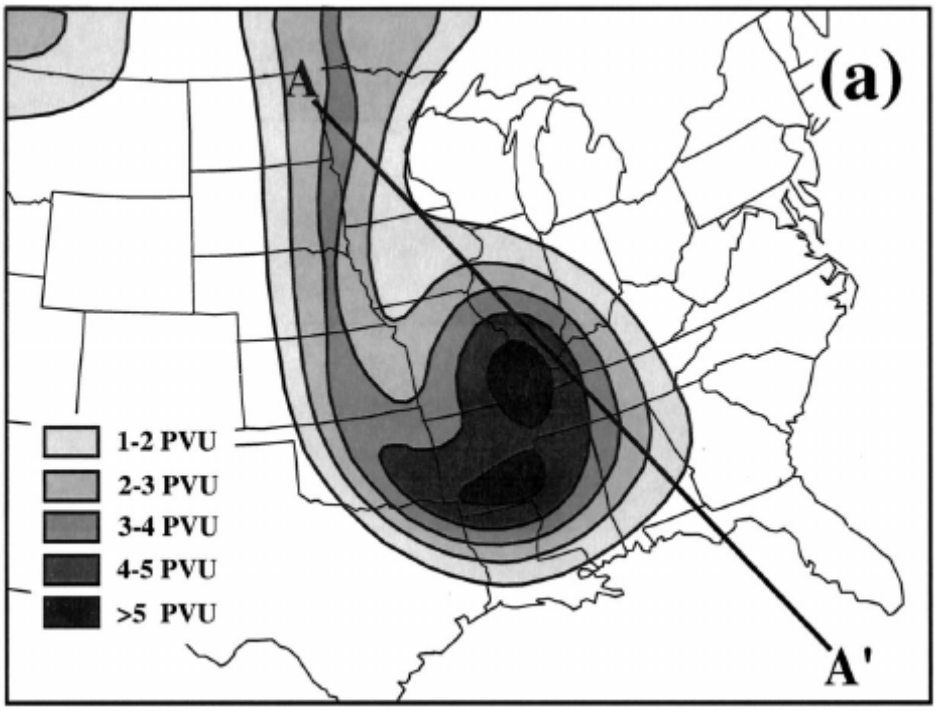

Figure 2.13. Schematic of treble-clef-shaped upper tropospheric PV structure described in the text. Solid lines are isopleths of PV on an isobaric surface contoured and shaded in PVU. (Posselt and Martin, 2004)

According to Hoskins et al. (1985) near-tropopause high value areas of potential vorticity sit atop relatively cold columns of air while regions of low values coincide with relatively warm air columns in the underlying troposphere.

These considerations imply that the treble clef configuration at upper-tropospheric levels is accompanied with a tropospheric thermodynamic structure as in fig. 2.14, which represents a vertical cross section across the treble-clef-shaped PV structure (AA’ in Fig. 2.13). At a closer look this cross sections turns out to be the canonical thermal structure of a warm occluded front.

Based on these considerations Martin (1999) suggests the upper tropospheric treble-clef-shaped PV configuration to be the sufficient condition for stating the presence of a warm occluded structure in the underlying troposphere.

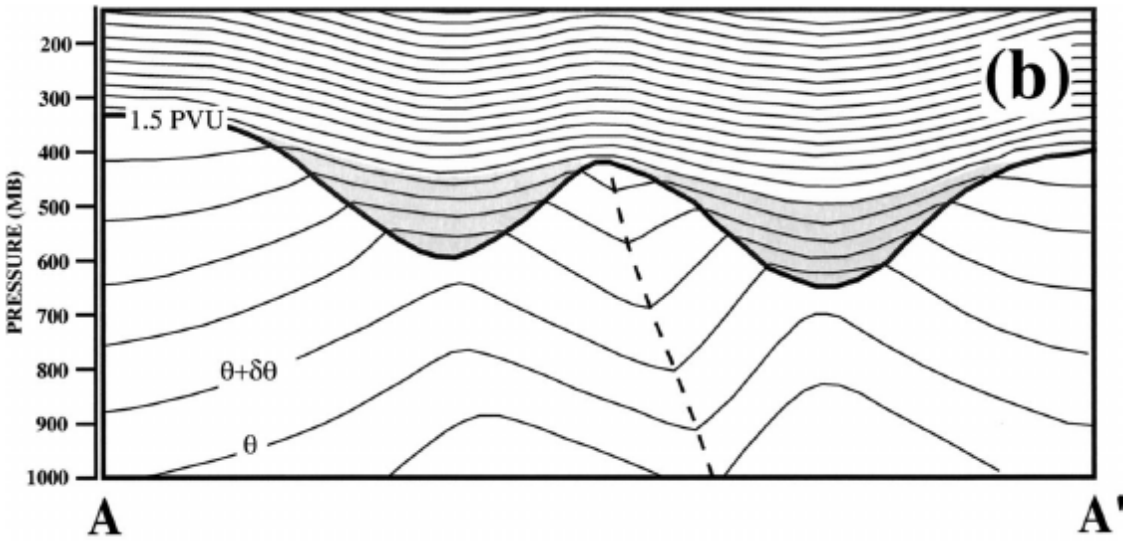

Figure 2.14. Schematic cross section of potential temperature (Θ) in the vicinity of a treble-clef-shaped upper tropospheric PV signature. The dashed axis denotes the sloping axis of warm air in the troposphere characteristic of an occlude cyclone (Posselt and Martin, 2004)

Posselt and Martin (2004) have recently proposed in their studies a mechanism inducing the formation of the treble clef. Their argumentation can be easily explained by means of fig. 2.15a-c: In the open wave stage (fig. 2.15a) the latent heat released in connection with ascent is concentrated along the cold front and in the vicinity of the surface low pressure of the developing cyclone, usually located downstream of an upper-tropospheric positive PV anomaly. Persistent diabatic erosion contributes in creating a notch in upper tropospheric PV contour northwest of the surface occluding cyclone, affecting also the flow in that vicinity at the tropopause level (fig. 2.15b).

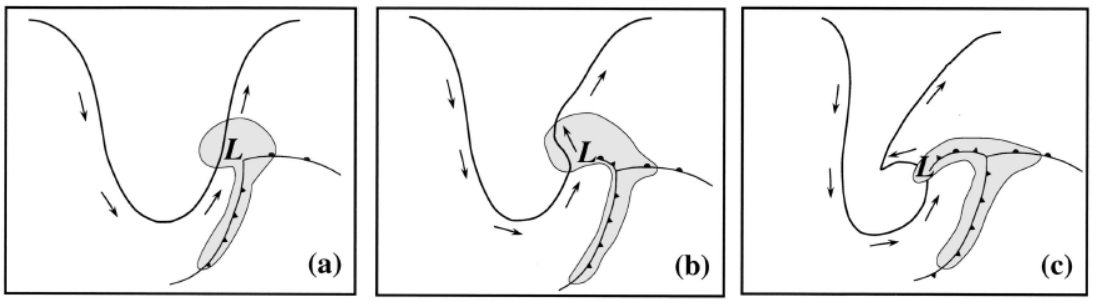

Figure 2.15. Schematic illustrating the synergy between diabatic erosion of PV and negative advection of PV at the tropopause during occlusion. Gray shading represents the erosion of tropopause PV by adiabatic heating associated with the cyclone, the surface low of which is marked by "L". Traditional frontal symbols indicate surface frontal locations. The thick solid line represents the PV=2 PVU isopleths at the tropopause. Arrows represent the tropopause-level flow associated with the upper tropospheric PV feature. (a) The open wave stage. (b) Commencement of occlusion. (c) Fully occluded stage (Posselt and Martin, 2004).

The eastward progression of the upstream ridge also contributes in beginning the

isolation of a low-latitude high-PV region, while the surface low is far removed from the peak of the surface warm sector. At this stage the heating is no longer affecting the process, but it is the large scale circulation modified by the ongoing process that contributes to the advection of low PV values into the developing notch, further isolating the low-latitude high PV reservoir (fig. 2.15c).

2.3.4 The role of latent heat release

In the study of Posselt and Martin (2004) the effect of latent heat release on the development of the occluded thermal structure was investigated. In their study a strong marine winter cyclone is examined through comparison of full physics (FP) and no-latent-heat-release (NLHR) simulations of the event performed using the Mesoscale Model MM5.

It was shown that the latent heat release is essential when describing the process of occlusion, which in their studies is defined as the process yielding a trowal-like thermal structure, i.e. trough of warm air aloft. In fact, though both simulations exhibit a well-developed occluded thermal ridge near the surface, the FP simulation depicts the canonical, troposphere-deep warm occluded thermal structure, whereas the NLHR simulation produces only a shallow, poorly developed one.

This result can be considered as an addition to the classical frontal model, which handled only the kinematics of the frontal bands.

As highlighted by Posselt and Martin (2004), the latent heat released in the occlusion process plays an essential role in maintaining the thermal ridge, because it compensates the adiabatic cooling due to rising motion associated with the Q_s convergence (see chapter 2.3.2), which in turn tends to weaken the warm anomaly characterizing the occluded process.

Posselt and Martin (2004) thus suggest a view of the occlusion as a process created by the interaction of synoptic-scale dynamics and latent heat release, which is itself a result of the dynamical forcing.

3. OCCLUSION IN OPERATIONAL WEATHER FORECASTING

One of the main tasks of this work is the revision and eventual adjustment of the occlusion as a tool, i.e. conceptual model, used in operational weather forecasting.
As seen in the previous chapter the Norwegian model for cyclone developments was initially created to provide a better forecasting tool to meteorologists and to offer at the same time theoretical means for understanding the structure of mid-latitude cyclones and their development. The classical model has since successfully been adopted into operational weather forecasting routines.
In the last twenty years the ever increasing precision and versatility of numerical model outputs and observations (e.g. satellite images) has notably weakened the role of the classical occlusion as a prognostic conceptual model especially in short and medium range weather forecasting.
In this context the concept of occlusion needs to go through a comprehensive revision.

3.1 FMI synoptic interpretation guidelines for occlusions

In the Finnish Meteorological Institute's (FMI) weather offices the classical model is generally used when performing the so called frontal analysis on synoptic weather charts.
A set of guidelines has been assembled by the FMI staff in order to offer a coherent tool within the classical framework, which helps forecasters make synoptic frontal analysis. In the following text these guidelines will be referred to as FMI synoptic interpretation guidelines and abbreviated as FMI guidelines.

According to FMI guidelines the occlusion is divided into four types which can be distinguished in a constant pressure level framework by means of temperature and temperature advection fields on 850 hPa level and jet stream's configuration on 300 hPa. In vertical cross sections, in order to identify the different types, the use of temperature advection and equivalent potential temperature fields is suggested.
The classification leads to warm, cold, neutral and back-bent type occlusions.

All the occlusion types exhibit the following common features (equivalent potential

temperature is marked as Θ_e):

- a warm tongue is observed in 850 hPa temperature and Θ_e fields
- the occluded front is characterized on the surface by a trough in the pressure field, or in general by a cyclonic wind shear
- in case of an elongated occluded front the type may change at different points along the front
- in vertical cross sections a distinct trough structure in Θ_e field is observed, which indicates the warmer air lifted aloft
- an occluded cyclone always has a cold and warm front structure in its earliest stage of formation

In the following discussion the specific features of the above mentioned occlusion types are discussed in detail according to the FMI guidelines. On the basis of these configurations the meteorologist is supposed to define the type of the occlusion. It must be highlighted that the above mentioned rules represent a set of bulk rules which help the forecaster approximately identify the type of the occluded cyclone in question. Even in the hypothetic case that the classical model would perfectly describe the post-mature stage of cyclones these rules provide a direction towards the identification of the type. A definitive and (hypothetical) correct verification of the type in question would require a much deeper investigation of the cyclone structure throughout the troposphere.

The back-bent type represents a further development experienced by occlusions and is not therefore discussed in details in this context.

3.1.1 Warm occlusion

According to the NCM warm-type occlusions are supposed to form when the air mass on the rear side of the occluding cyclone is warmer than the one on its leading side
In case of warm-type occlusion the jet stream is continuous on the fore side of the occluded and warm front; a separate jet stream is placed on the rear side of the cold front, usually intersecting the cyclone over its triple point (fig 3.1, right side).
At 850 hPa intense warm advection and high temperature gradients are located in front of the occluded (and warm) front, while behind it advection and gradients are in

comparison very weak (fig. 3.1, left side). Surface temperatures and dew point temperatures are higher behind the occluded front than on its fore side; for old occlusion such differences can be barely observed.

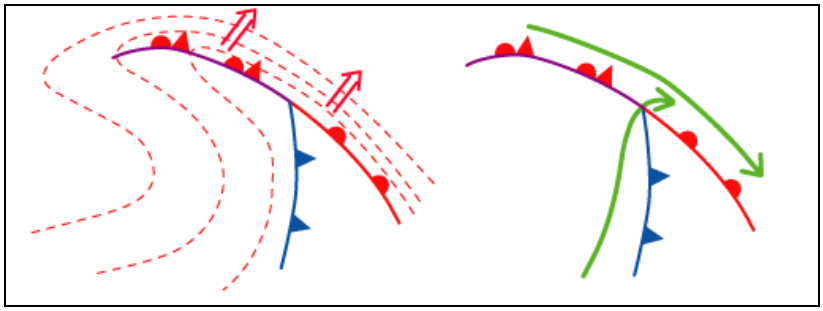

Figure 3.1. Warm-type occlusion schematic according to FMI guidelines. Left: surface fronts and temperature field at 850 hPa (red dashed lines); open red arrows indicate the highest temperature gradient direction (warm advection). Right: surface fronts and jet streams (green arrows) at 300-400 hPa (Lehkonen, 2002).

In vertical cross sections the occlusion is characterized, as mentioned earlier, by an upper through most easily recognizable in Θ_e field and by the two crowding zones related to the surface fronts on both sides of the trough. In warm occlusions the zone of high Θ_e gradient related to the warm front reaches the ground as an occluded front. There is usually intense warm advection within and ahead of the warm and the occluded front (fig. 3.2, right).

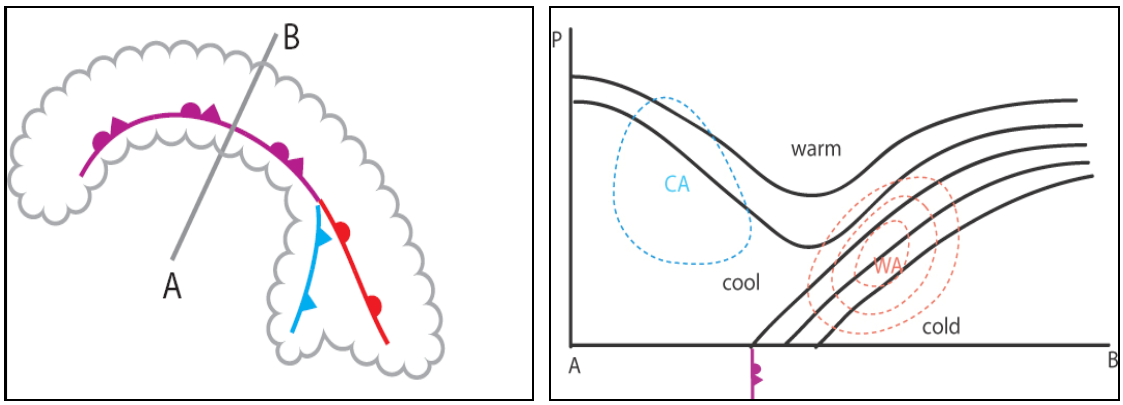

Figure 3.2. Schematic vertical cross section through a warm-type occluded front. Left: position of the cross section. Right: vertical cross section: potential or equivalent potential temperature (black lines), temperature advection (dashed lines: blue for cold and red for warm); warm refers to the warm air mass, while cold and cool to the different temperature properties of the cold air mass.

.

A specific feature of the structure of classical warm-type occluded fronts is the forward inclination of the related frontal band as shown in fig. 3.2.

3.1.2 Cold occlusion

Cold-type occlusions, contrary to the warm-type, are formed when the air mass on the rear side of the occluding cyclone is colder than the one on its fore side.

The cold-type occlusion is characterized by a jet stream which splits into two branches, one following the occluded front on its rear side and the other bending through the triple point to area ahead of the warm front. Temperature advection and gradients at 850 hPa are very weak in front of the occlusion while intense cold advection and strong temperature gradients are located behind it (fig. 3.3, left).

Surface temperature and dew point temperature values are in this case lower behind the front.

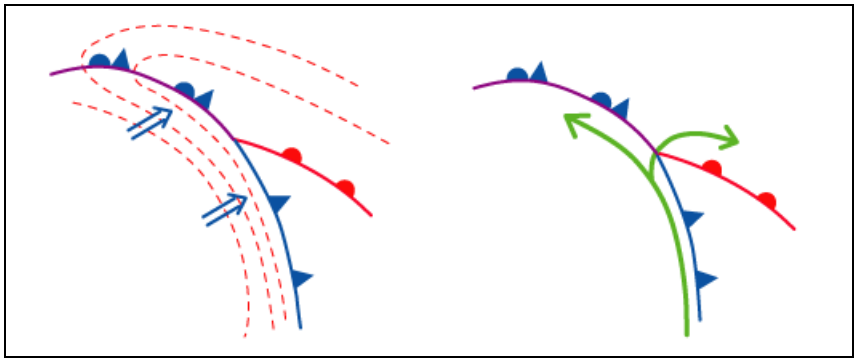

Figure 3.3. Schematic of cold-type occlusion according to FMI guidelines. Left: surface fronts and temperature field at 850 hPa (red dashed lines); open blue arrows indicate highest cold advection areas. Right: surface fronts and jet streams (green arrows) at 300-400 hPa (Lehkonen, 2002).

In vertical cross sections the same general argumentation as for the warm-type occlusion structure is valid, with the difference that it is the thermal band related to the cold front that reaches the ground as an occluded front and that the occluded front has a backward slope. Cold advection maxima are located behind and across the cold and occluded front, usually in the low or middle troposphere (fig. 3.4, right).

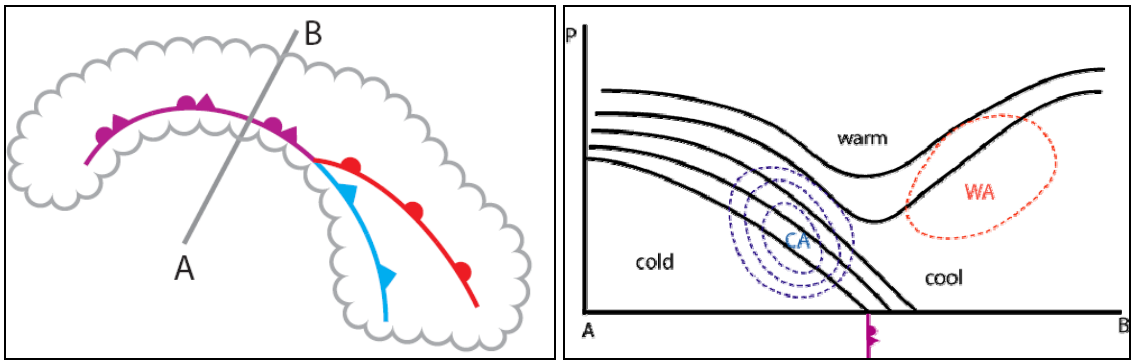

Figure 3.4. Schematic vertical cross section through cold-type occluded front. Left: position of the cross section. Right: vertical cross section: potential or equivalent potential temperature (black lines), temperature advection (dashed lines: blue for cold and red for warm); warm refers to the warm air mass, while cold and cool to the different temperature properties of the cold air mass.

3.1.3 Neutral occlusion

Neutral occlusion is thought to be achieved when there is not any major difference in the properties of the two air masses wrapping the shrinking warm sector

The neutral occlusion is characterized by one jet stream which crosses the occluded front over its triple point. Warm and cold advections as well as temperature gradients at 850 hPa are of the same intensity on both side of the occlusion and not very intense. Also temperatures and dew point are similar on both sides of the occlusion.

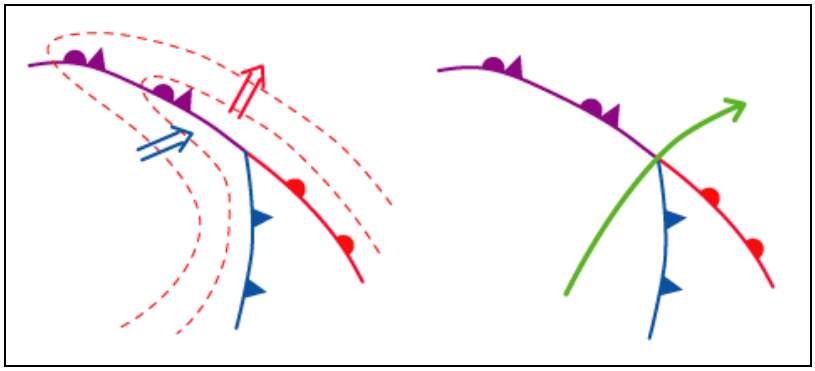

Figure 3.5. Schematic of neutral-type occlusion according to FMI guidelines. Left: surface fronts and temperature field at 850 hPa (red dashed lines); open blue and red arrows indicate respectively highest cold and warm advection areas. Right: surface fronts and jet streams (green arrows) at 300-400 hPa (Lehkonen, 2002).

In vertical cross sections the neutral-type occlusion structure is characterized like the other types by a distinct trough of lifted warm air aloft but a recognizable frontal structure in the lower troposphere is nearly absent or at least very weak, with no prevailing inclination (fig. 3.6, right).

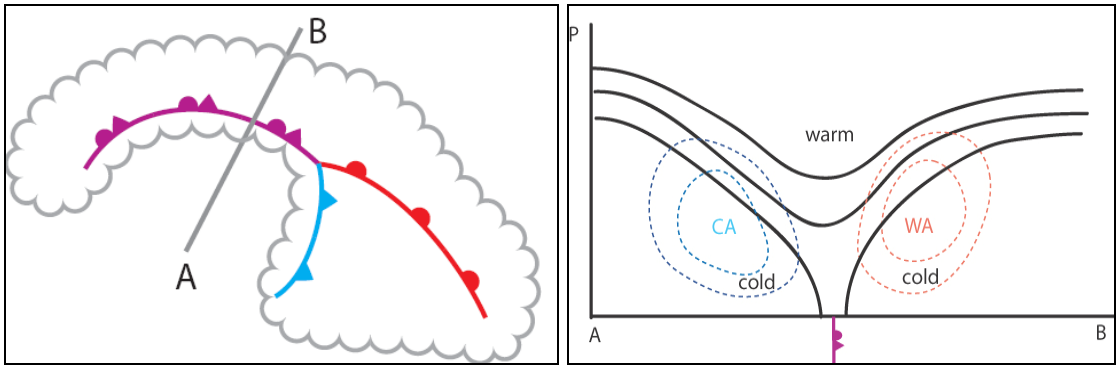

Figure 3.6. Schematic vertical cross section of a neutral-type occluded front. Left: position of the cross section. Right: vertical cross section: potential or equivalent potential temperature (black lines), temperature advection (dashed lines: blue for cold and red for warm); warm refers to the warm air mass, while cold and cool to the different temperature properties of the cold air mass.

In this case temperature advection on both sides of the weak neutral occluded front is very weak or at least of the same intensity.

3.1.4 The occlusion process

In FMI guidelines the life cycle of the classical cyclone development is also described and hints are given about the typical appearance in numerical fields at different stage of the occlusion process.

The cyclone begins the occlusion process from the surface when the cold front reaches the warm one and the warm sector begins shrinking and lifting upwards, exactly as claimed in the classical Norwegian model.

In the beginning of the occlusion process an open wave is usually observed in the temperature field at middle and upper levels in slightly different phase with respect to the geopotential height anomaly; the jet stream is still consisting of a unique core (fig. 3.7).

As the occlusion process continues the warm sector is pushed upwards and narrowed at each level, being completely detached from the surface. The surface low pressure center does not deepen anymore; aloft at the tropopause level the jet stream weakens and begins to split into different branches starting from the triple point, i.e. the apex of the warm sector at the surface, according to the type in question.

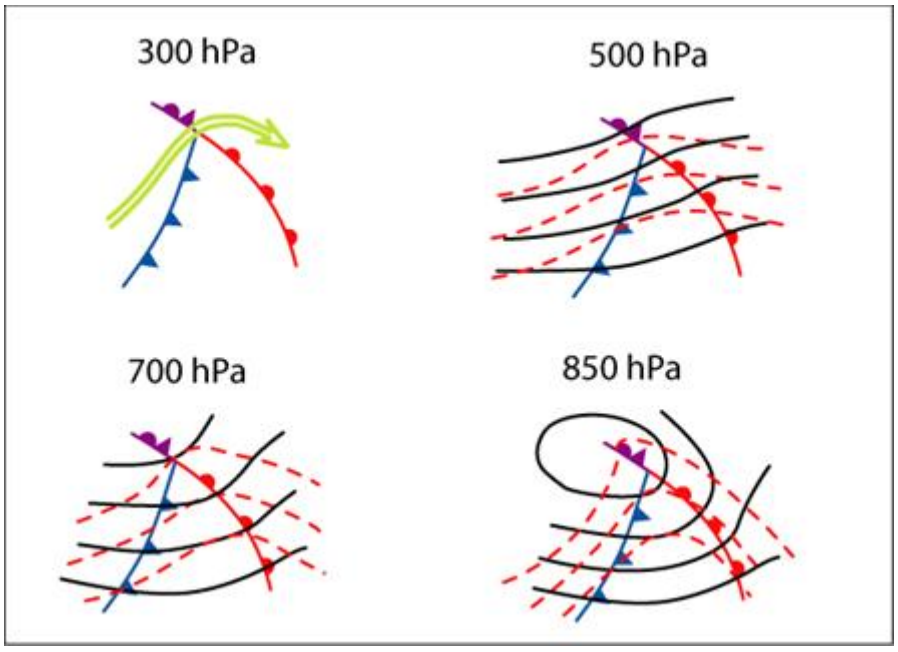

Figure 3.7. Appearance of a young occlusion in numerical fields at different pressure levels. Upper left: surface frontal analysis and jet streak; elsewhere solid black lines for geopotential height and red dash lines for temperature fields (Lehkonen, 2002).

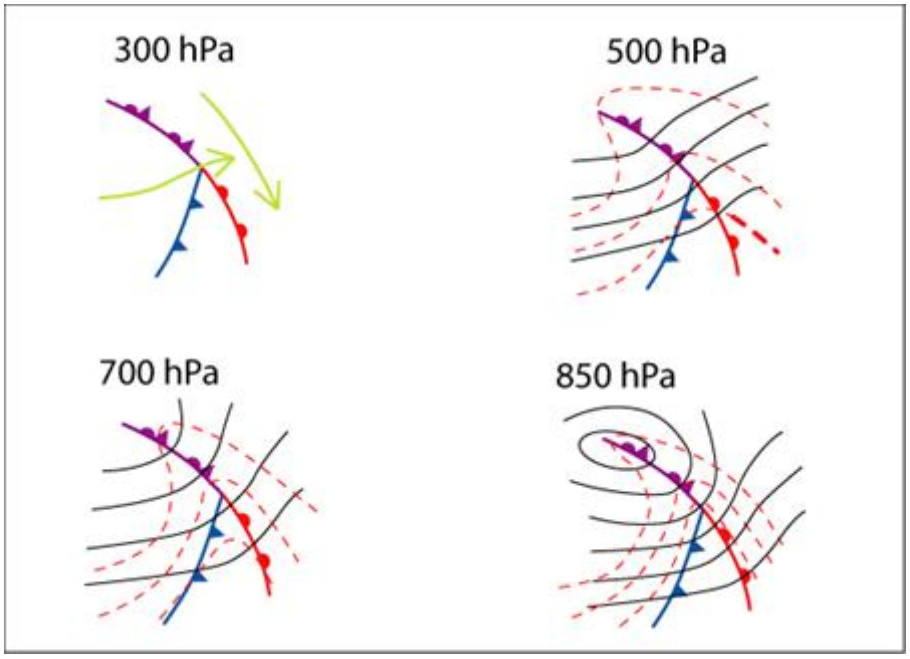

Figure 3.8. Appearance of an occlusion in numerical fields at different pressure levels in the middle stage of life. Upper left: surface frontal analysis and jet streak; elsewhere solid black lines for geopotential height and red dash lines for temperature fields (Lehkonen, 2002).

In the latest stage of the occlusion process the warm sector is no more present on the surface. The axis of the low pressure at different levels is almost vertical. The occluded front typically curls around the surface low and the gradient in the temperature field is now very weak. In case of strong developments a warm air pool called seclusion may be

observed at 850-500 hPa (fig. 3.9).

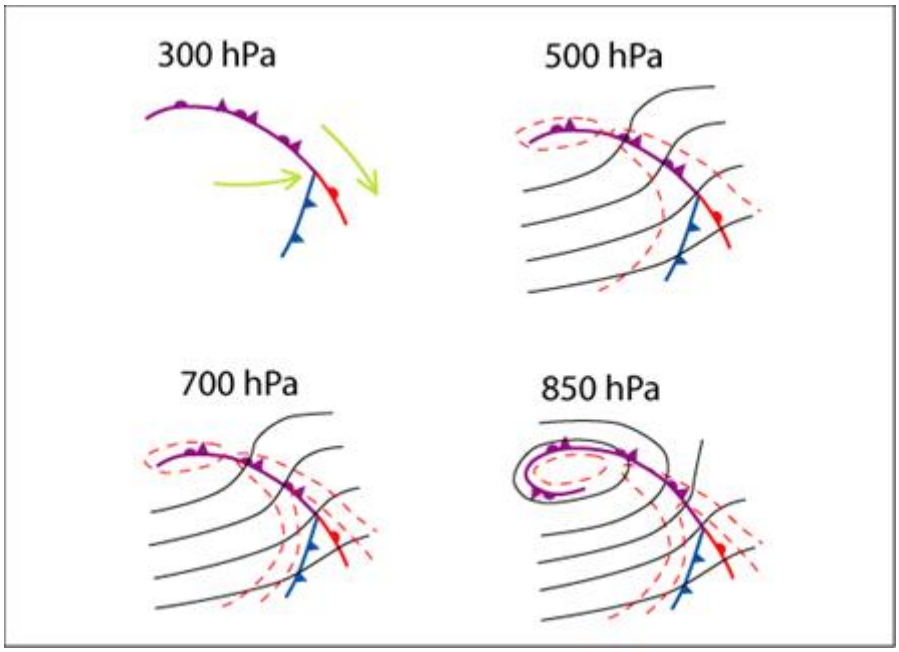

Figure 3.9. Appearance of an occlusion in numerical fields at different pressure levels in the final stage of its life cycle. Upper left: surface frontal analysis and jet streak; elsewhere solid black lines for geopotential height and red dash lines for temperature fields (Lehkonen, 2002).

3.2 Occlusion as a diagnostic and forecasting tool

The conceptual model of occlusion is widely used in weather offices when performing the frontal analysis, along with many other classical conceptual models.

The meaning and usefulness related to the use of the conceptual model of occlusion in operations is somehow questionable, at least in the way it is done nowadays.

The main meaning of the use of conceptual models has been traditionally related to the fact that it helps the forecaster depict in his mind a four-dimensional picture of the synoptic scale atmospheric structure. On this basis the forecaster is able to diagnose and forecast, not only over synoptic but also over sub-synoptic scales, the probability of distribution of the relevant meteorological variables, mostly according to the season. The most common variables are cloudiness, type and amount of precipitation, surface wind, temperature and humidity but also, thinking especially of aviation weather, visibility on the surface correlated with significant weather like fog and mist, stratus clouds and eventually icing conditions.

Before the era of operational numerical models the interpretation of weather systems as conceptual models had a central role in forecasting. The very important characteristic of the occlusion was the fact that it represented a phase of the cyclone's life cycle: the forecaster was aware that the cyclone, observed in its developing stage, would transform into an occlusion, with its specific weather pattern, and would soon after decay.
The occlusion's intrinsic meaning and power therefore relied on being part of the wider and more complex Norwegian conceptual model for mid-latitude cyclones.

The occlusion is nowadays used in operational forecasting basically as interpretation of numerical model outputs.
When investigating medium and long term weather evolution, which is performed almost exclusively on the basis of numerical model predictions, the forecaster can identify some patterns observed in the numerical fields (fig 3.10a, b, c) and interpretate them as a conceptual model and therefore get an instantaneous snapshot about the behavior of the relevant meteorological events in that specific situation (fig 3.10d), without browsing and interpreting other additional fields. This is of great advantage because it allows saving time and energy, which are very important matters in operational forecasting.
On the other hand the conceptual models help the forecaster understand better the outputs of the numerical model and put them in a proper dynamical framework. Otherwise there is a big risk that the forecaster handles numerical model predictions as black boxes and therefore looses any capacity of control about their quality and precision.

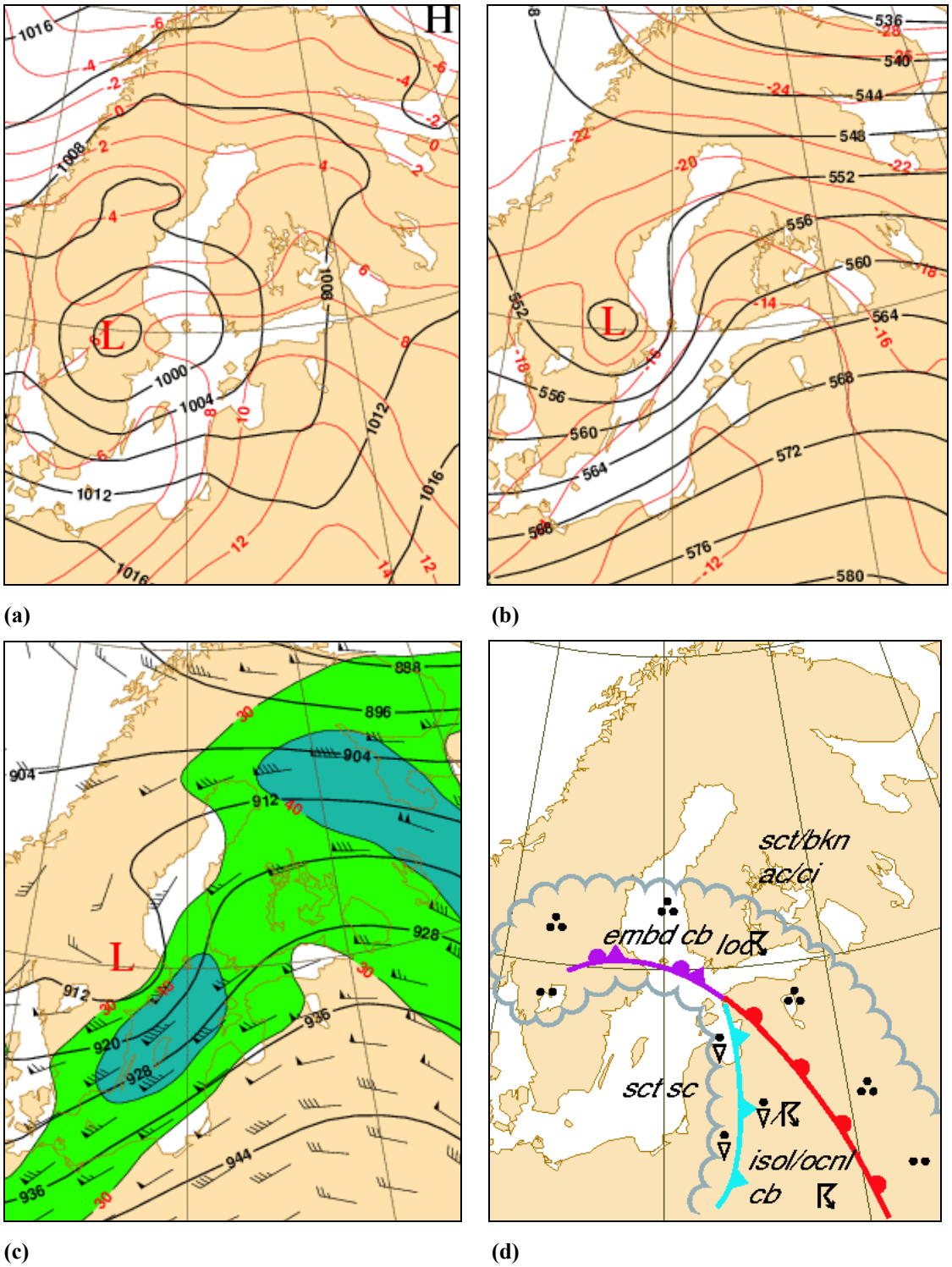

(a) (b)

(c) (d)

Figure 3.10. 24h numerical model forecast (ECMWF) for 09.06.2003, 12 UTC. (a) surface level pressure (black line) and 850 hPa temperature (red line). (b) 500 hPa geopotential height (black lines) and temperature (red lines). (c) 300 hPa geopotential height (black lines), isotachs at 10 kt intervals starting from 60 kt and wind vectors (black wind barbs). (d) example of frontal and significant weather forecast on the basis of conceptual models and numerical model outputs as in (a), (b) and (c).

Again the occlusion as a conceptual model helps the forecaster figure in his mind a picture of the weather system closer to the one furnished by remote sensing systems and

less abstract than the information provided by numerical fields. Fig 3.11 shows how the process of adopting conceptual model described above leads to results which sometimes very well fit the reality.

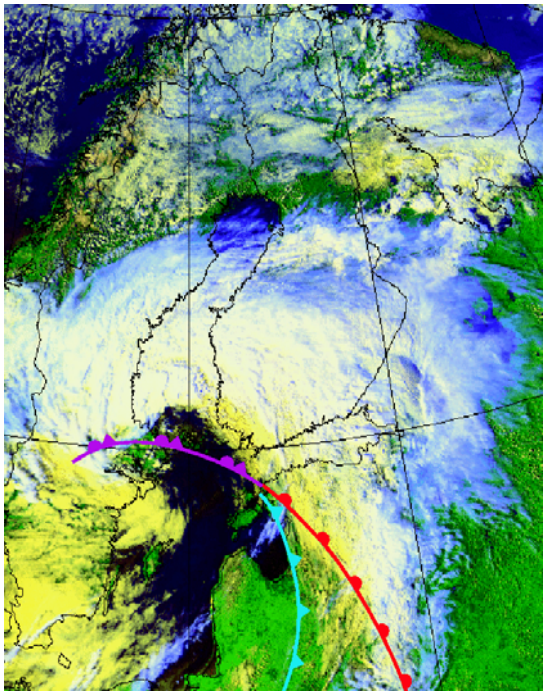

Figure 3.11. NOAA AVHRR composite image (channels 1, 2 and 4) from Scandinavia at 13.19 UTC of 09.06.2003; the frontal system forecast as in picture 3.7(d) is superimposed.

In very short range forecasting the synoptic diagnosis of weather systems by means of all the available observational tools plays a central role, so that also the use of the occlusion as conceptual model is different than in medium and long range forecasting.
In this context the conceptual model works more as the base where the mosaic made up of all the observations is built on. The forecaster on duty puts the observations collected in a certain time window all together into a single coherent configuration, in this case the occlusion. New observations are added to update the details and the structure of the specific occluded system; at the same time the forecaster extrapolates into the near future the development of the system.

From the above mentioned considerations it can be stated that in nowcasting the innermost structure of the conceptual model of occlusion comes in question as there is interest also in investigating and forecasting the eventual stirring of smaller scale systems and weather: the diagnostic properties of occlusion are therefore mainly used.
In longer range forecasting the nature of the occlusion as part of the cyclone life cycle is

instead highlighted and the concept of probable weather associated with it is applied.

The above considerations bring out very clearly two main aspects related to the use of occlusion in present-day weather forecasting (which can be extended to many other conceptual models): first the conceptual model is needed to help the forecaster in interpreting the numerical model outputs and put them together into one coherent picture; secondly the conceptual models allow the forecaster to collect the ever increasing amount of observations into one framework, which help them understand better their interaction and evolution, especially in the closest future (partly Hobbs et al., 1996).

3.3 Outstanding problems

Among the synoptic conceptual models traditionally used in weather forecasting occlusion seems to be the most problematic.
One reason is due to the wide variety of configurations the post-mature cyclone may exhibit both in numerical fields and when observed with remote observation systems. The forecaster is not often able to properly identify the system in question as a classical occlusion and, even if many parameters don't agree with this interpretation, the system is anyway labeled as an occlusion. This process undoubtedly affects the quality of the diagnosis and the forecast itself, because the forecaster implies features typical of the occlusion process to a system that might not be an occlusion.
Browning (1990) forewarns about the settled practice of forecasters of wrongly analyzing instant occlusions and also upper cold fronts or split-front systems as occlusions. On the other way Lehkonen (personal communications) has noticed during the last years that very many cold occlusions are analyzed as cold or split fronts.

In many other cases the forecaster supplies the lack of firm reference points by means of subjective analysis based only on satellite or, if available, radar imagery, which may work only in few cases and mostly leads to incorrect pictures of the atmospheric structure: the meaning of conceptual model is indeed to concatenate together observations from different sources in a coherent and structurally correct way.

Many problems thus arise when trying to identify an observed structure as a certain conceptual model, which are not always fitting with each other. The disagreement often leads meteorologists to force observations into the conceptual model box, which is a very unscientific procedure.
Similar problems were already observed and reported by Postma (1948) who noted how Norwegian analysts drew occluded fronts despite any evidence that the occlusion had ever occurred, faced with the separation of the surface low from the warm sector.
So, the analyzing of occlusions has created much confusion, which has lead to extensive discussions among meteorologists during the second half of the last century.

Another very controversial feature of occlusions is the process by which an occlusion is formed, which has raised a long debate especially during the last quarter of the past century among scientists, with a clear division between those claiming the classic occlusion process does occur (e.g., Schultz and Mass 1993; Reed et al. 1994; Martin 1998) and those demonstrating that alternative processes are observed (e.g., Palmén 1951; Wallace and Hobbs 1997; Hoskins and West 1979; Shapiro and Keyser 1990). Despite the debate, it still remains a fact that proving the existence of the occlusion process is not always a straightforward or even solvable task.

It is nowadays an accepted fact, as extensively summed by Schultz and Mass (1993), that the post-mature stage of extra-tropical cyclones can be achieved in some other different ways than the one depicted in the classical theory and can show up in very different structures.

Hartonen (1994) has shown that the type of occlusion is very often analyzed in different ways in different operational environments, which undoubtedly leads to the conclusion that something is wrong in the conceptual model itself and the way it is interpreted in different context.
It is well known in operational meteorology, as extensively commented by Doswell (1999) in his personal notes, that in some contexts more than one conceptual model may describe the same meteorological system, at least in some stage of development. If the application of a conceptual model leads frequently to different and controversial conclusions, revisions ought to be done.

It can be that there are not objective argumentations for determining the type of occluded fronts and the whole classification turns out to be idealistic.

All the above mentioned argumentations lead to the conclusion that the occlusion needs to be further studied under many different points of view, in order to provide a solid basis that allows a proper and scientifically correct use of the concept.

4. STATISTICAL INVESTIGATION OF OCCLUSIONS

4.1 Aims of the investigation

The central part of the work is the comprehensive investigation of the occlusion processes occurred over a relatively long period of time.
The purposes of the investigation include the creation of statistics about the occurrence of the different types of occlusions, gaining some insight about their relation with respect to the seasonal and geographical occurrence, and the assessment to what extent, from a statistical point of view, the classical model is able to describe the observed features.

4.2 Area and period of the investigation

The period of investigation spans the year 2003.
The area of investigation includes Europe and the north part of Atlantic (fig. 4.1).

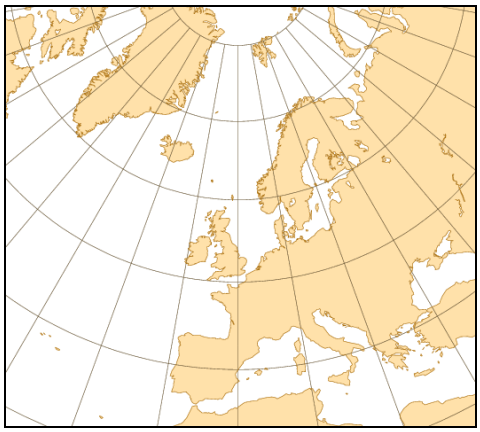

Figure 4.1. The area of the investigation

4.3 Investigation: methodology and classification

The work deals mainly with the well developed late stage of the extra-tropical cyclone: this is identified as the occluded stage in the NCM as well as in the FMI guidelines.

As will be shown later, the cyclones reaching a well-developed stage do not always fit in the classical framework, often exhibiting only some features of it, if any at all.
In the light of these considerations it is proper to say that the investigation considers all those low pressure developments reaching the so called post-mature stage, which is not necessarily an occlusion. Occlusion does refer to a specific process having its own structural characteristic as depicted within the FMI guidelines, while the goal is indeed to study how the structure of post-mature cyclones eventually differs from that of the classical framework.

Stating when a cyclone has reached the post-mature stage is sometimes rather arbitrary, because of the fact that the development doesn't always exhibit clear features as supposed in the classical model: an interim definition of post-mature stage is needed.
In this work a cyclone is typically considered to have reached the post-mature stage at the time the surface low pressure center begins detaching from the peak of the warm sector; accompanied by the formation of a sharp warm air tongue in the temperature field or a ridge in (equivalent) potential temperature field in the lower layers of the troposphere. Satellite imagery has been also used occasionally as an additional tool in very critical situations, but never as a definitive parameter.
Each development has been analyzed throughout its whole life cycle in order to recognize non-classical occlusion-like structures, e.g. instant occlusions.

In order to look for the cyclones which have reached the post-mature stage, certain numerical fields at interval of six hours based on the data archived into the MARS database of ECMWF have been thoroughly examined. The investigation has been pursued by means of the same set of fields for each interval of time, which includes the ones suggested in the FMI Interpretation Rules for occlusion identification and type

classification (table 4.1). On the other hand the same fields are the same traditionally used by operational forecaster during routine frontal analyses of weather charts.

Table 4.1. The levels and numerical fields used in the investigation.

LEVEL	FIELDS
Surface	pressure (mslp)
850 hPa	temperature (t), equivalent potential temperature (Θ_e), geopotential height (Z)
700 hPa	geopotential height (Z), relative humidity (rh)
500 hPa	geopotential height (Z) and temperature (t)
300 hPa	geopotential height (Z), wind vector, and isotaches

The investigation is actually like routine frontal analysis, the focus being on well-developed cyclones.

At first each development reaching the post-mature stage is comprehensively examined through its entire life cycle and classified on this basis either as classical or non-classical.

A classical development exhibits features which fit throughout its life cycle the structural and kinematical development of the classical model, while a non-classical one exhibits features which strongly differ from the classical model, usually the absence or anomalous position of the jet stream or the absence of a recognizable warm air tongue.

Again for sake of clearness, for classical model it is meant the model as treated in the FMI guidelines. Clear cases of instant occlusions and developments which entered the area in question in their latest phase of life are not further considered in this investigation.

It should be said that this kind of analysis is not always straightforward and some unclear developments have been left out, because it could not be assessed by means of available tools whether it was the case of a post-mature stage or the sample of a different synoptic weather system.

Once the development has been classified as classical, which means that we are dealing now with what a forecaster would call a traditional occlusion, a closer examination of its structure is pursued, which yields a further sub-classification, intrinsically connected with determining the type of the occlusion.

At this stage we compare the observed cyclone's structure with the ideal one proposed in the FMI guidelines, at the same time trying to assign a type to the occlusion. If the type can be assigned according to all the parameters as in FMI guidelines, then we consider the occlusion as perfect and assign it a type (warm, cold or neutral); if instead the type can be clearly assigned on the basis of at least one parameter, but not all, then the occlusion is classified as imperfect.

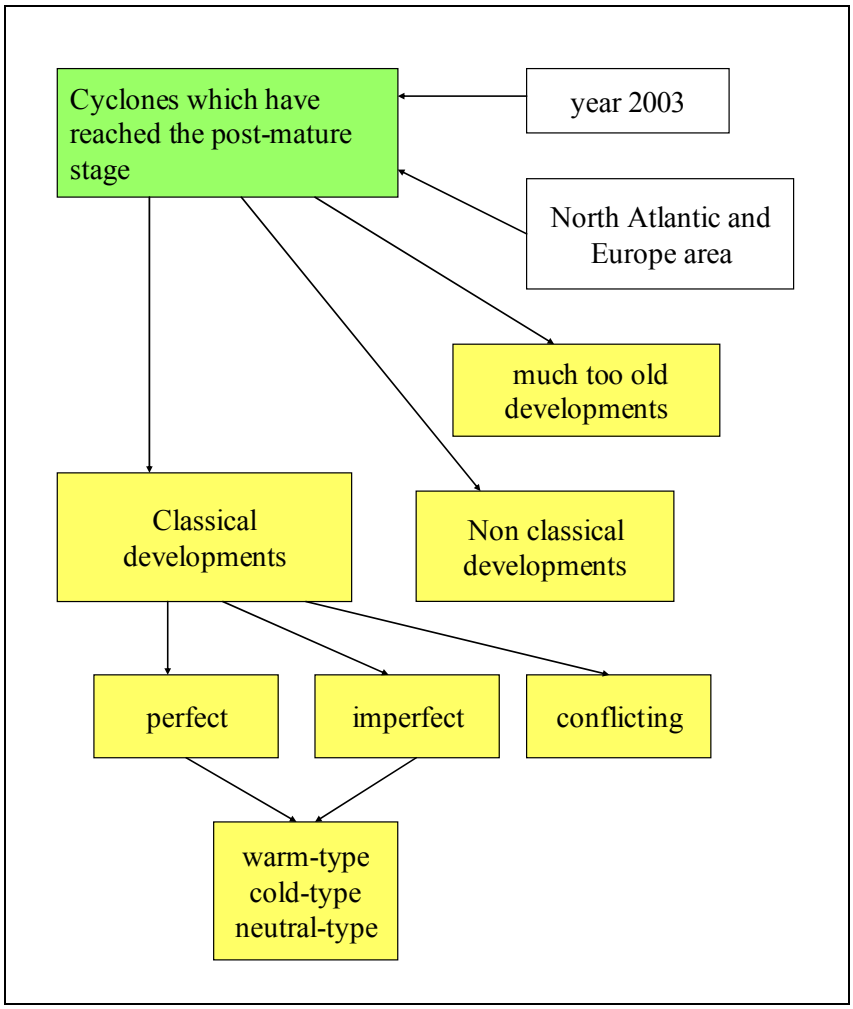

Figure 4.2. Diagram showing the classes produced in the investigation (yellow filled boxes) from the initial ensemble of post-mature cyclones observed over Europe and North Atlantic during year 2003 (green filled box). The class 'much too old developments' refers to the cyclones which came to the area of the investigation already in the latest stage of their life cycle.

In some cases the parameters lead to the determination of different types for the same development in the same phase: in this case the occlusion is classified as conflicting, which means that the type cannot be assigned on the basis of the available tools.
Fig. 4.2 shows all the classes and the corresponding relations discussed earlier.

4.4 Collection and statistics

The total number of cases collected from year 2003 over the area in question was 275.
This number includes few multiple cases, which refer to those ones whose class clearly changed into another one in a way that the system has been treated as two different systems at two different times. For each case that has reached the post-mature stage, date and coordinates have been recorded, together with the class assigned to it on the basis of the diagram shown in fig. 4.2. All the material collected has been further investigated in order to gain some insight of the capability of classical model to describe the thermal structures observed in the post-mature stage of the extra-tropical cyclones.
On the other hand the results have been inspected regarding the types of occlusions and their intrinsic validity.

4.4.1 Statistics and geographical distribution of occlusion types

Reliable statistics about occlusion types is nearly absent from the literature. The investigation pursued in this work furnishes material which allows the creation of a very short-term statistics. As highlighted in the FMI guidelines the type is assigned on the basis of the configuration of the cyclone's thermal structure, which is not often straightforward, and refers only indirectly to the temperature distribution in the lowest troposphere and especially over the surface.
The relation between the thermal structure throughout the troposphere and the surface temperature distribution is discussed in detail later in the conclusions.

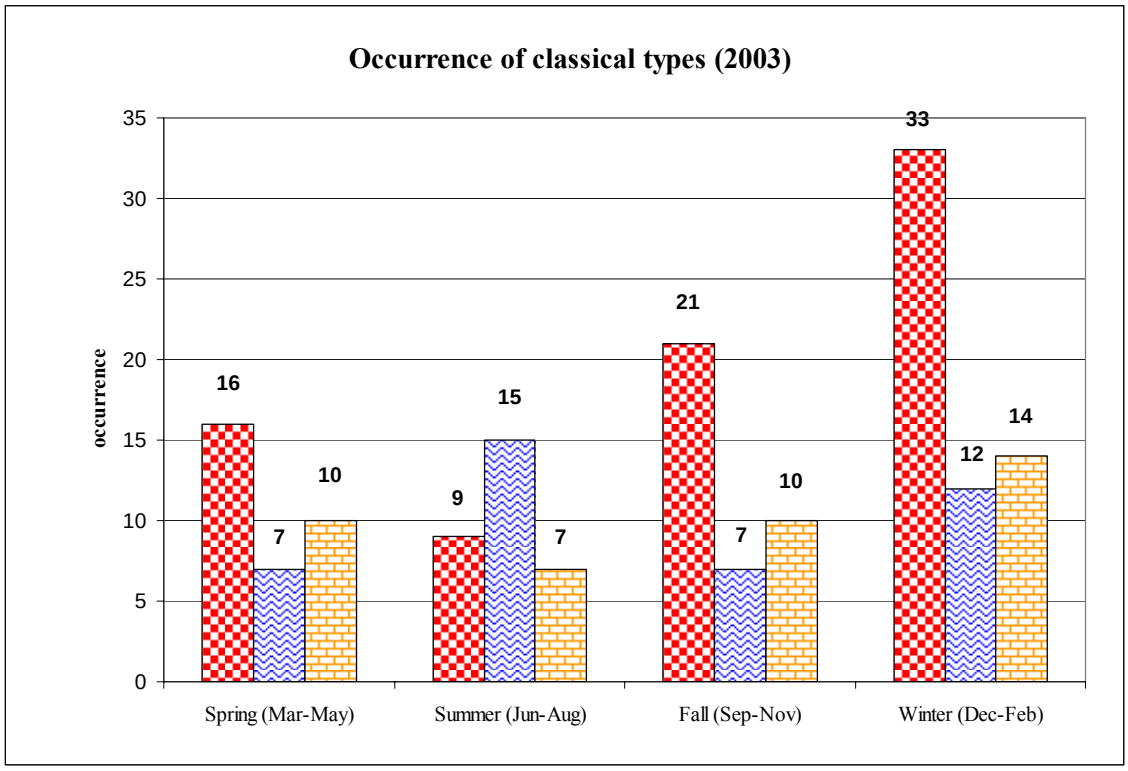

Figure 4.3. Seasonal occurrence of classical occlusions (perfect and imperfect) according to their type during the year 2003 over the area of the investigation. Columns filled with red squares, blue wave-like segments and orange bricks represent warm, cold and neutral occlusions respectively.

If we consider both perfect and imperfect classical developments, the seasonal occurrence of the different types of occlusion over the investigation area (fig. 4.3) shows that during fall and winter times, and in a lesser extent during the spring time, there is a predominance of warm-type occlusions, generally more than half of the total, whereas the occurrence of cold-type cases is only from 15 to 20% (fig. 4.4).

During the summer time there is instead predominance of cold-type occlusions (nearly 60%) and fewer warm-type cases.

Neutral-type occlusions occur nearly with the same seasonal incidence with an average of 25%.

Figures 4.5-8 show the seasonal geographical distribution of the occlusion types, including both perfect and imperfect cases. The comparison of the different seasons shows that the cyclones occluding over the easternmost part of the Atlantic and Western Europe are usually warm- and, in a lesser extent, neutral-type, except in the summer when the majority is cold-type.

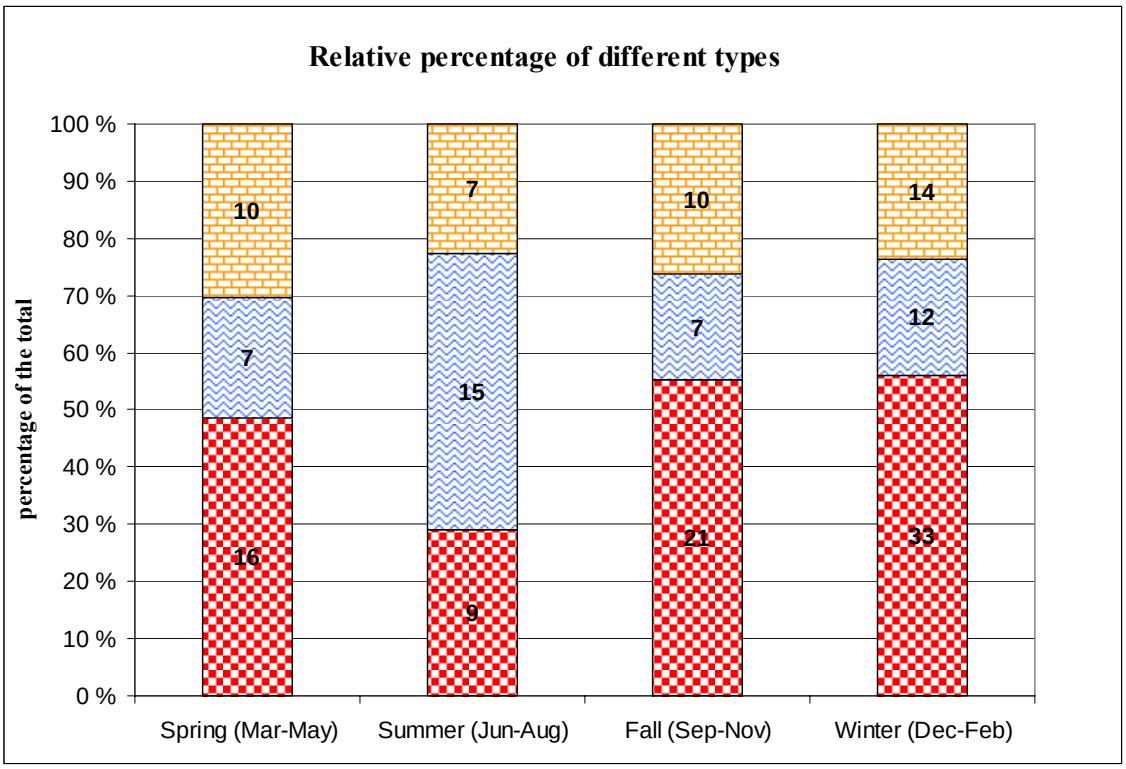

Figure 4.4. Relative percentage of the seasonal distribution of classical (perfect and imperfect) occlusion cases according to their type with respect to the total number of cases occurred over the area of the investigation during year 2003. Legend as in figure 4.3.

Over northern Atlantic there is predominance of warm-type cases during fall and winter times, while cold- and neutral-type dominate during spring and especially summer times.

On the other hand neutral-type occlusions seem to be homogeneously distributed over the Atlantic and European area, with a slightly higher, but not significant, density during the spring time.

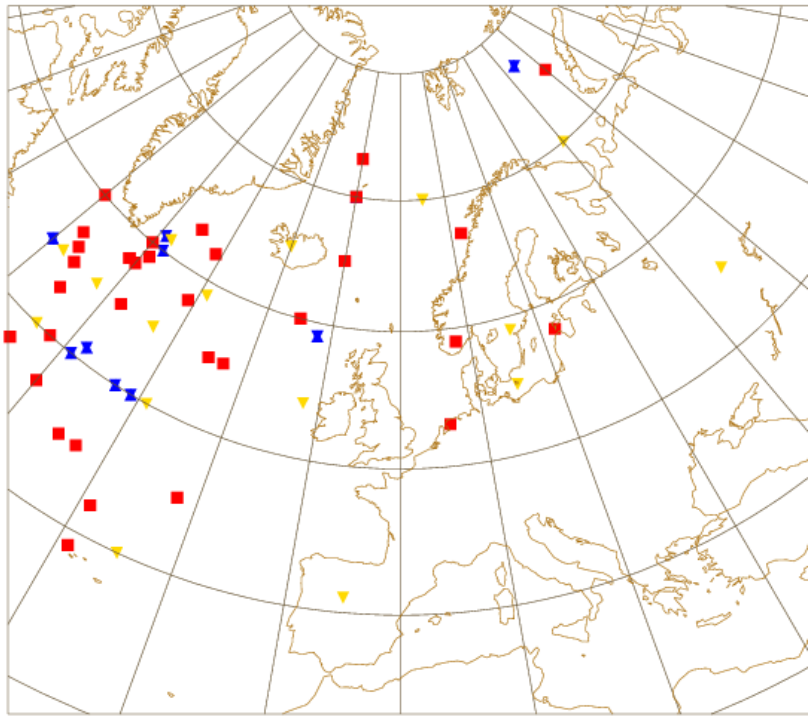

Figure 4.5. Geographical distribution of the types of the occlusions (perfect and imperfect cases) over the area of the investigation during winter 2003. Red squares, blue hourglasses and yellow triangle represent for warm-, cold-, and neutral-types respectively.

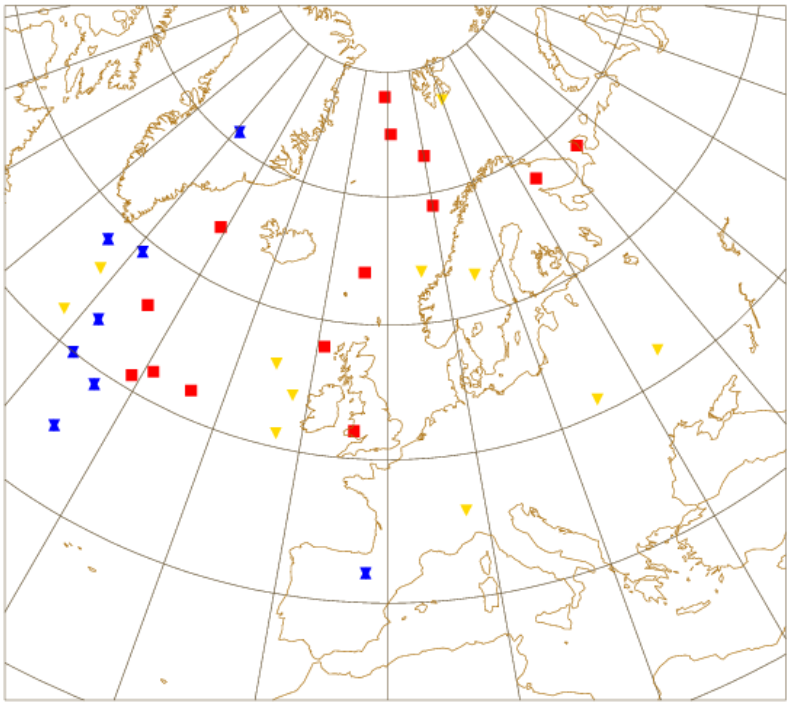

Figure 4.6. Geographical distribution of the types of the occlusions (perfect and imperfect cases) over the area of the investigation during the spring 2003; legend as in figure 4.5.

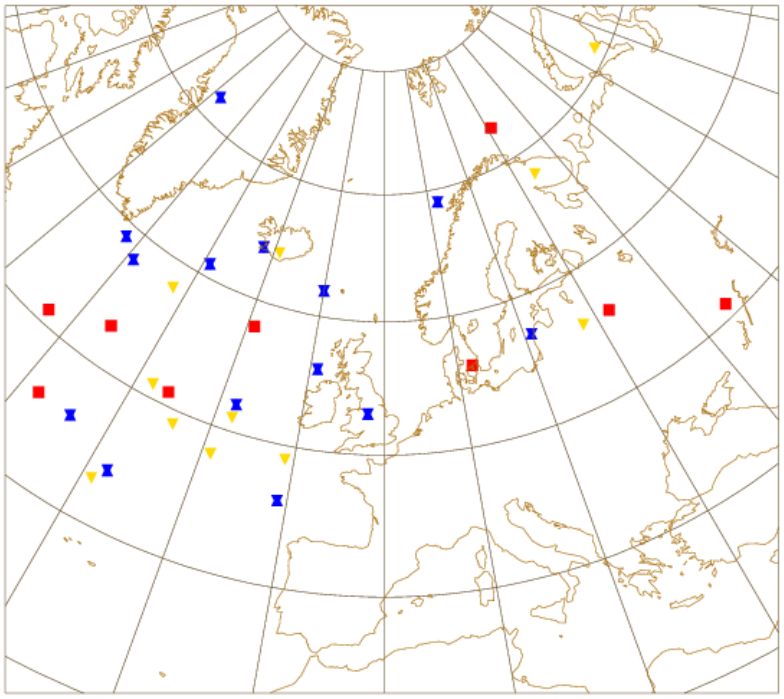

Figure 4.7. Geographical distribution of the types of the occlusions (perfect and imperfect cases) over the area of the investigation during the summer 2003; legend as in figure 4.5.

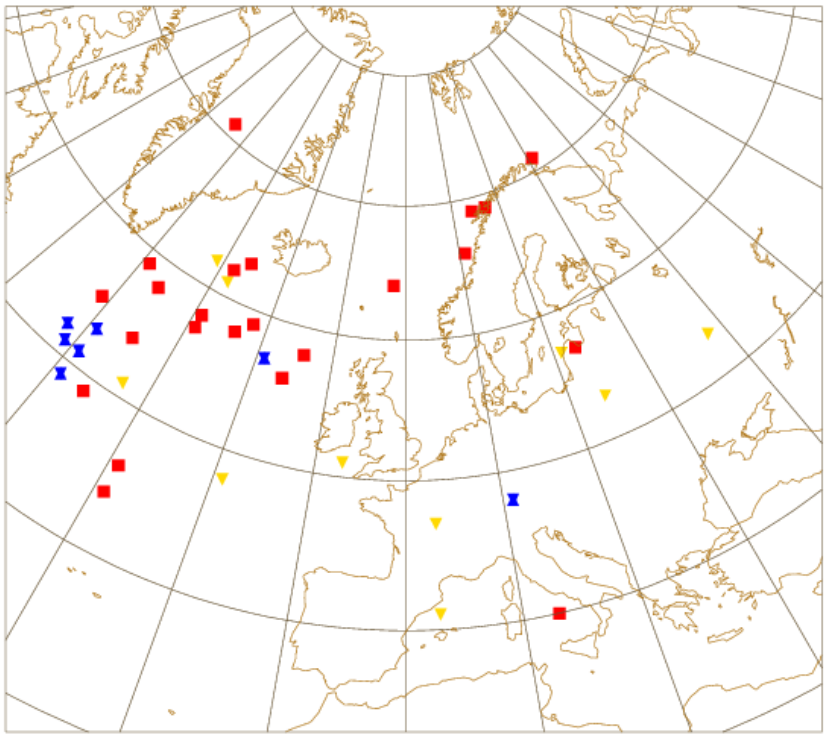

Figure 4.8. Geographical distribution of the types of the occlusions (perfect and imperfect cases) over the area of the investigation during the autumn 2003; legend as in figure 4.5.

It should be kept in mind that each point on the maps represents the approximate instant and place where the occlusion process begins and that the average path of the cyclones

is from west to east, even if there are many exceptions, especially over southeastern Europe. According to this argumentation at high latitudes cyclones usually occlude over the Atlantic and reach Europe at already a well-developed stage. On the other hand Scandinavian Peninsula can be considered an area with a modest density of occluding cyclones throughout all the year.

4.4.2 Statistics and geographical inspection about the intrinsic nature of the types of the occlusions

As already mentioned several times the determination of the type of the occlusions collected during the investigation has not been a straightforward task. Figure 4.9 shows the percentage of the different classes of classical occlusions with respect to the total number of cases. Only a third of the classical occlusions has been classified as perfect, which means that relatively seldom all the parameters together allow a clear determination of the occlusion type. It instead happens very often that either the determination of the type is possible on the basis of only some of the parameters, yielding an imperfect case (41% of the total), or different parameters lead to the determination of different types, yielding what in this investigation is classified as a conflicting case (23% of the total). Also the classification of the imperfect cases bears anyway a certain amount of uncertainty.

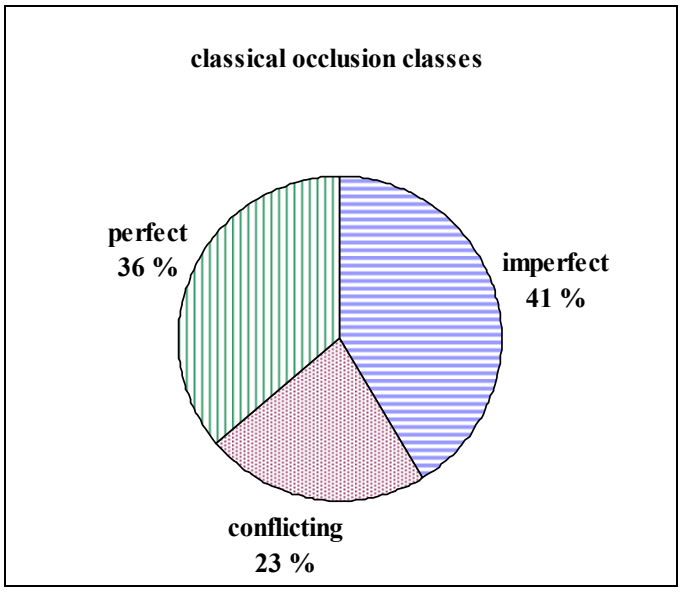

Figure 4.9. Diagram showing the percentage of different types of occlusions classified according to their classical features. Blue horizontal lines: imperfect occlusions; vertical green lines: perfect occlusions; close-fitting red dots: conflicting occlusions.

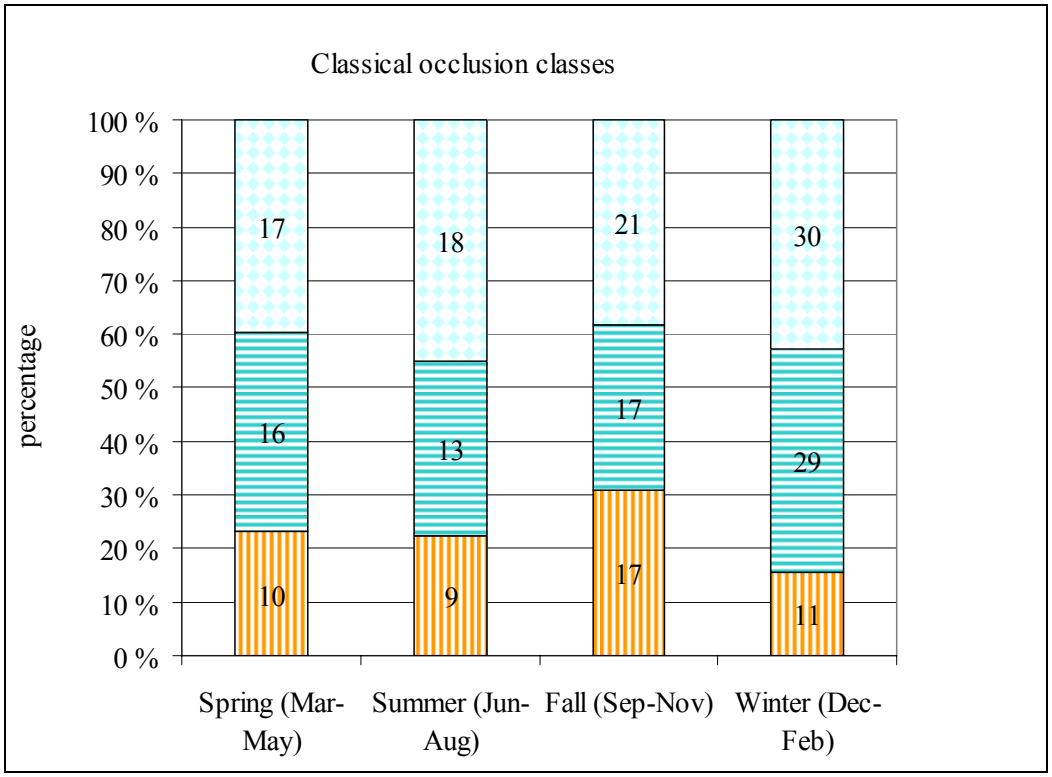

Fig. 4.10. Diagram showing the seasonal distribution of the different types of occlusions classified according to their classical features. Orange-yellow vertical lines filled columns: conflicting occlusion; blue horizontal lines: perfect occlusions; light blue squares imperfect occlusions.

Figure 4.10 shows the seasonal distribution of the occlusions classified according to their classical features, i.e. perfect, imperfect and conflicting. With the aid of this histogram representation it is possible to inspect the earlier argumentation within a seasonal frame. The relative percentage of perfect classical occlusion is higher in spring and winter times, about 40 %, while during the summer and the fall is significantly smaller, 30 % or less. Imperfect occlusions experience a constant incidence, about 40 % in each season, while conflicting cases show a peak during the fall time and a minimum during the winter.

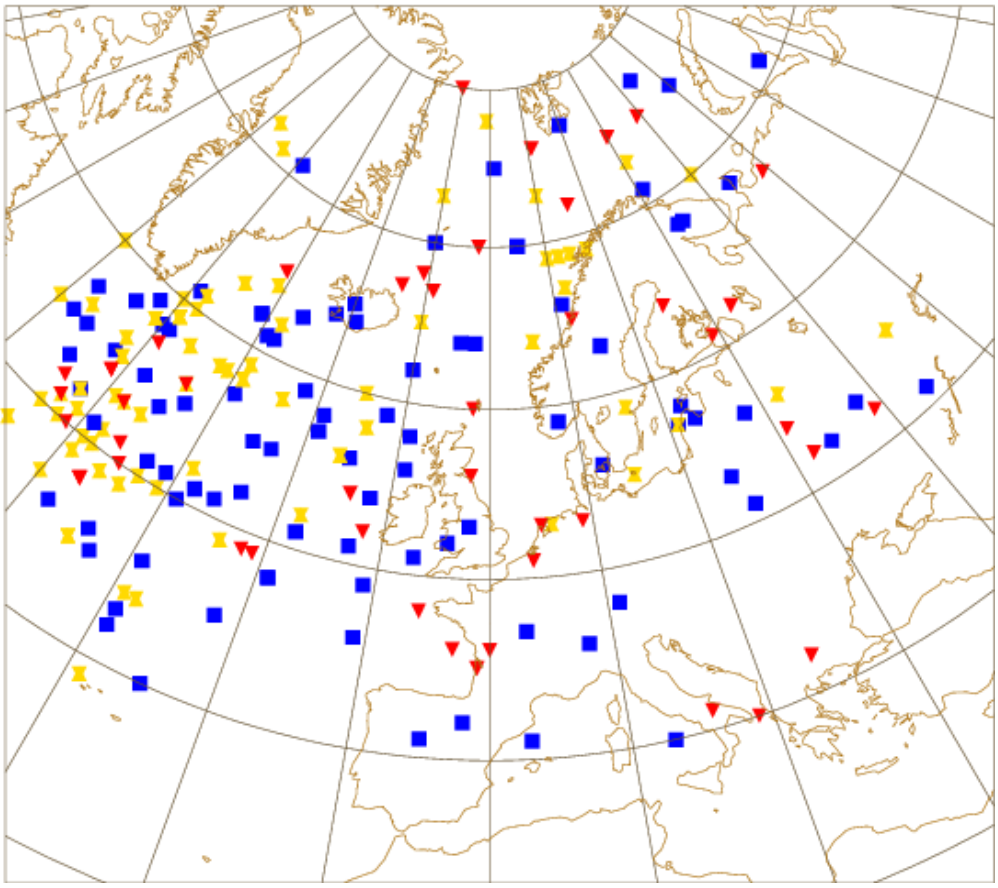

Figure 4.11. Geographical distribution of perfect, imperfect and conflicting occlusions. Blue square: imperfect occlusion; red triangle: conflicting occlusion; orange-yellow hourglass: perfect occlusion.

Figure 4.11 shows the geographical distribution of the three classes of classical occluded cyclones produced in the investigation, the same treated in fig 4.9 and 4.10. The distribution reveals that the conflicting occlusions are proportionally equally distributed over the investigation are, while over the European continent, except eastern part of Scandinavia, a remarked predominance of imperfect cases is observed.

4.4.3 Statistics and geographical inspection about the classical occlusion model

The material furnished by the investigation has been also analyzed in order to get some quantitative estimate of the capability of the classical model to describe the structure of the collected post-mature cyclones. In figure 4.12 the seasonal distribution of classical occlusion cases and so called non-classical occlusions show that the classical model significantly experiences difficulties in describing the structure and evolution of extratropical cyclone's post-mature stage. In winter the classical occluded model fits

better the observed cyclones' post-mature structure, as can be seen from the gap between classical and non classical occlusions is bigger than in other seasons.

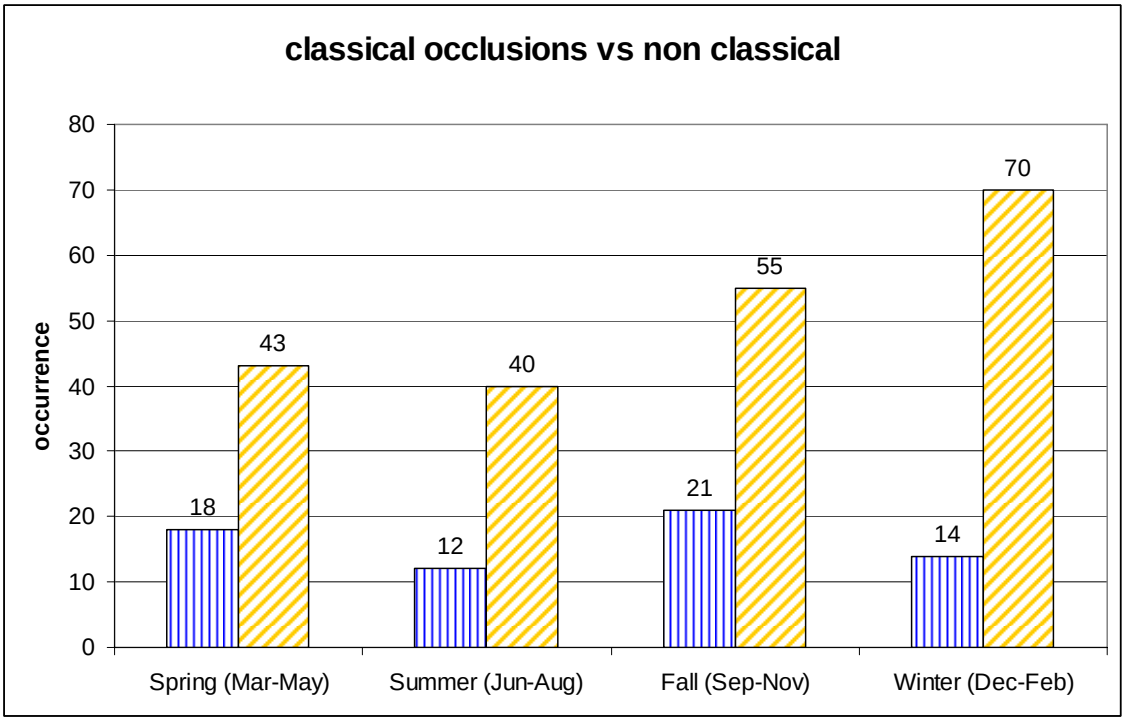

Figure 4.12. Seasonal distribution of classical occlusions (perfect, imperfect and conflicting) and cyclones yielding non-classical post-mature stage. Columns filled with yellow oblique lines: classical occlusions; columns filled with blue vertical lines: non-classical developments.

The geographical distribution of the entire year (fig. 4.13) reveals that non-classical occlusions are more likely to occur over the whole European continent, with slightly higher density over Mediterranean basin and western Russia, than over the Atlantic Ocean. On the other hand classical cyclones occur with nearly the same density over Europe, while over the ocean the majority of the development can be defined as classical. Only around southern Greenland non-classical occlusions show a local maximum.

In figure 4.14 a similar distribution is shown with the difference that only perfect classical occlusions are considered instead of the entire ensemble of classical occlusions. This geographical distribution shows a clear separation between ocean and continent: occlusions developing over the ocean seem to exhibit structures which are well described by the classical model, while over Southern and Eastern Europe the density of non-classical development is predominant.

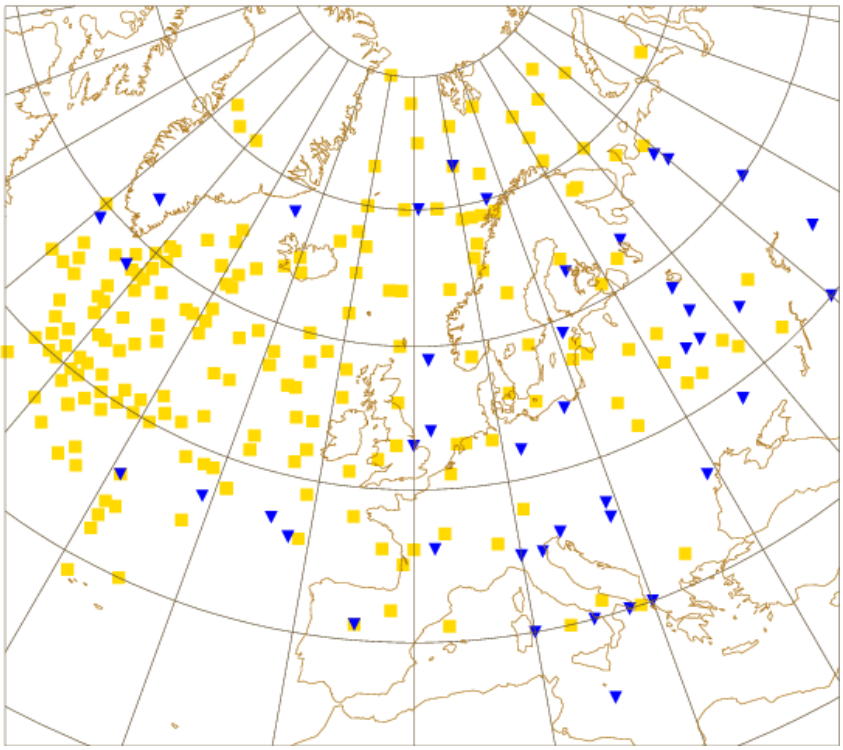

Figure 4.13. Geographical distribution of classical occlusions (perfect, imperfect and conflicting) and post-mature cyclones which couldn't be considered as classical occlusion. Yellow-orange squares represent classical occlusions and blue triangles non-classical developments.

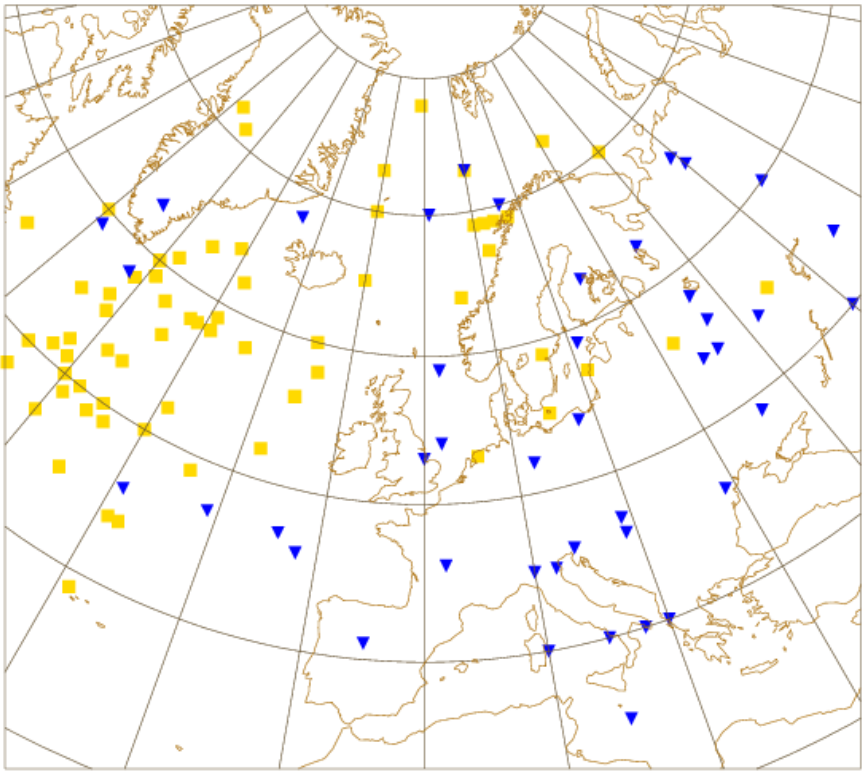

Figure 4.14. Geographical distribution of classical perfect occlusions and non-classical occlusion. Legend as in figure 4.13.

5. CASE STUDIES

In this section some interesting cases chosen from the ones collected during the investigation will be studied in detail. Not all the classes defined in table 4.1 will be represented by a case: those classes are a product of the statistical investigation, while in this section the purpose is to analyze certain aspects of the occlusion process through specific cases and not to go through samples of each class.
The way each case is examined is different from case to case, according to the specific features we want to highlight: we will not examine each development from a synoptic point of view throughout its life cycle but will focus the attention on certain aspects of the development, which will be discussed more extensively later.

5.1 Classical perfect warm-type occlusions

5.1.1 Cyclone over Southern Scandinavia 27.-30.4.2003

This cyclone has reached the post-mature stage over southern Scandinavia during the early morning of 27.4.2003 and yielded a classical perfect warm-type occlusion. Both in a constant pressure level and in a vertical cross section framework the structure of the development fits the FMI guidelines.
At 00 UTC of April 27th the presence of a nearby dissipating occlusion can be still traced by means of the warm tongue at 500 and 700 hPa (fig. 5.1, left) stretching across southern part of Sweden and Norway. The axis of maximum values of the Θ_e-ridge is on with the rear edge of the precipitation area related to this old occlusion, as can be verified comparing the two images of figure 5.1. In the same images the frontal band and the precipitation area related to the occluding cyclone under investigation can be observed over Denmark and the southernmost part of Sweden.

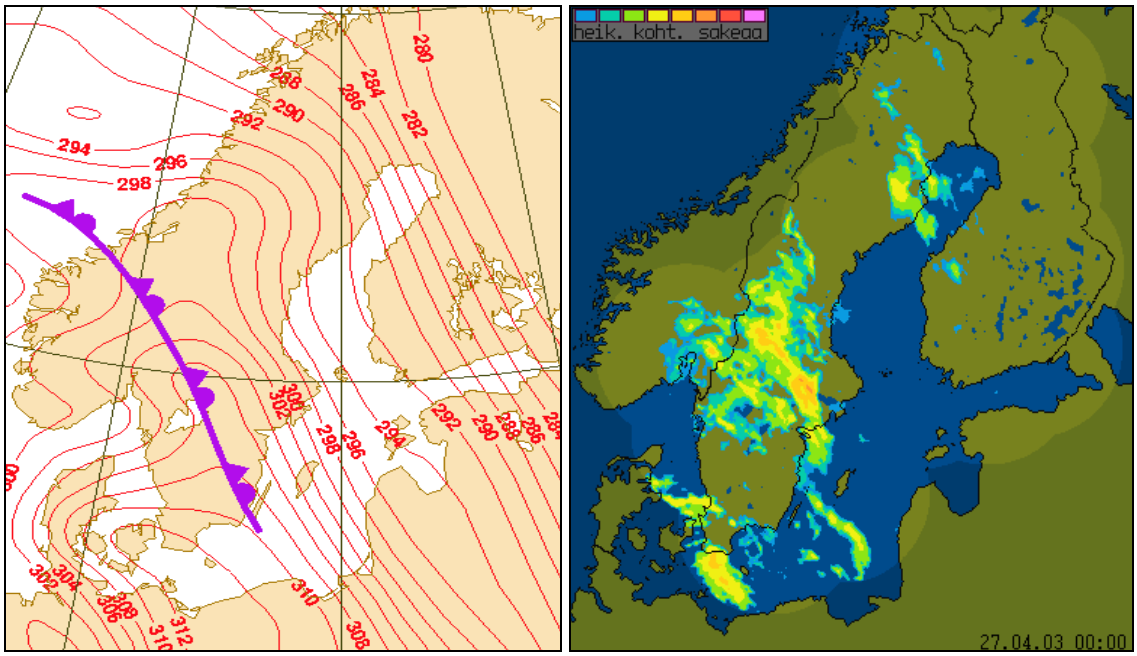

Figure 5.1. Left: 700 hPa Θ_e-field from 27.4.2003 at 00 UTC and frontal analysis. Right: radar composite picture at 00 UTC of 27.4.2003.

Stating when the cyclone has occluded, only by means of observations and numerical fields on constant pressure levels, has not been possible with absolute precision: within this framework it is possible to state that the cyclone is assuming, between 00 and 06 UTC, features typical of the post-mature stage, but not exactly where the cyclone is occluding. Figure 5.2(left) shows the subjective frontal analysis of the occluded cyclone at 06 UTC performed on the basis of numerical fields as explained in the FMI guidelines: the cyclone seems to have gone far into the occluded stage.

The jet stream is well split into two branches in accordance with a typical warm-type structure, with the one related to the cold front being very weak; a stronger temperature gradient is observed at 850 hPa on the fore side of the occluded front (fig. 5.2). The equivalent potential temperature field at 700 hPa shows a well developed warm tongue over Southern Sweden, not to be confused with the one over central part of Sweden and Norway related to the earlier mentioned dissipating occlusion (fig. 5.3, right). For this younger occluded cyclone the isentropic ridge correlates with the rear edge of the cloud distribution shown in the satellite images in figure 5.3(left).

Despite the use of additional information furnished by surface synop-observations, the surface warm sector has been rather arbitrarily located: the framework we are working with does not offer enough details in order to depict an exact three-dimensional picture of the system.

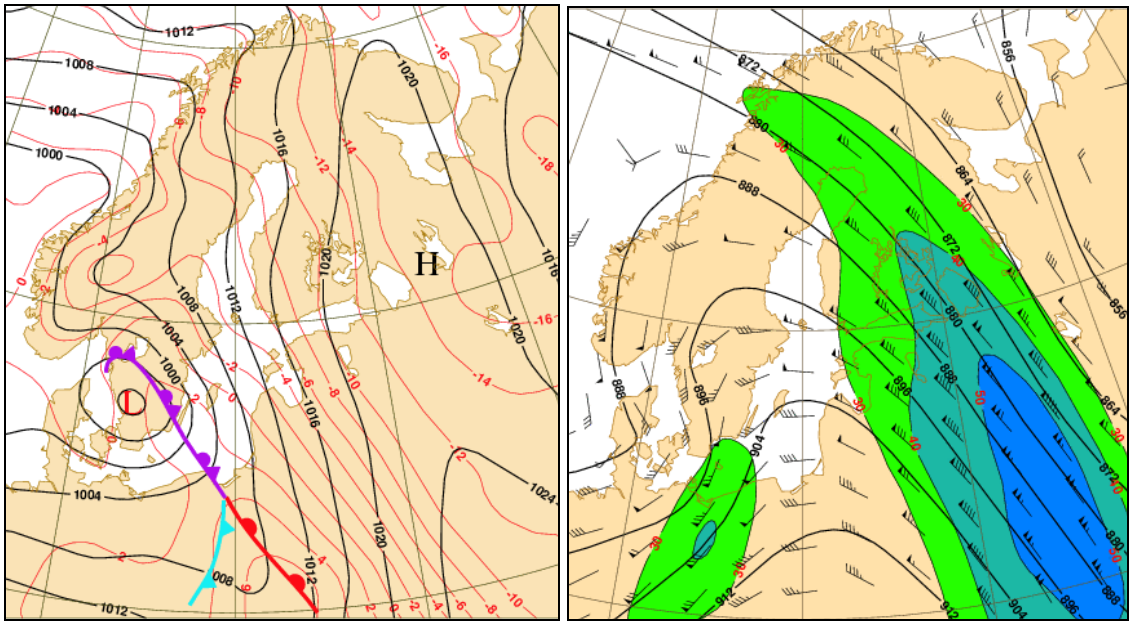

Figure 5.2. Numerical fields and frontal analysis from 27.4.2003 at 12 UTC. Left: 850 hPa geopotential height (solid black lines) contoured every 4 dam, equivalent potential temperature (thin red lines) contoured very 2 k and subjective frontal analysis; right: 300 hPa isotaches (colored starting from 30 m/s at interval of 10 m/s), geopotential height (solid black lines) contoured every 8 dam and wind vector barbs in knots.

Cross sections at 00 and 06 UTC of April 27th do not either exhibit very clear frontal structures: a kind of double frontal pattern is present, as the cross section in figure 5.4 shows, one in the middle troposphere and the other more classical but weaker in the lower part, both discernible by related frontal bands and temperature advection maxima. Cross sections exhibit more classical features, i.e. a recognizable occlusion structure fitting the FMI guidelines, only starting from 12 UTC.

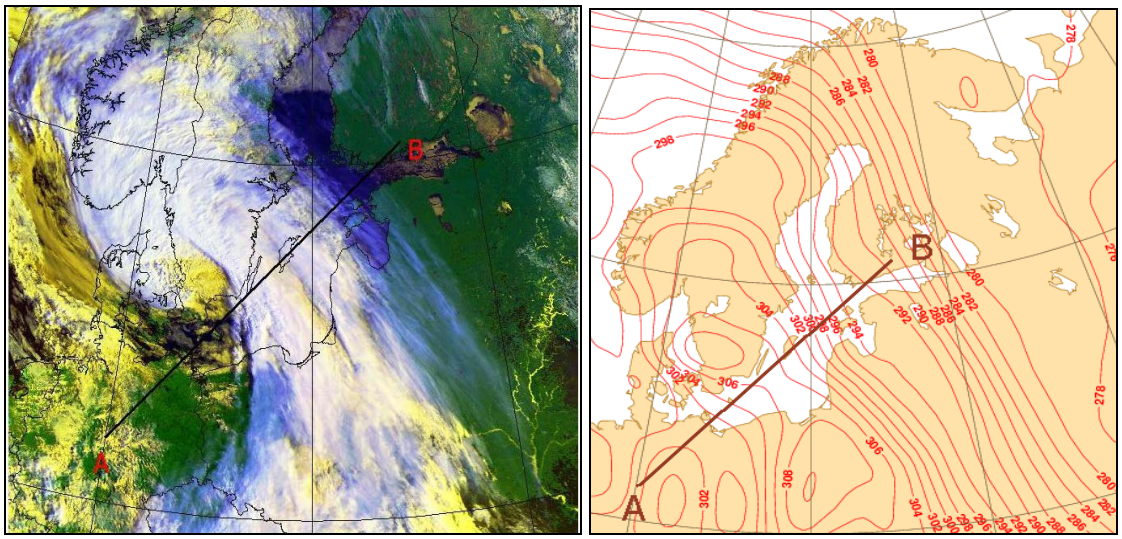

Figure 5.3. Left: NOAA AVHRR satellite RGB composite image (channels 1, 2 and 4) at 06.22 UTC of 27.4.2003 and the position of the cross section. Right: 700 hPa Θ_e-field (contoured every 2 K) at 06 UTC and the position of the cross section.

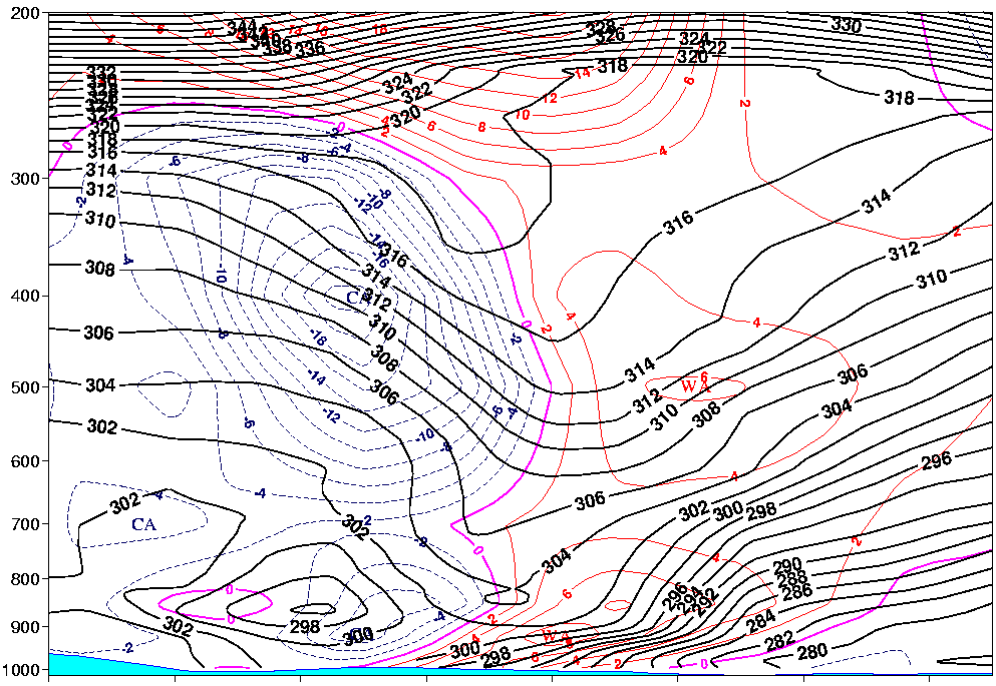

Figure 5.4. Cross section at 06 UTC of 27.4.2003. Solid black lines: isentropes, contoured every 2 K; thin lines: temperature advection (dashed blue lines for cold advection, red solid for warm advection and solid violet for value 0, contours every 2 x 10^{-4} K s^{-1})

At 12 UTC the occluded cyclone keeps all the features described for 06 UTC, as can be verified from figure 5.5. The 850 hPa warm advection on the fore side of the occlusion is predominant with respect to the cold advection on the rear side (fig. 5.6, left). A very well developed warm tongue can still be observed in the lower troposphere: figure 5.5(left) and 5.6 (right) shows this feature in the temperature field at 850 and in the equivalent isentropic field at 700 hPa.

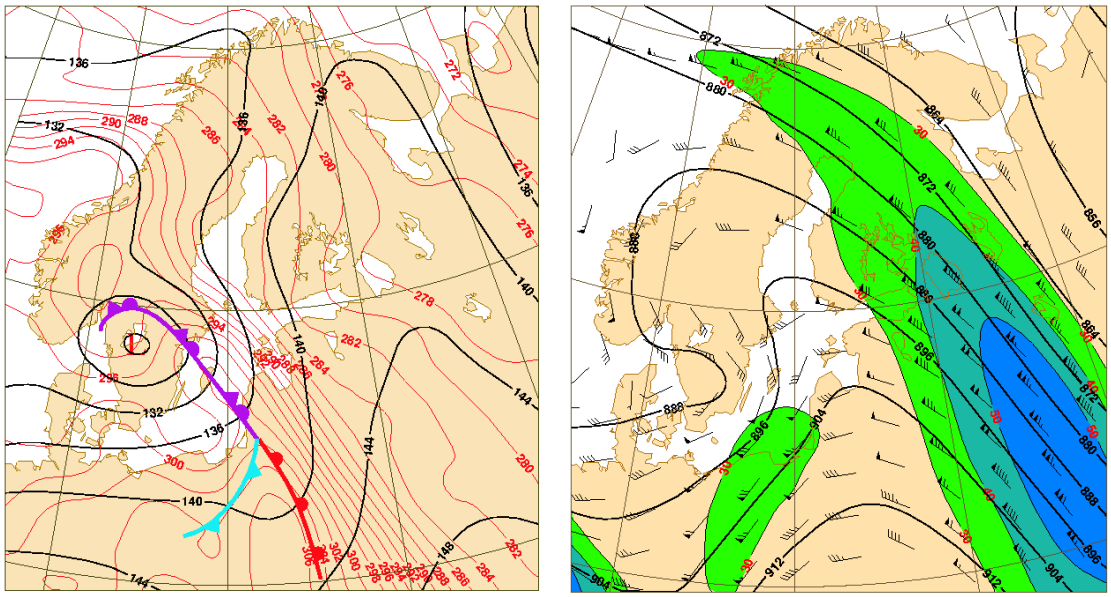

Figure 5.5. Numerical fields and frontal analysis for 27.4.2003 at 12 UTC. Right: 850 hPa geopotential height contoured every 4 dam (solid black lines), equivalent potential temperature (thin red lines) contoured every 2 K and subjective frontal analysis; left 300 hPa isotaches (colored starting from 30 m/s at interval of 10 m/s), geopotential height (solid black lines) contoured every 8 dam and wind vector barbs in knots.

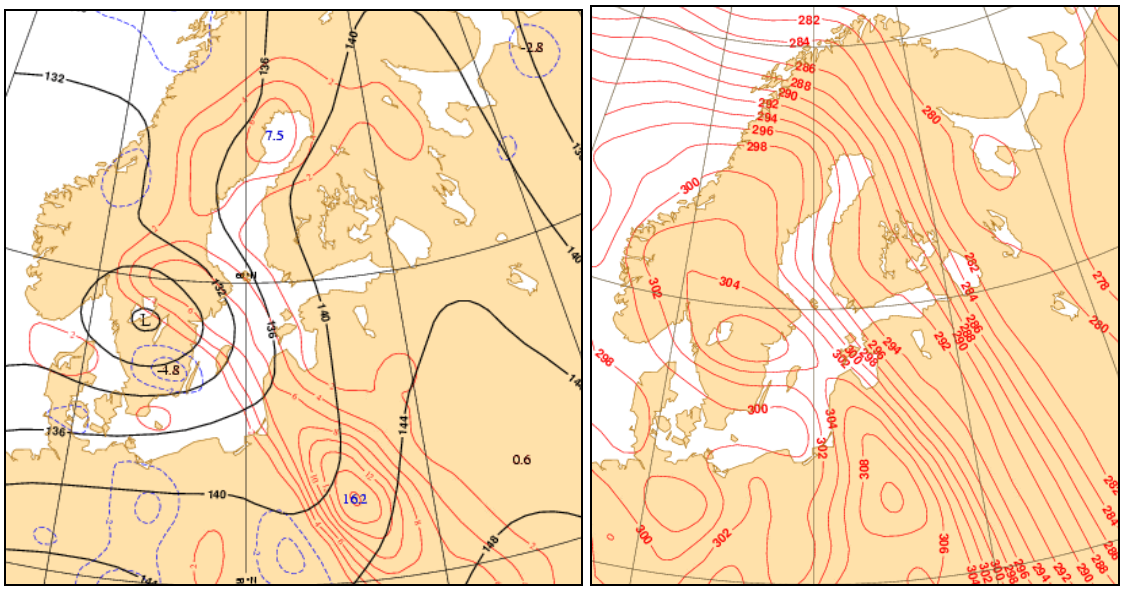

figure 5.6. Numerical fields for 27.4.2003 at 12 UTC. Left: 850 hPa, solid black lines: geopotential height contoured every 4 dam, red solid lines: warm advection, blue dashed lines: cold advection; temperature advection contoured every 2 x 10^{-4} K s^{-1}. Right: 700 hPa, red lines: equivalent potential temperature contoured every 2 K.

At 12 UTC the surface temperature distribution (fig. 5.7) shows a warmer air mass in the rear part of the occluded front, about 3-4, locally even 5-6, degrees, which may be also due to a differential surface heating due to the difference in cloud cover amount and

thickness.

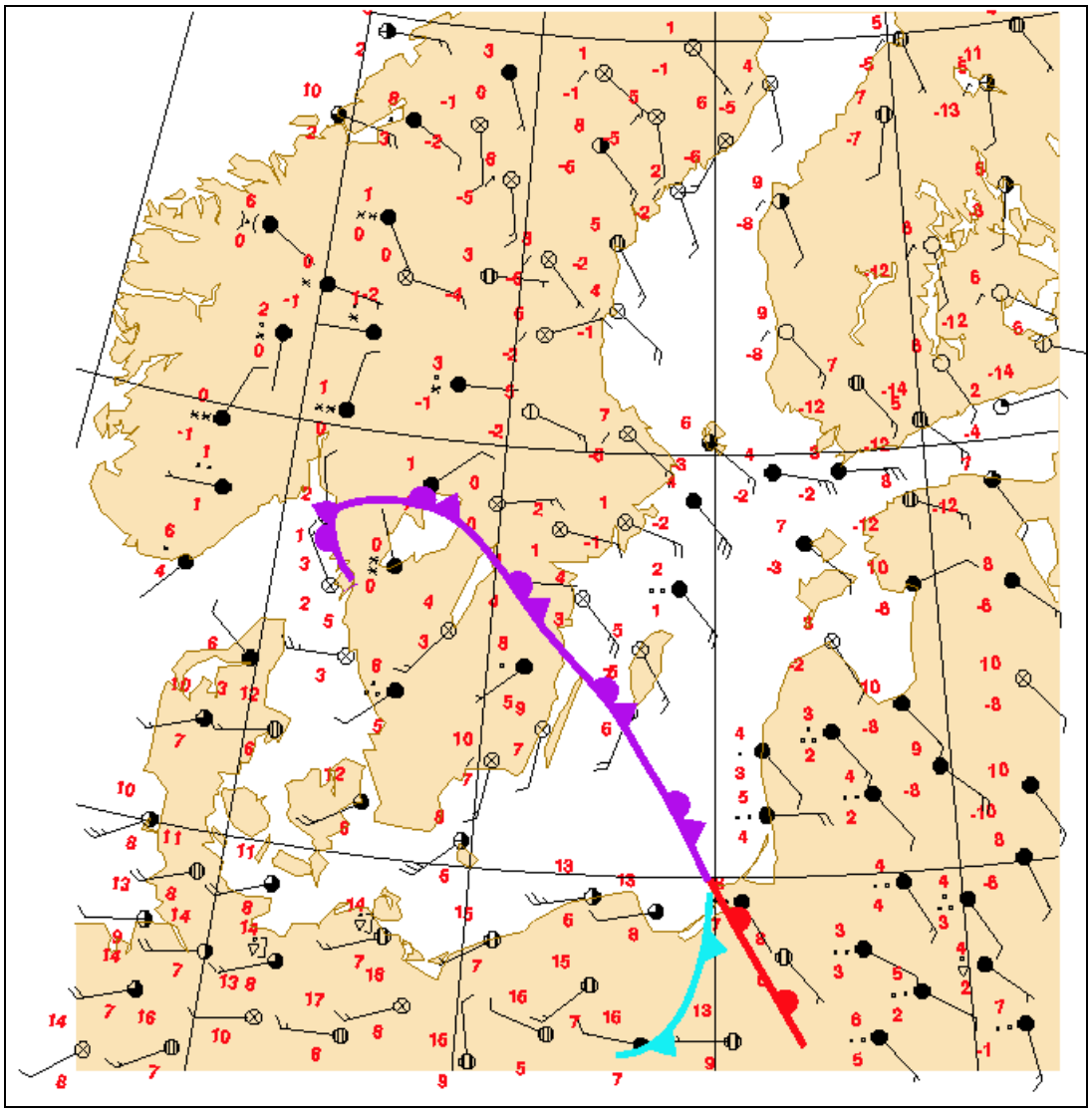

Figure 5.7. Synop observations at 12 UTC of 27.4.2003 and classical frontal analysis. Each synop observation include only temperature and dew point temperature, current weather symbol, wind barb (m/s), total cloudiness amount.

The comparison of temperature values from areas of total cloudiness shows differences in the same direction, though smaller; during the following night, at 00 UTC of 28.4.2003 (fig. 5.8), the same argumentation is valid. A cross section of the temperature field through the occluded front at 12 UTC of April 27th (Fig 5.9) exhibits warmer temperature in the lowest part of the troposphere behind the occluded front, so that we can finally conclude that the surface temperatures generally rise after the passage of the front.

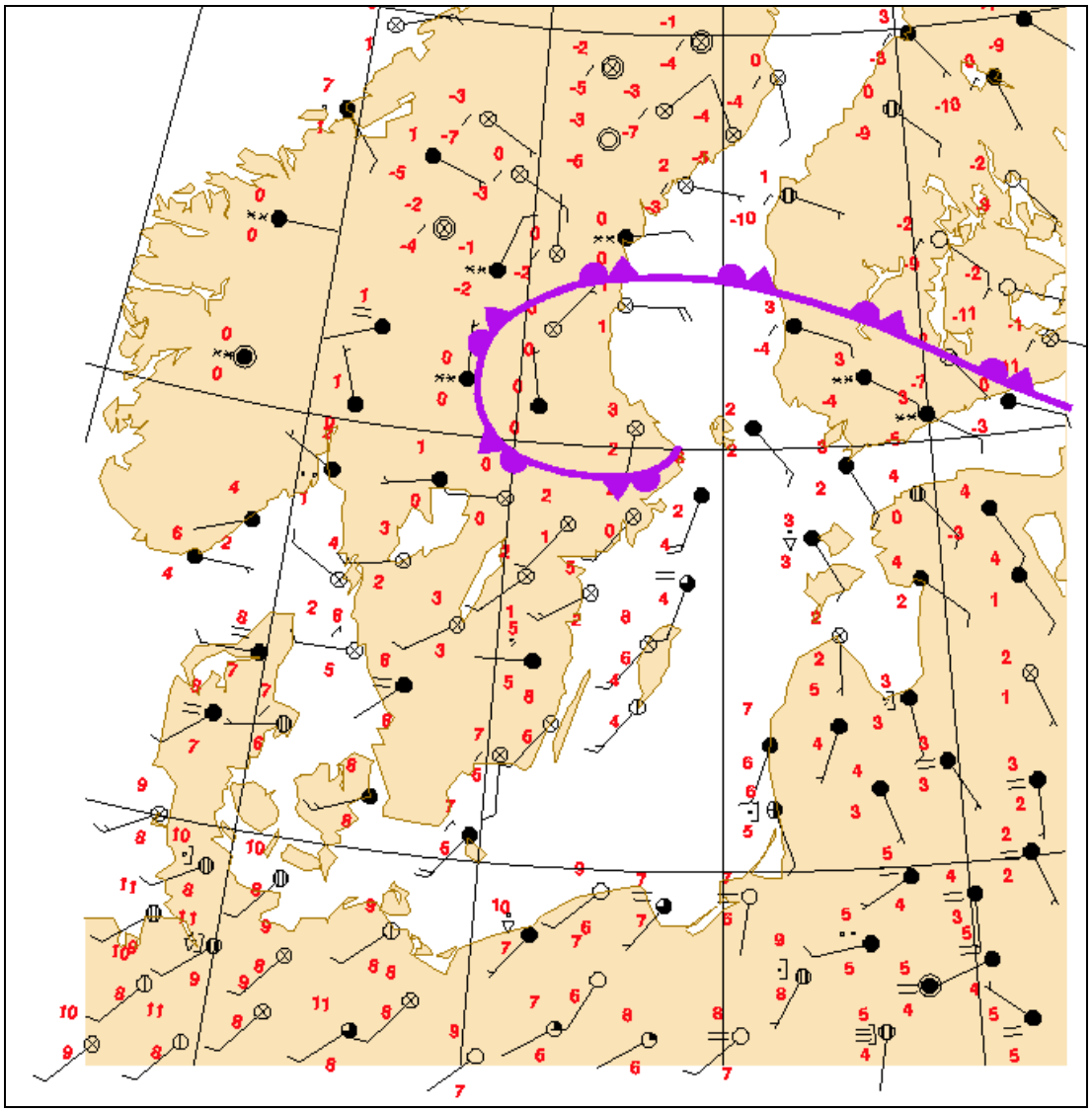

Figure 5.8. . Synop observations at 00 UTC of 28.4.2003 and classical frontal analysis. Each synop observation include only temperature and dew point temperature, current weather symbol, wind barb (m/s), total cloudiness amount.

The cross section of Θ_e-field across the occluded front shows that it slopes forward, in accordance with the classical definition of warm-type structure as in FMI guidelines: in figure 5.10 the subjective frontal analysis is superimposed to the fields. In the same image we can see that intense warm advection is located around the occluded front, partly also behind it, in the lowest layers.

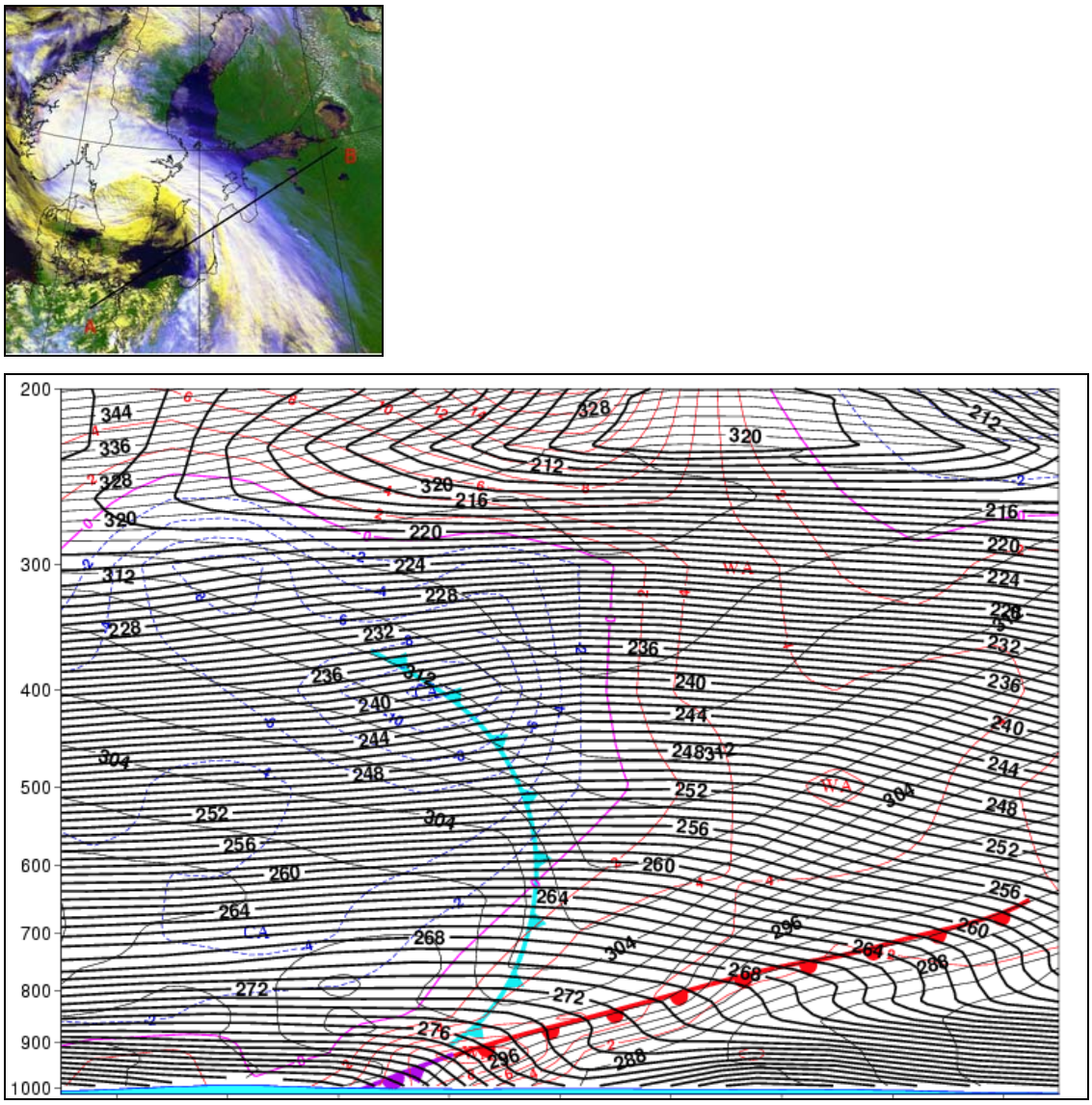

Figure 5.9. Upper: NOAA AVHRR satellite RGB composite image (channels 1, 2 and 4) at 12.12 UTC of 27.4.2003 and the position of the cross section. Lower: cross section at 12 UTC of 27.4.2003. Thin black lines: isentropes (K); thick black lines: temperature (K); dashed blue lines: cold advection, red lines: warm advection and violet lines: temperature advection = 0, contoured every 2 x 10^{-4} K s^{-1}.

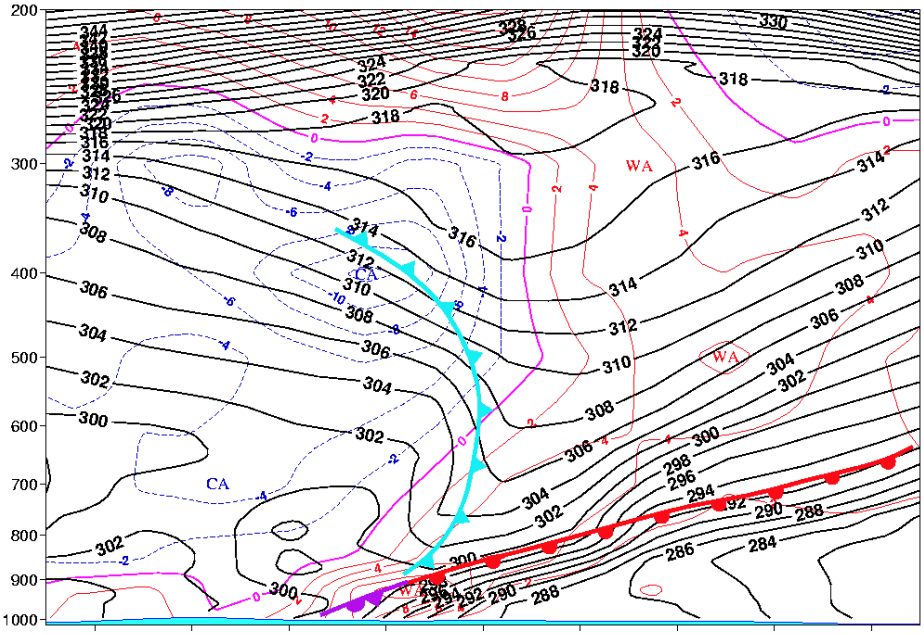

Figure 5.10. Cross section at 12 UTC of 27.4.2003 across axis shown in fig. 5.9. Solid black lines: isentropes (K); dashed blue lines: cold advection, red lines: warm advection and violet lines: temperature advection = 0, contoured every 2 x 10^{-4} K s^{-1}.

Cross sections made in the pre-dissipating stage across the surface low, i.e. where the occluded front usually coils around the low assuming the characteristic cloud spiral shape, as in the satellite image of figure 5.11(left), show in the middle atmosphere structures remind of occlusion, i.e. Θ_e-troughs, but completely detached from the lower part of the atmosphere, where instead a statically unstable configuration may take place. Depending on the cross section axis often two occlusion structures may be observed, which refer to the same occluded front coiling around the surface low. This is the case of the cross section of fig. 5.11(right) whose axis across the surface low pressure intersects the occluded front in two different points, as shown in fig. 5.11(left): the equivalent isentropic field shows in the correspondent coordinates two separate trough, tough very weak.

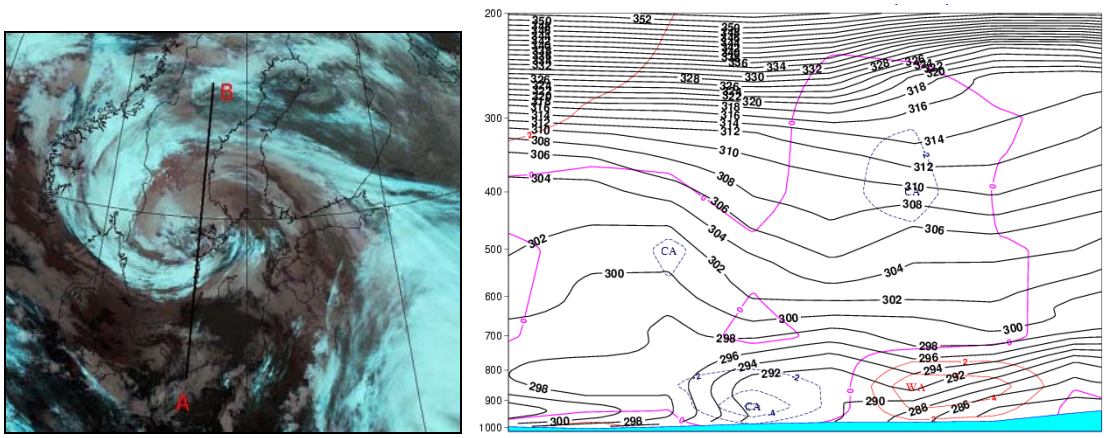

Figure 5.11. Left: NOAA satellite AVHRR RGB composite image (channels 3, 4 and 5) at 00.22 UTC of 28.4.2003 and the position of the cross section. Right: cross section at 00 UTC of 28.4.2003. Solid black lines: isentropes (K); dashed blue lines: cold advection, red solid lines: warm advection and solid violet lines: value 0, contoured every 2 x 10^{-4} K s^{-1}.

When the occlusion reaches its last stage of life, before it breaks up into different smaller scale systems, it seems that 700 hPa and, even better, 500 hPa thetae fields show the structure of the occlusion better than 850 hPa, which is to be expected, since the warm air has ascended.

Also the typical features of an occlusion are weaker: the original cold front is not anymore discernible and the warm sector has risen upwards and mixed with the colder air.

5.1.2 Cyclone over Southern Scandinavia 9.-10.6.2003

This cyclone having developed over Southern Scandinavia during the 9. and 10. of June 2003 has been classified as a perfect warm-type occlusion: the jet stream configuration and the 850 hPa temperature field structure lead to a warm type structure, even if the thermal gradient on the fore side of the occlusion is not extremely intense when compared to the rear side.

In this case the time when the occlusion process begins is determined by means of vertical cross sections. In the following all the mentioned times refer to the 9 of June.

Numerical fields on constant pressure levels do not offer an exact picture of the occurring occlusion process: a sharpening warm tongue is present in temperature fields at 00 and 06 UTC (and also in correspondent Θ_e-fields) but the 300 hPa jet stream structures would lead to an occlusion process already at 00 UTC (fig. 5.12).

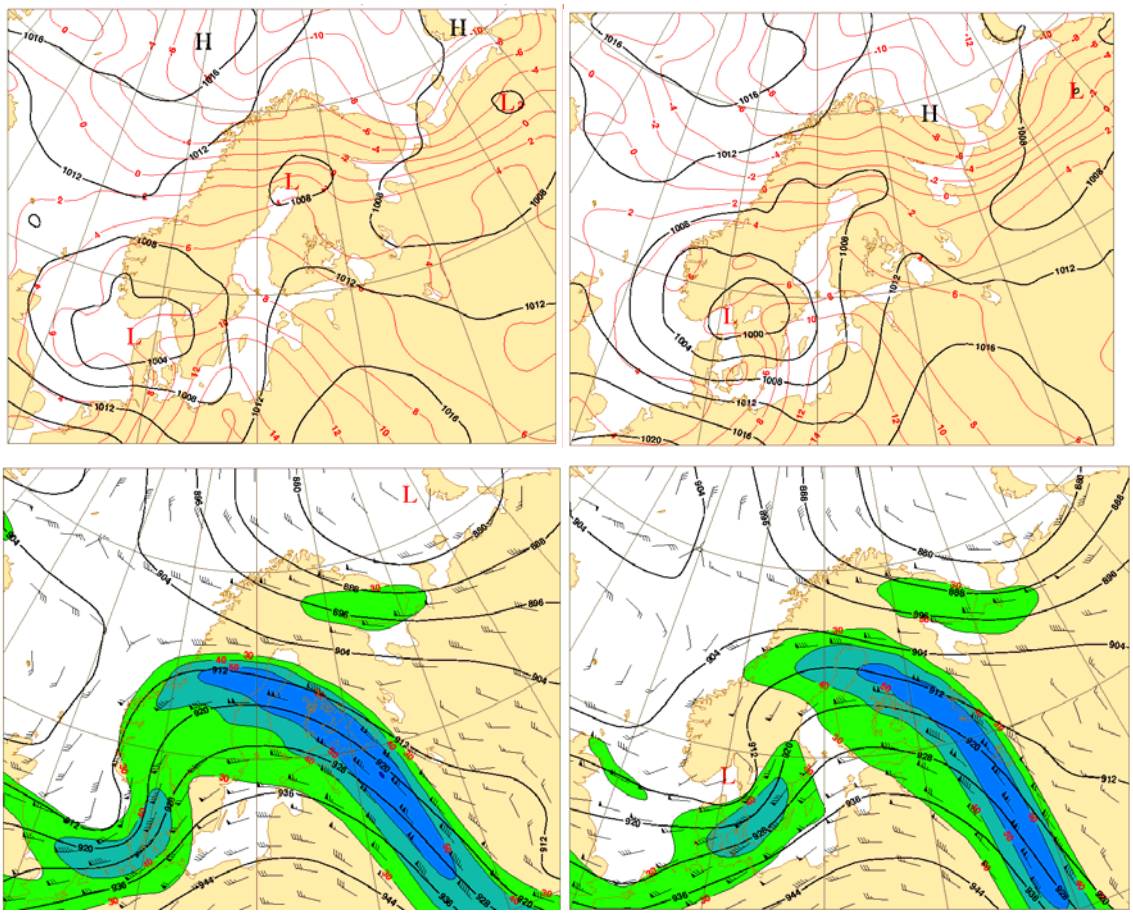

Figure 5.12. Upper: temperature at 850 hPa (thin red lines) every 4 dam and MSLP (solid black lines) every 4 hPa at 00 UTC (left) and 06 UTC (right) of 09.06.2003. Lower: 300 hPa isotaches (colored starting from 30 m/s at interval of 10 m/s), geopotential height (solid black lines) contoured every 8 dam and wind vector barbs in knots at times correspondent to upper images.

As can be seen from the cross section at 00 UTC, taken over the possible occlusion point, the cold and warm frontal zones are still separate from each other.

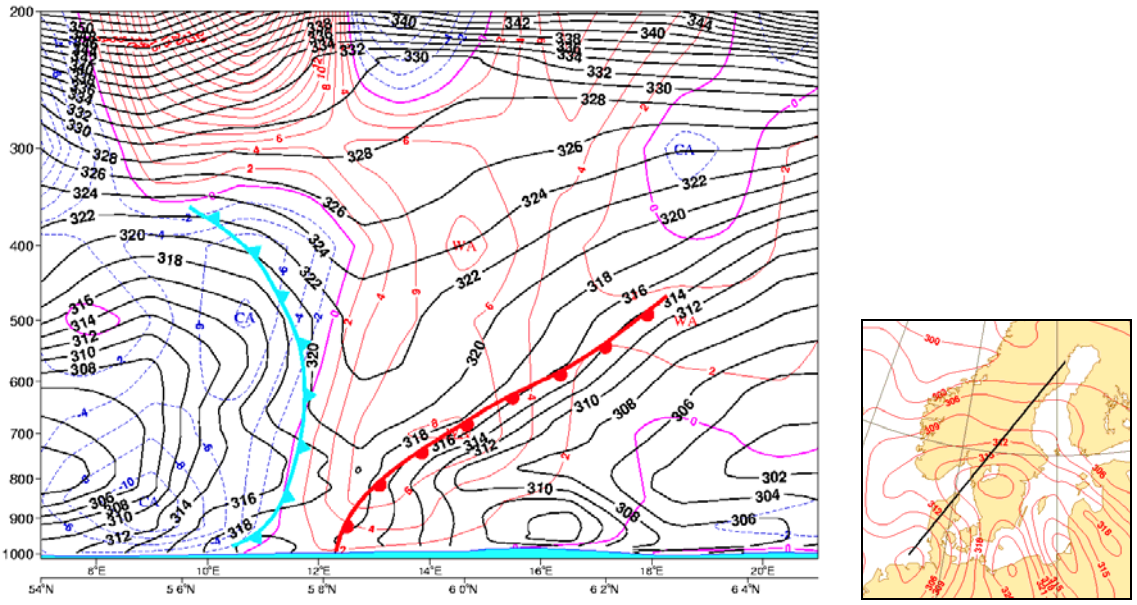

Figure 5.13. Vertical cross section (axis shown in the box on the right, where 700 hPa equivalent isentropes are plotted in red every 2 K) across the frontal structure at 00 UTC of 9.6.2003 and frontal subjective analysis. Solid black lines: isentropes (K); dashed blue lines: cold advection, red solid lines: warm advection and solid violet lines: value 0, contoured every 2 x 10^{-4} K s^{-1}.

In light of these argumentations we can state that occlusion process has not yet occurred at 00 UTC. The tongue of warm air stretching to the North Sea belongs to another system in the southwestern part of Norway.

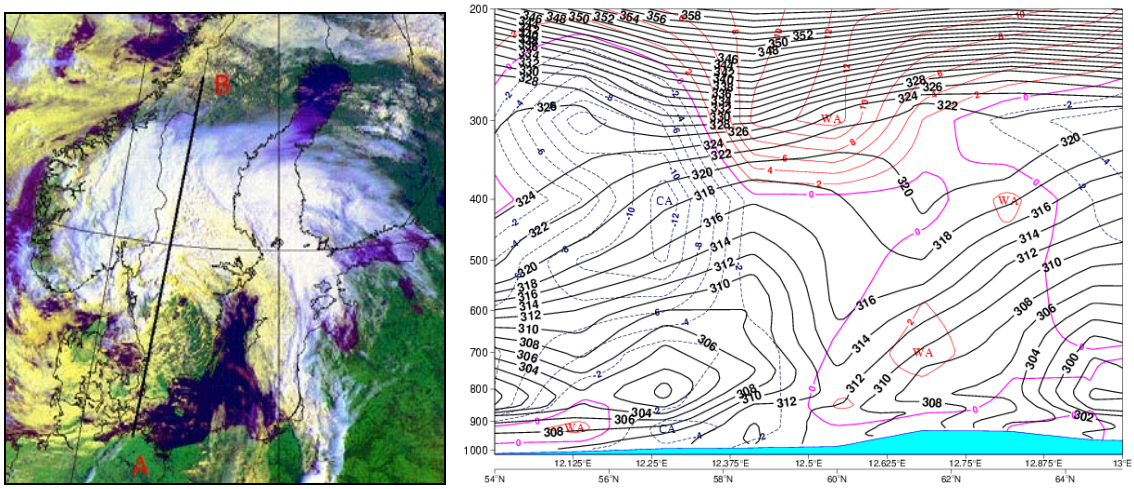

Figure 5.14. Left: NOAA satellite AVHRR RGB composite image (channels 1, 2 and 4) at 6.22 UTC of 9.6.2003 showing the occluded cyclone over central Scandinavia and the position of the cross section. Right: vertical cross section of equivalent potential temperature and temperature advection; Solid black lines: isentropes (K); dashed blue lines: cold advection, red solid lines: warm advection and solid violet lines: value 0, contoured every 2 x 10^{-4} K s^{-1}.

At 06 UTC the occlusion process has already begun. A cross section made through the occluded front (fig. 5.14) shows the typical occlusion pattern in the Θ_e-field, even if it is not possible to state the type of the occlusion according to the classical model

argumentations: only very tiny evidences of warm-type structure are present: the frontal band related to the warm front seems to reach the ground while the upward cold frontal band intersects the warm aloft. The temperature advection field doesn't offer in this case any hint for the determination of the occlusion type.

Also the temperature advection field at 850 hPa (fig. 5.15) shows that on either side of the occluded front the temperature advection has about the same intensity and thus does not offer any support to the warm-type nature of the occlusion.

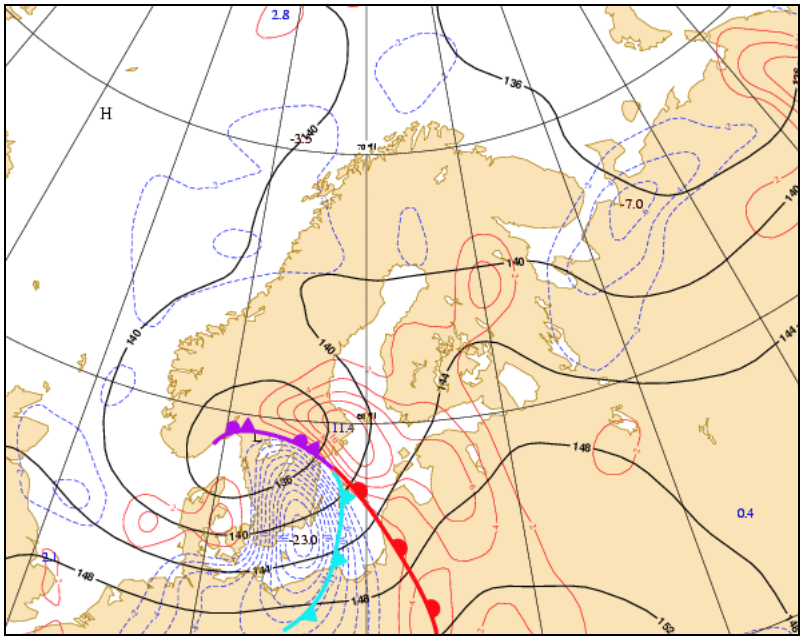

Figure 5.15. 850 hPa Geopotential height (solid black lines every 4 dam) and temperature advection field at 06 UTC of 09.06.2003; red solid lines: warm advection, blue dashed lines: cold advection; temperature advection contoured every 2 x 10^{-4} K s^{-1}. Subjective frontal analysis superimposed.

The location of the triple point can be estimated with the help of the jet stream. Also, the temperatures and dew points within the warm sector are clearly higher than elsewhere. In this case both factors lead to the same conclusion, supporting the FMI rules.

A look at the surface temperature distribution on both sides of the occluded front at 06 and 12 UTC (fig. 5.16) reveals minimal differences, even when differential heating factors and land-sea distribution are taken into account: the air mass seems to be slightly warmer on the rear side, in accordance to the warm-type nature of the occlusion previously stated by means of the upper tropospheric structure.

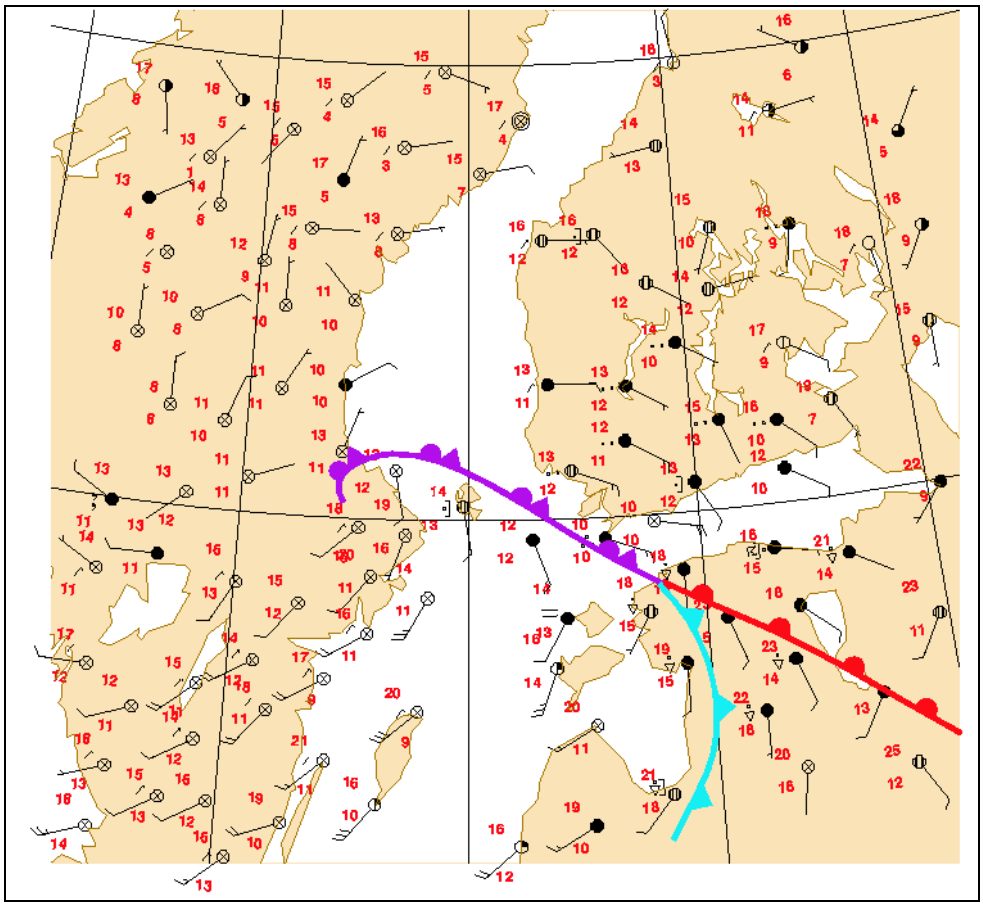

Figure 5.16. Synop observations at 12 UTC of 9.6.2003 and surface frontal analysis. Each synop observation include only temperature and dew point temperature, current weather symbol, wind barb (m/s), total cloudiness fraction.

The temperature advection field computed on the 850 hPa pressure level at 12 UTC shows this time a structure closer to the warm-type occlusion: along the whole occluded front warm advection on its fore side is more intense than cold advection on the rear side (fig. 5.17).

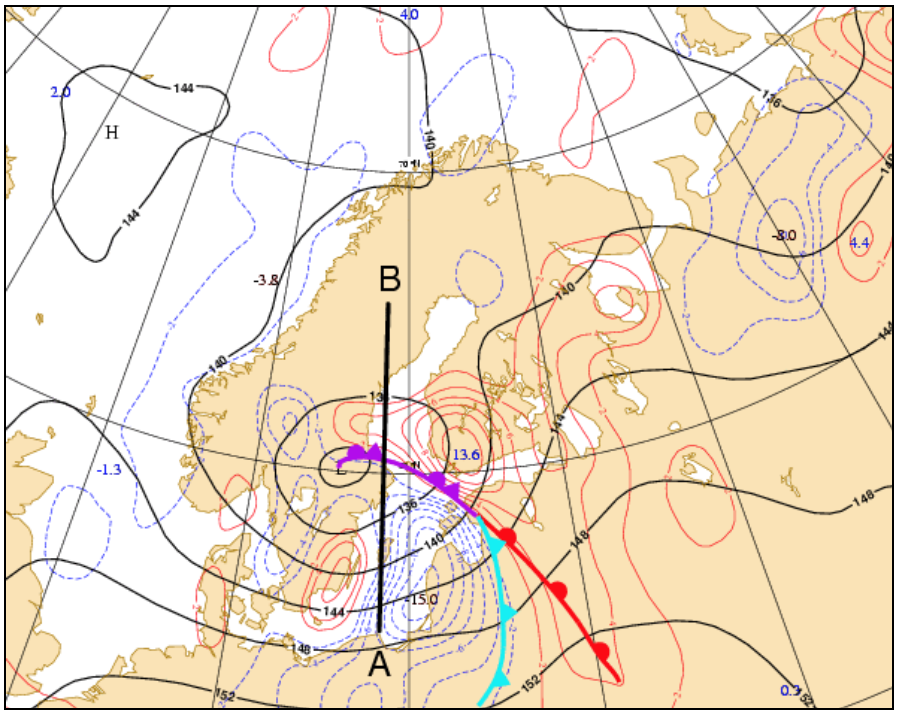

Figure 5.17. Temperature advection at 850 hPa: red lines: warm advection, blue dashed lines: cold advection (contoured every 2 x 10^{-4} K s^{-1}) and geopotential height at the same level every 4 dam (solid black lines) at 12 UTC of 9.6.2003; frontal subjective analysis and cross section axis AB are superimposed.

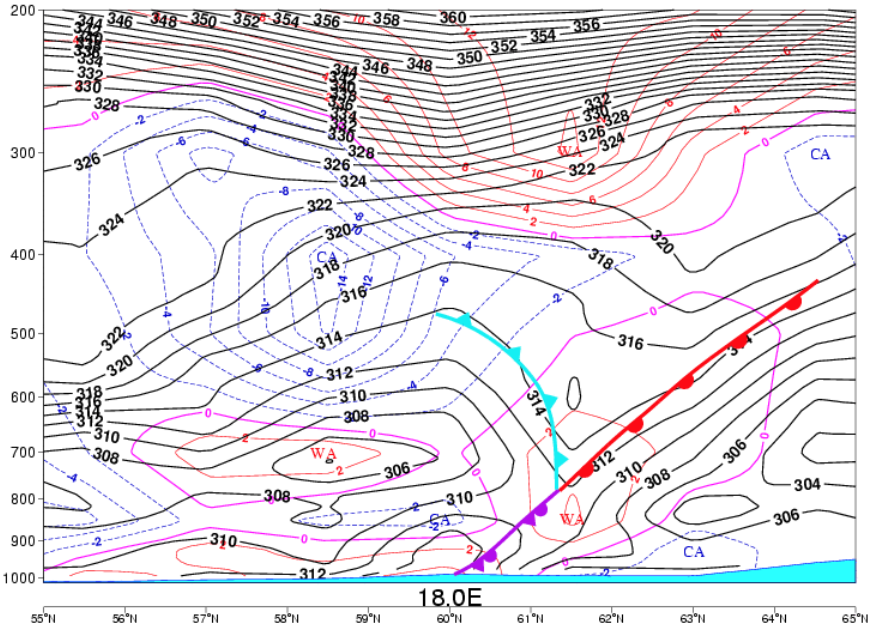

Figure 5.18. Vertical cross section (left and right extreme respectively A and B of the axis in figure 5.15) of equivalent potential temperature (K) and temperature advection; red lines: warm advection, blue dashed lines: cold advection, violet line: advection=0, (contoured every 2 x 10^{-4} K s^{-1})

Also the cross section taken across the occluded front at 12 UTC (fig. 5.18) exhibits features very close to the ideal structure depicted in the FMI guidelines, as demonstrated by the subjective frontal analysis superimposed. Immediately behind the

occluded front the air mass is unstable (the value of equivalent isentropes decreases with height): this feature affects the shape of the isentropes in such a way that it is difficult to exactly identify the position of the occluded front on the surface.

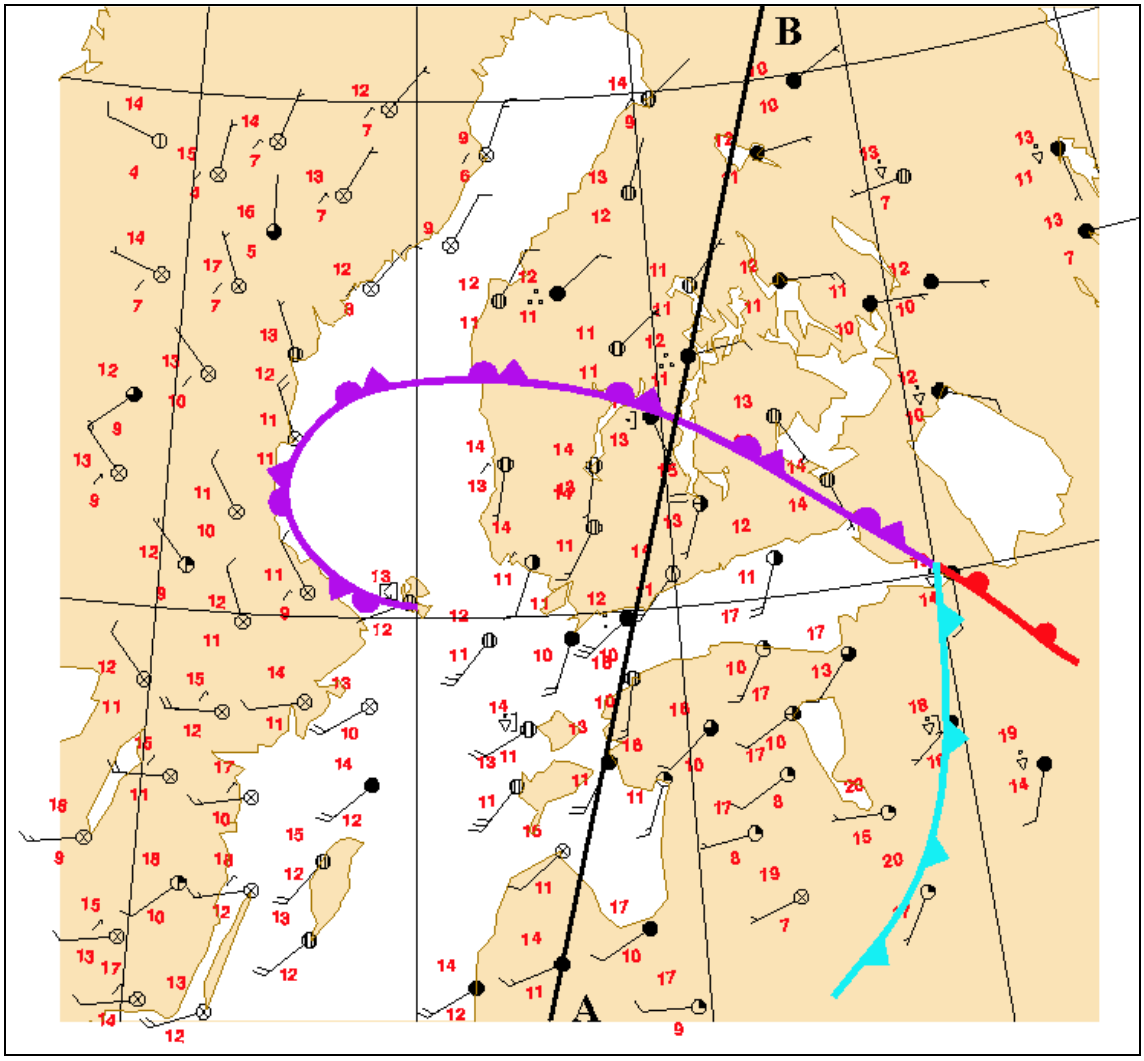

Figure 5.19. Synop weather observations at 18 UTC of 09.06.2003 over Southern Finland. The classical surface subjective frontal analysis is carried out on the basis of upper air numerical analysis and surface synop-observations. Line AB refers to the axis of vertical cross section in figure 5.19. Each synop observation include only temperature and dew point temperature, current weather symbol, wind barb (m/s), total cloudiness fraction.

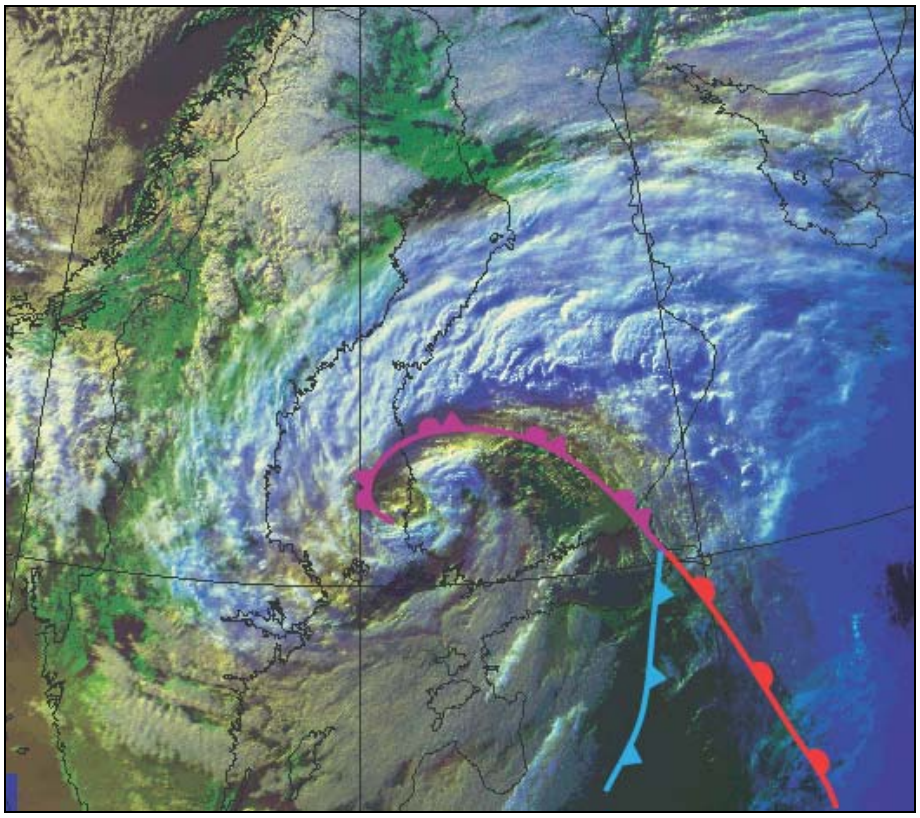

Figure 5.20. Noaa satellite RGB composite image (channels 1, 2 and 4) at 18.45 UTC of 09.06.2003. The frontal analysis performed at 18 UTC (fig. 5.19) is superimposed.

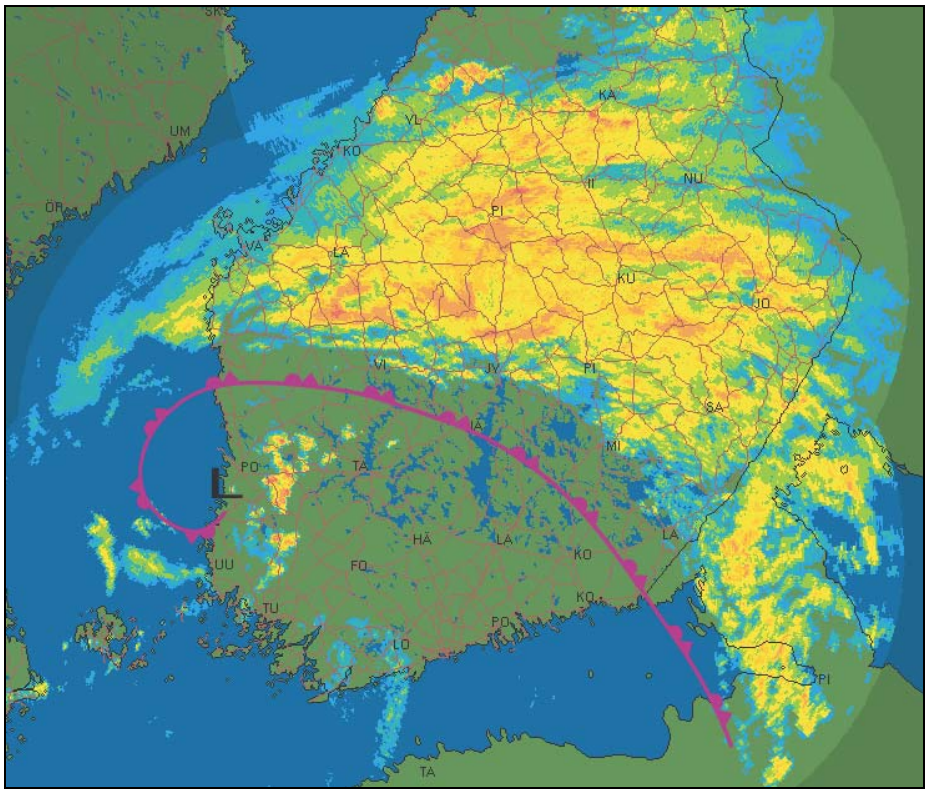

Figure 5.21. Doppler weather radar image at 18 UTC of 09.06.2003 over southern Finland. The frontal analysis performed at 18 UTC (fig. 5.19) is superimposed.

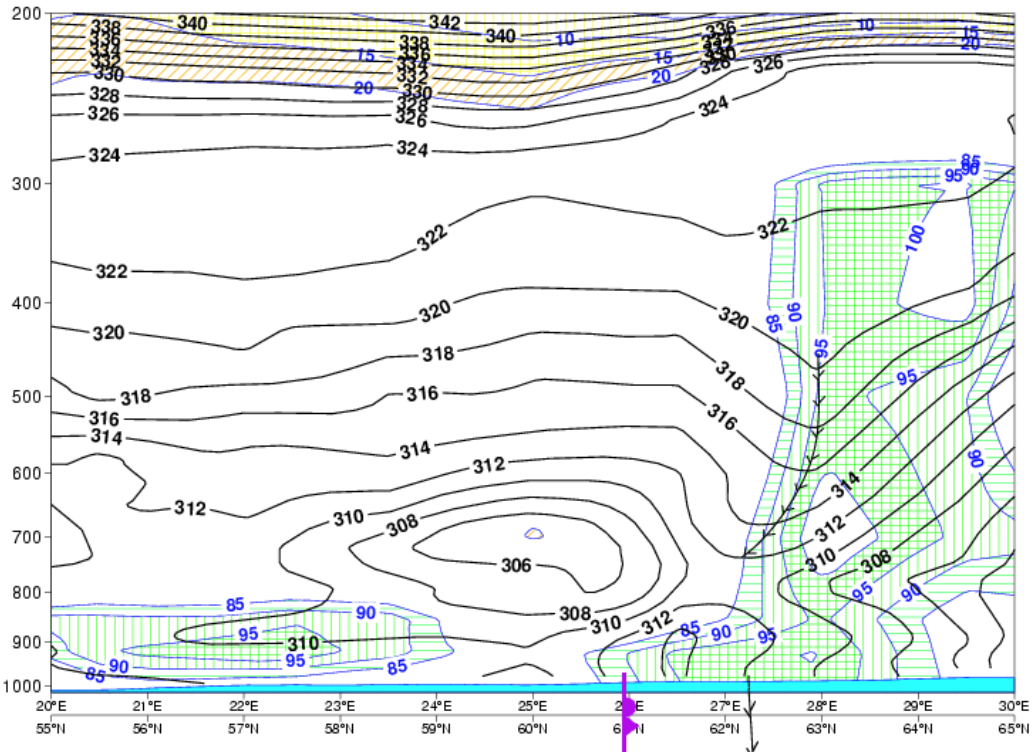

Figure 5.22. Vertical cross section at 18 UTC of 09.06.2003. Equivalent potential temperature every 2 K (solid black lines) and relative humidity every 5 percentage unit below and above 20 and 85 unit, respectively (thin blue solid lines). The trough line in the cross section is placed along the axis of locally smallest isentropic values. The occlusion sign is placed across the coordinate axis in the position inferred from the weather chart of figure 5.19, while the trough sign represents the projection on the surface of the rear side of the rainfall area inferred both from the humidity distribution and from the radar image of figure 5.21.

At 18 UTC the occlusion process continues keeping its classical features. An interesting insight into its structure comes out when comparing surface analysis, cross sections, satellite and radar imagery with each other. The forward inclination of the occluded front has shown up already in the cross sections made in earlier instances, but the combination of these different images brings up this feature in an extremely noticeable manner.

In figures 5.20 and 5.21 there are the satellite image at 18.45 UTC and the radar image at 18 UTC, respectively. In both images the surface occluded front analyzed on the basis of the numerical fields and the wind cyclonic shear on the surface weather chart at 18 UTC (fig. 5.19) is superimposed. The occluded front on the surface lies about 50-60 km from the rear edge of the rainfall and nimbostratus cloud area.

In figure 5.22 the cross section taken across the axis AB shown in fig. 5.19 offers an alternative perspective into this feature: again the surface occluded front lies far behind the rear edge of the rainfall area, represented by a trough sign across the coordinate axis.

Moreover the axis of the isentropic trough aloft, i.e. the trowal, is located exactly on the rear side of the humidity zone corresponding to the highest values (95% or more), which we can consider to be related to the thick nimbostratus cloud yielding the precipitation shown in the radar picture of figure 5.21.
This is a typical characteristic of the classical warm occluded front which represents a central point in the trowal model introduced by Canadian scientists in the second half of the last century and still used nowadays in operation.

5.2 Classical perfect cold type occlusion process: Northern Atlantic 3.-6.1.2003

The cyclone in question has developed over Northern Atlantic during 3-6 January 2003 in a classical manner leading to an occlusion classified as perfect cold-type. Looking at numerical fields at constant pressure levels and vertical cross sections, this development matches exactly with the features described in the FMI rules concerning cold-type occlusions, at least starting from the post-mature stage as it will be shown in the following.

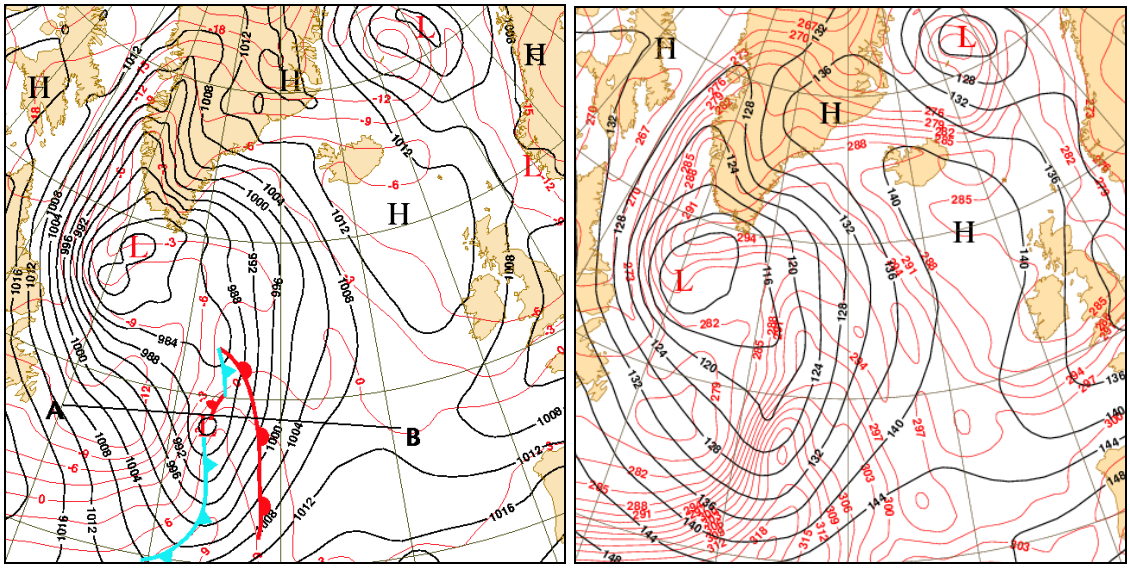

Figure 5.23. Numerical analysis fields at 18 UTC of 03.01.2003. Left: MSLP every 4 hPa (solid black lines) and 850 hPa temperature every 2 K (red thin lines); axis AB of vertical cross section shown in figure 5.25 and surface frontal analysis superimposed. Right: 850n hPa geopotential height every 4 dam (solid black lines) and equivalent potential temperature every 2 K (red thin lines).

The cyclone development can be inspected by means of surface pressure, 850 hPa temperature and 300 hPa isotaches.

At 18 UTC of 3.1.2003 the jet streak begins to break up into two branches according to the cold type occlusion scheme (fig. 5.24, left)

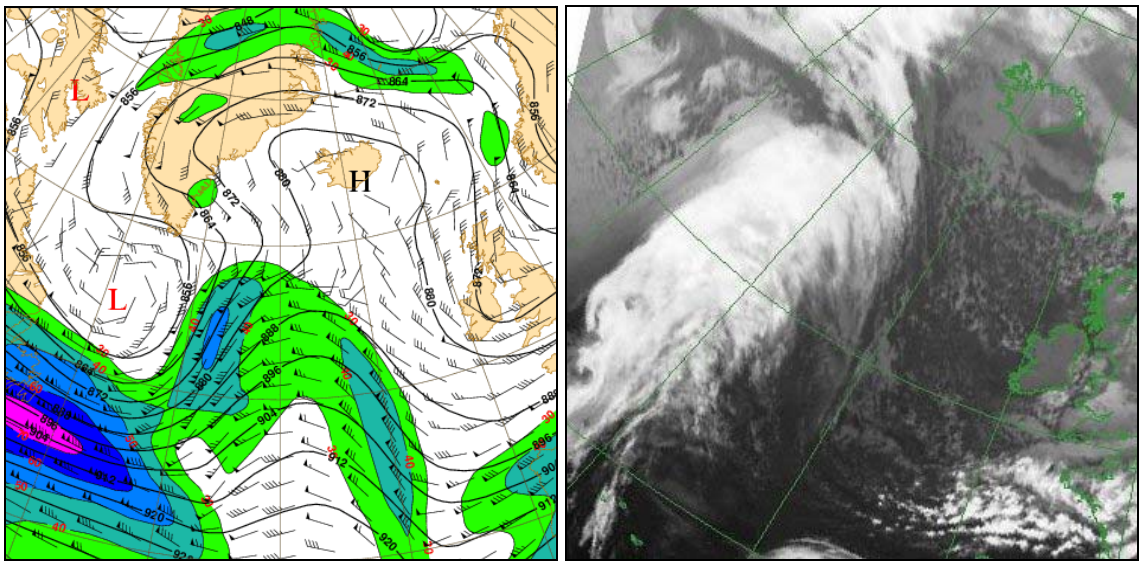

Figure 5.24. Left: 300 hPa isotaches (colored starting from 30 m/s at interval of 10 m/s), geopotential height (solid black lines) contoured every 8 dam and wind vector barbs in knots at 18 UTC of 03.01.2003. Right: Meteosat 7 IR image at same instant as left side fields.

At 18 UTC no occlusion process has yet occurred: the temperature and equivalent potential temperature fields at 850 hPa (left and right side of figure 5.23) show an open warm sector whose apex is located over the surface low pressure; in fact there is also a small wave which will rapidly die out. The cloud mass is characterized by an elongated distribution (fig. 5.24, right), which may lead to misleading interpretations, namely an occlusion process already begun. Vertical cross sections support pressure level fields, like the one shown in figure 5.25: it shows very nicely the presence of separate cold and warm front reaching the surface and the shrinking warm sector, thus identifying a cyclone still in its mature stage and very close to the post-mature phase.

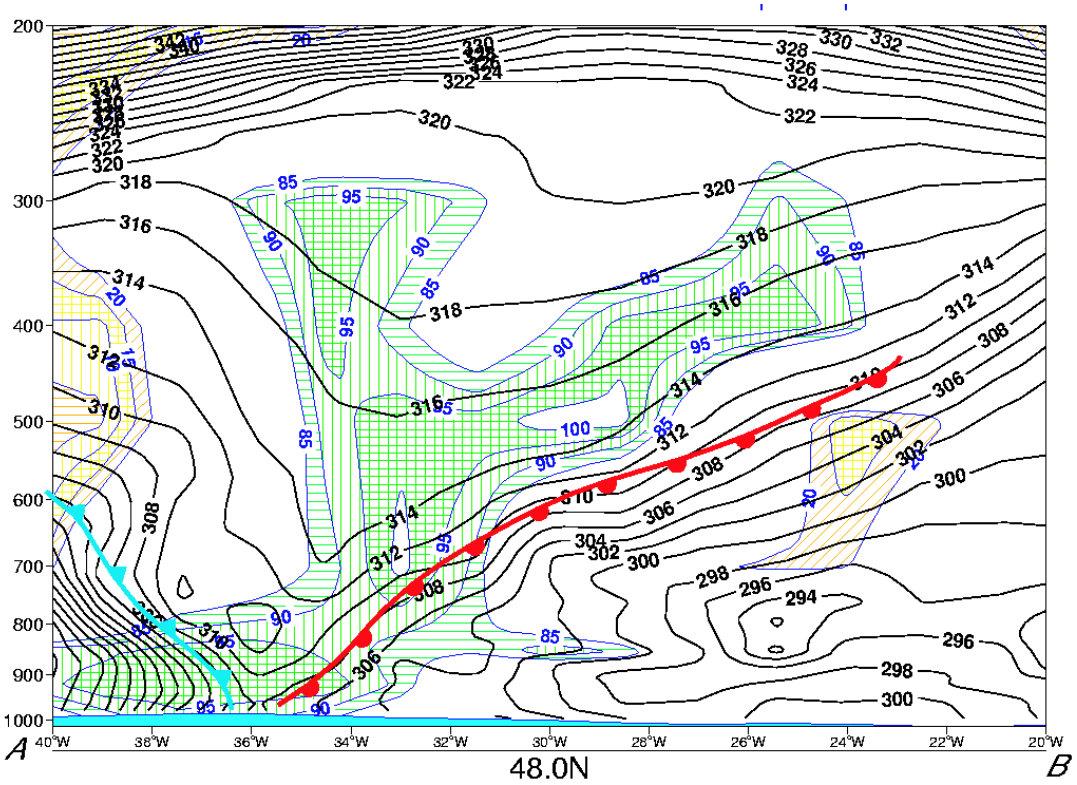

Figure 5.25. Vertical cross section of equivalent potential temperature and relative humidity across the axis AB of figure 5.23(left) at 18 UTC of 03.01.2003. Equivalent potential temperature contoured every 2 K (solid black lines) and relative humidity every 5 percentage unit below and above 20 and 85 unit, respectively (thin blue solid lines).

After 6 hours, at 00 UTC of January 4th, the cyclone has rapidly developed further and the occlusion has process begun. The warm air tongue is very narrow, which makes it difficult to determine the triple point: vertical cross sections are the only available tool for it. Cross sections taken at this time show that the occlusion process has already occurred around latitude 52-53N; south of this latitude there is no sign of occlusion, because in vertical cross sections both fronts reach the surface. Figure 5.26 shows the cross section which intersects the cyclone at about latitude 48 N (axis AB in fig. 5.27): the detached cold and warm frontal bands are well discernible, supporting the existence of warm sector still over the surface.

Figure 5.27 shows the subjective frontal analysis carried out on the basis of the earlier argumentations.

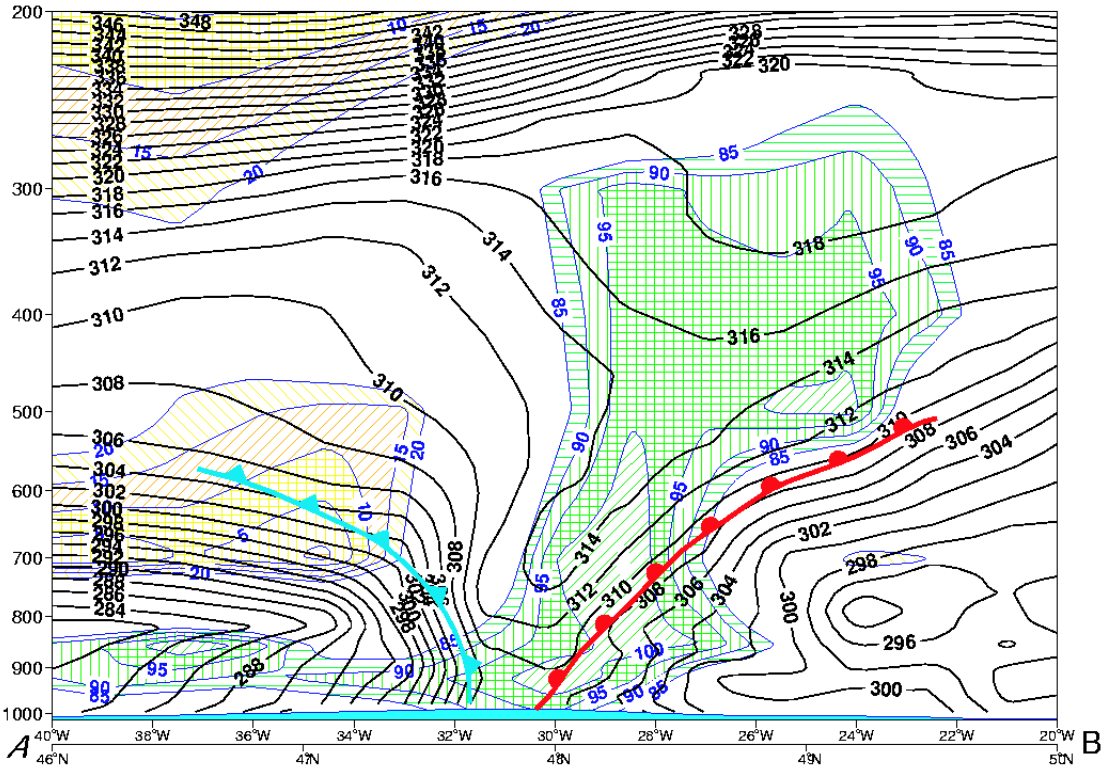

Figure 5.26. Vertical cross section (axis AB shown in figure 5.25) trough the warm sector of the cyclone at 00 UTC of 04.01.2003. Equivalent potential temperature contoured every 2 K (solid black lines) and relative humidity every 5 percentage unit below and above 20 and 85 unit, respectively (thin blue solid lines).

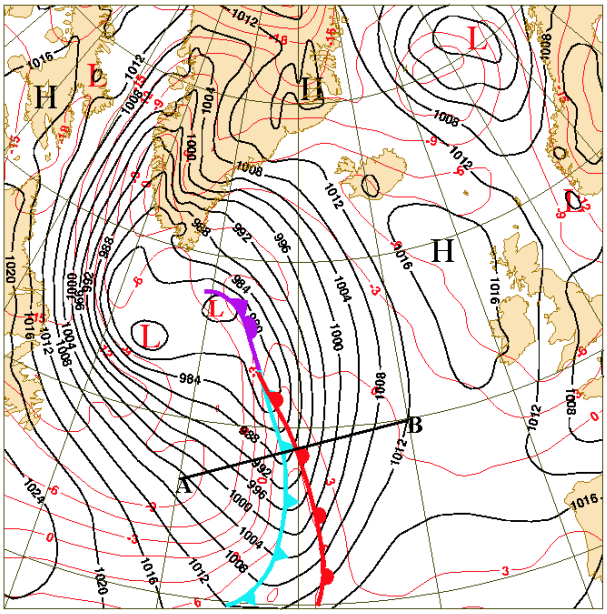

Figure 5.27. Frontal subjective analysis of the cyclone over north Atlantic at 00 UTC of 4.1.2003. Solid black lines for MSLP contoured every 4 hPa and thin red lines for 850 hPa temperature contoured every 2 K.

At 06 UTC the temperature advection fields clearly show predominant cold advection in the rear part of the occluded front (fig. 5.28, left side), giving an additional support to

the cold type structure of the occlusion. The jet streak follows the occluded front along its rear side (fig. 5.28, right) and potential temperature fields at different pressure levels reveal a sharp warm air tongue, whose axis of maximum values at 700 hPa (fig. 5.29, left) is correlated with the rear edge of the cloud distribution shown by the correspondent satellite image in figure 5.29(right).

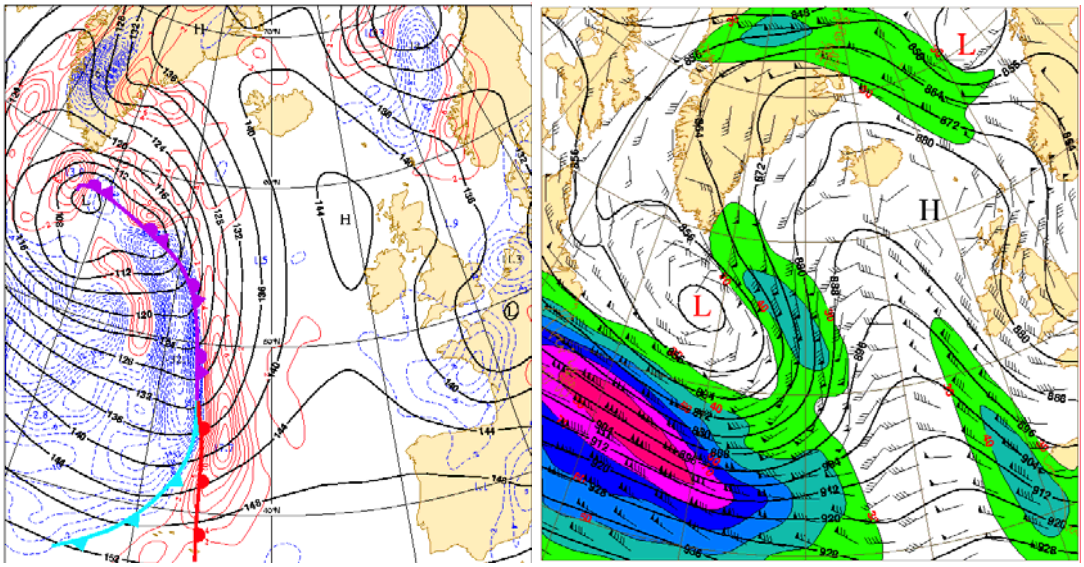

Figure 5.28. Left: temperature advection field and geopotential height at 850 hPa with surface frontal analysis superimposed at 06 UTC of 4.1.2003. Solid black lines for geopotential height contoured every 4 dam and thin lines for temperature advection (red thin for warm and blue thin dashed for cold) contoured every 2 x 10^{-4} K s^{-1}. Right: 300 hPa isotaches (colored starting from 30 m/s at interval of 10 m/s), geopotential height (solid black lines) contoured every 8 dam and wind vector barbs in knots, for the same instant as in left side.

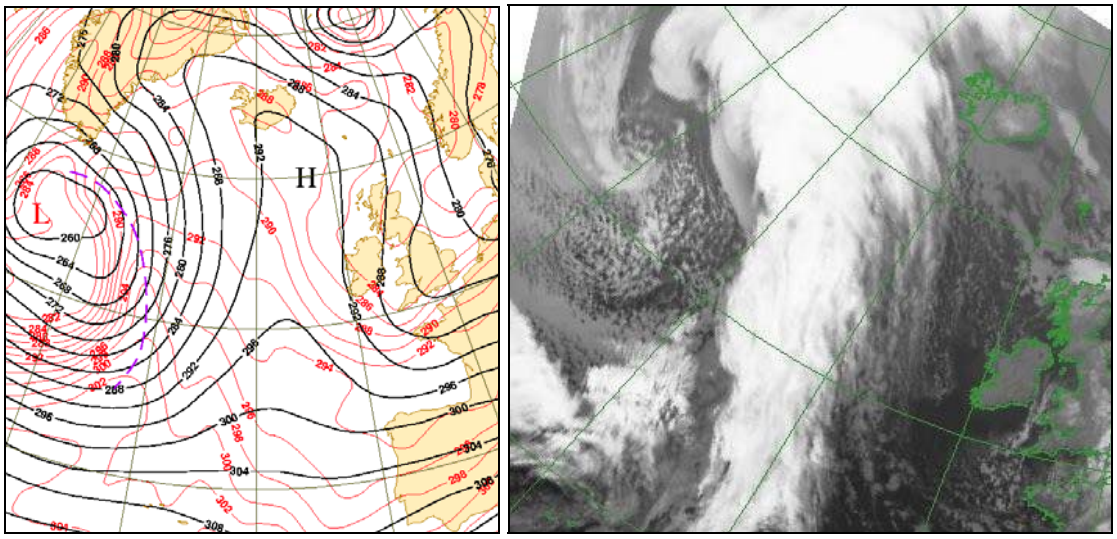

Figure 5.29. Left: 700 hPa geopotential height (solid black lines) contoured every 4 dam and potential temperature (red thin lines) contoured every 2 K at 06 UTC of 04.01.2003; violet dashed line represent the axis of highest values of potential temperature. Right: Meteosat 7 IR image at 06 UTC of 04.01.2003.

At 12 UTC several cross sections have been made, both for potential and equivalent potential temperature, in order to get an insight into the vertical structure of the cyclone, in particular of its occluded part (axes shown in figure 5.30).

The cross sections performed across the northernmost segment of the occluded front show features which match with the classical model, as can be observed from the cross section AA' and BB' (axes in figure 5.30) in figures 5.31 and 5.32, respectively. Both the cold and the warm front are well recognizable from the isentropes: the cold front reaches the surface, while the warm front is detached aloft, pushed up by the cold front and intersecting it at about 800-850 hPa. Very intense cold advection is present behind the cold and the occluded fronts, with frontal structures well developed up to the tropopause.

The cross section DD' carried out across the warm sector (fig. 5.33) shows the cold and warm front reaching the surface, apart; the vertical extension of the frontal bands is in this case confined to a more shallow layer than in the northern part of the cyclone.

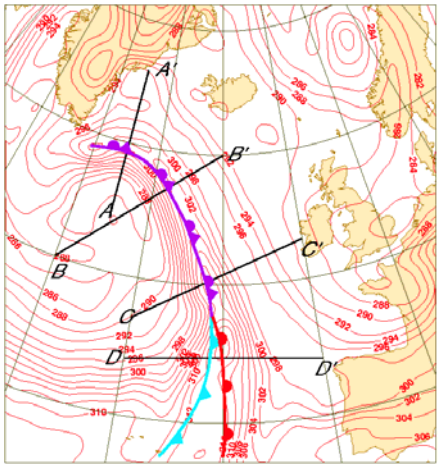

Fig. 5.30. Red: equivalent potential temperature at 700 hPa contoured every 2 K. Axis of the vertical cross section carried out across the occluded cyclone at 12 UTC of 4.1.2003. Axis AA' , BB' and DD' refer to cross sections shown in figures 5.31 (and 5.34), 5.32 (and 5.35) and 5.33, respectively.

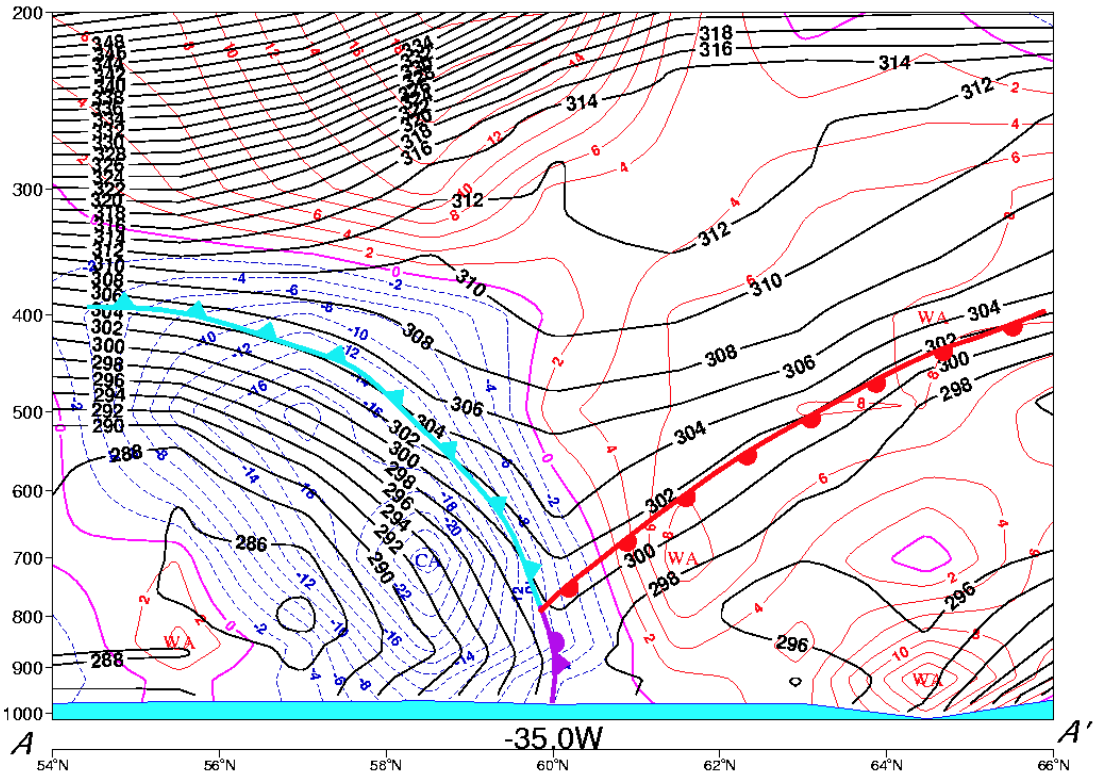

Figure 5.31. Cross section (axis AA' in fig. 5.30) at 12 UTC of 4.1.2003. Solid black lines: isentropes (K); dashed blue lines: cold advection, red solid lines: warm advection and solid violet lines: value 0, contoured every 2 x 10^{-4} K s^{-1}. Frontal subjective analysis superimposed.

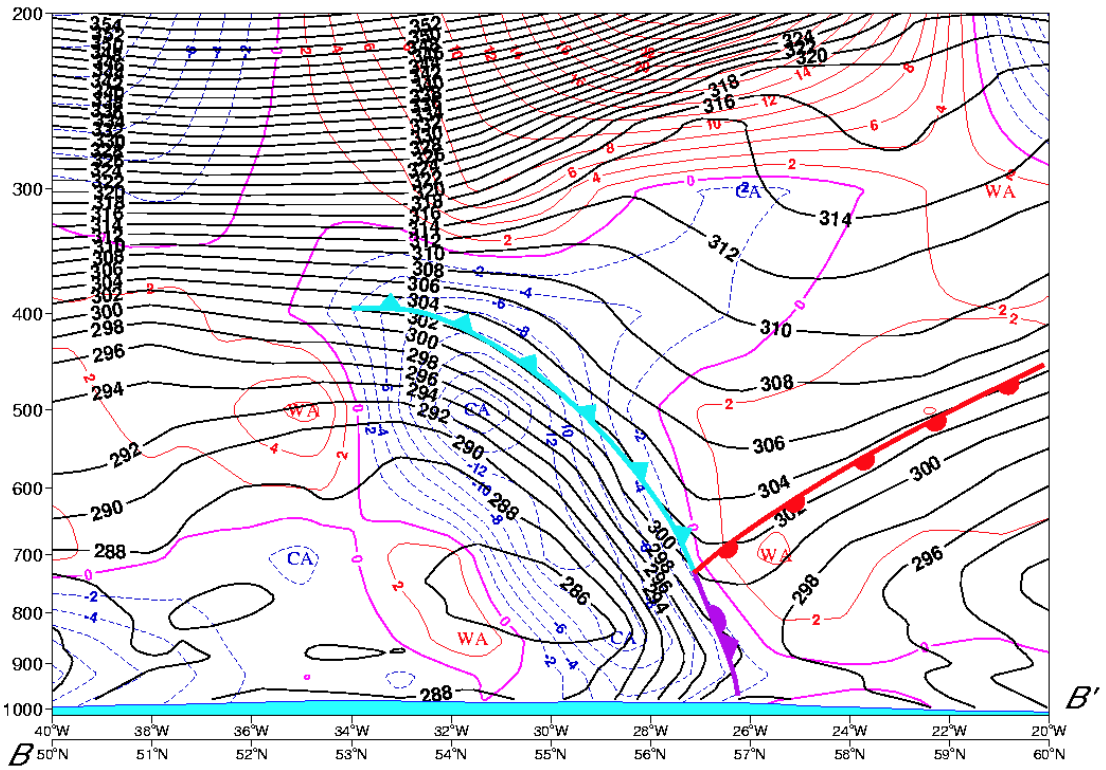

Figure 5.32. Cross section (axis BB' in fig. 5.30) at 12 UTC of 4.1.2003. Solid black lines: isentropes (K); dashed blue lines: cold advection, red solid lines: warm advection and solid violet lines: value 0, contoured every 2 x 10^{-4} K s^{-1}. Frontal subjective analysis superimposed.

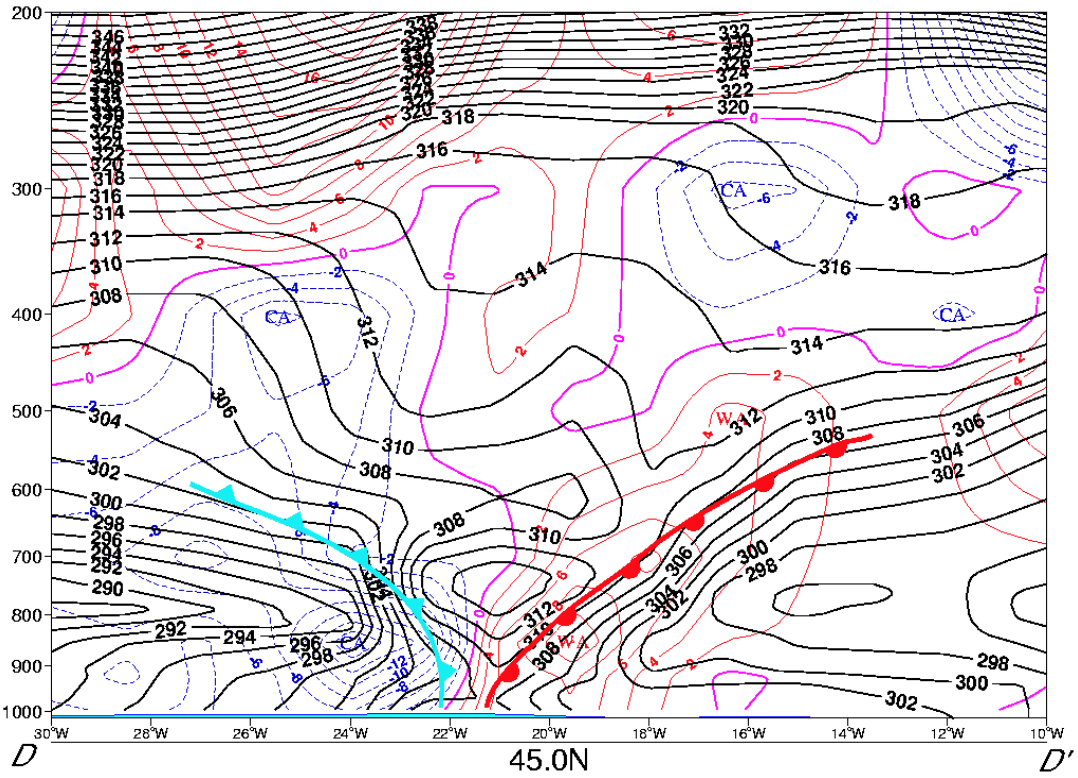

Figure 5.33. Cross section (axis DD' in fig. 5.30) at 12 UTC of 4.1.2003. Solid black lines: isentropes (K); dashed blue lines: cold advection, red solid lines: warm advection and solid violet lines: value 0, contoured every 2 x 10^{-4} K s^{-1}. Frontal subjective analysis superimposed.

Cross sections of potential temperature at the same time don't offer such good insights: the frontal structures are not clearly discernible, even if a clear warm air trough aloft is observed. From the cross section with equivalent potential temperatures it is possible to verify the static stability rule proposed by Stoelinga et al. (2002). According to the static stability rule the occlusion type is cold: a qualitative investigation of the static stability on both sides of the occluded front in cross sections AA' and BB', shown in figures 5.32 and 5.33, show slightly higher values on the cold side of the front, therefore supporting its backward slope, typical of a cold occlusion.

The surface temperature distribution, despite the fact that observations are very sparse, does not show remarkable differences between the two sides of the front: only in the northernmost part of the occluded front slightly colder values are observed in the rear part of the front. The fact that surface temperature and humidity values don't exhibit major differences is likely to be ascribed to the presence of the ocean surface, whose influence tries to equalize the differences of these parameters.

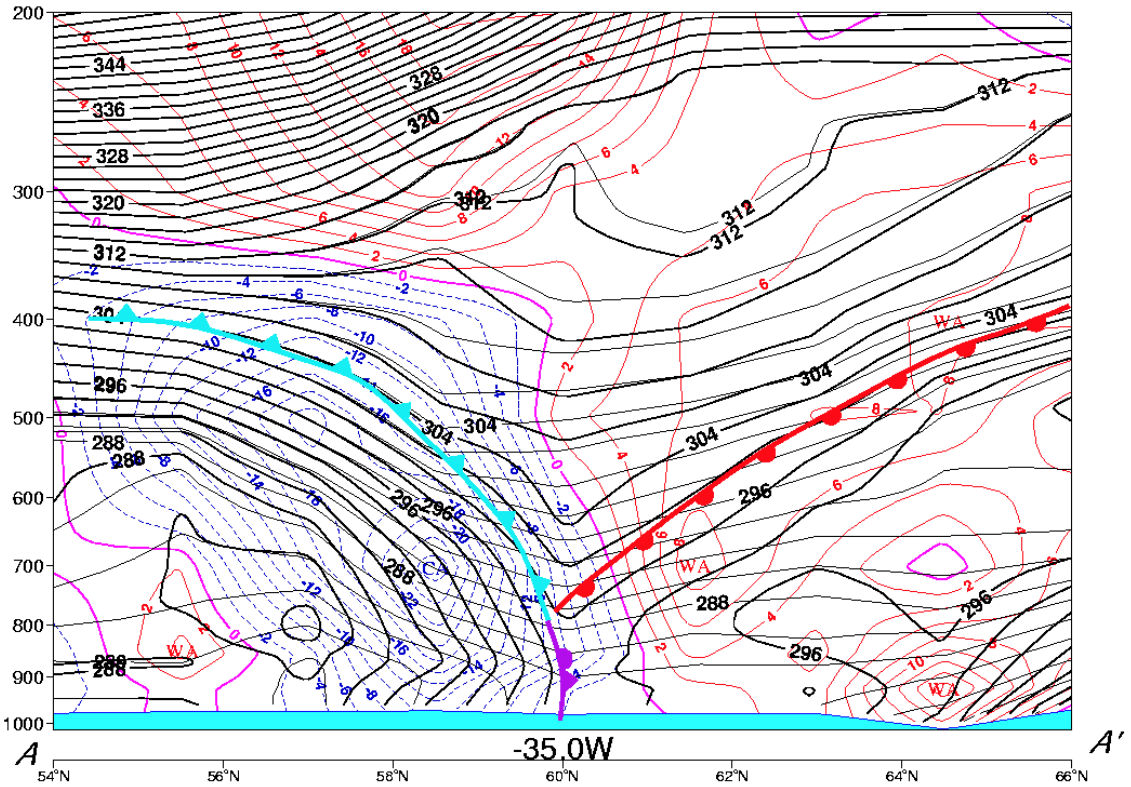

Figure 5.34. Cross section (axis AA' in fig. 5.30) at 12 UTC of 4.1.2003. Solid black lines: isentropes (K); thin black lines: potential temperature (K); dashed blue lines: cold advection, red solid lines: warm advection and solid violet lines: value 0, contoured every 2 x 10^{-4} K s^{-1}. Frontal subjective analysis superimposed. Note the higher vertical resolution of the isentropes in the rear part of the occluded front with respect to its fore side.

After 00 UTC of January 5th the occluded front, while moving eastward slowly due to the high pressure over British Isles, approaches another thermal band (a previous old dissipating occluded front) situated west of Great Britain. Due to the interaction with this dissipating occlusion, modifications occur in its thermal structure: the temperature and equivalent potential temperature gradient on both sides of the front is now about the same (respectively left and right hand side of fig. 5.36), whereas earlier it was more intense on the cold side.

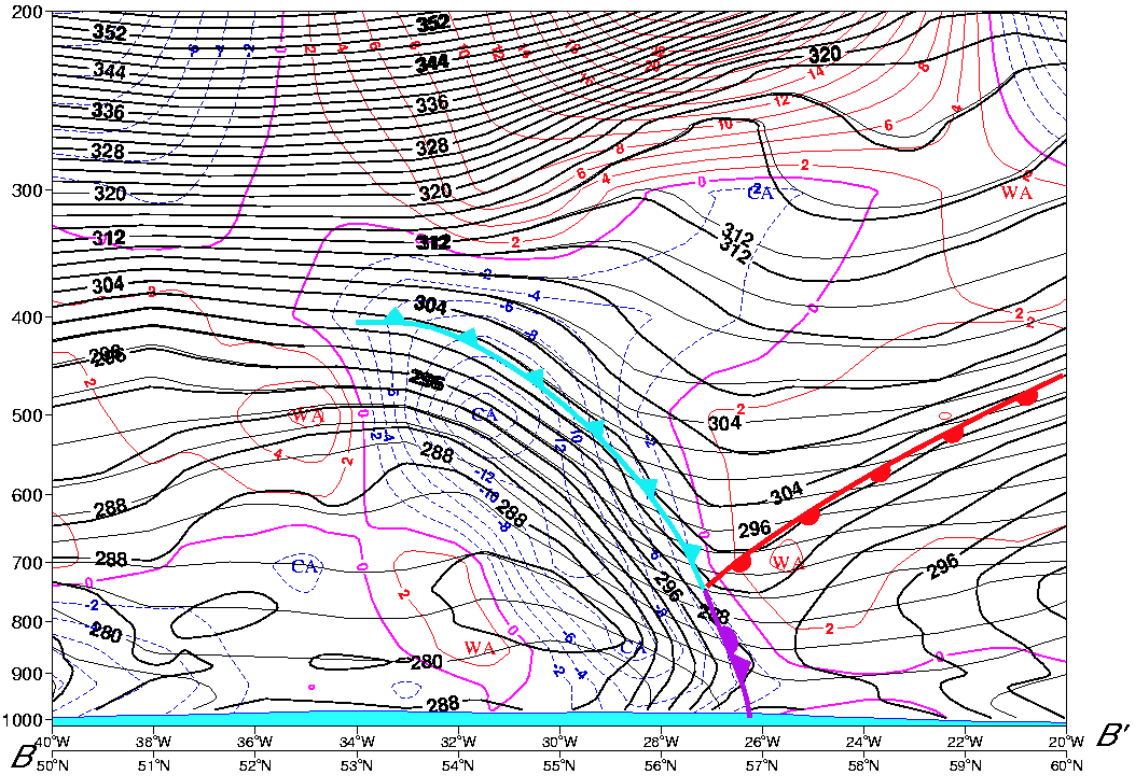

Figure 5.35. Similar cross section as in figure 5.34 but across axis BB' of fig. 5.30. Same consideration as for 5.34 are valid.

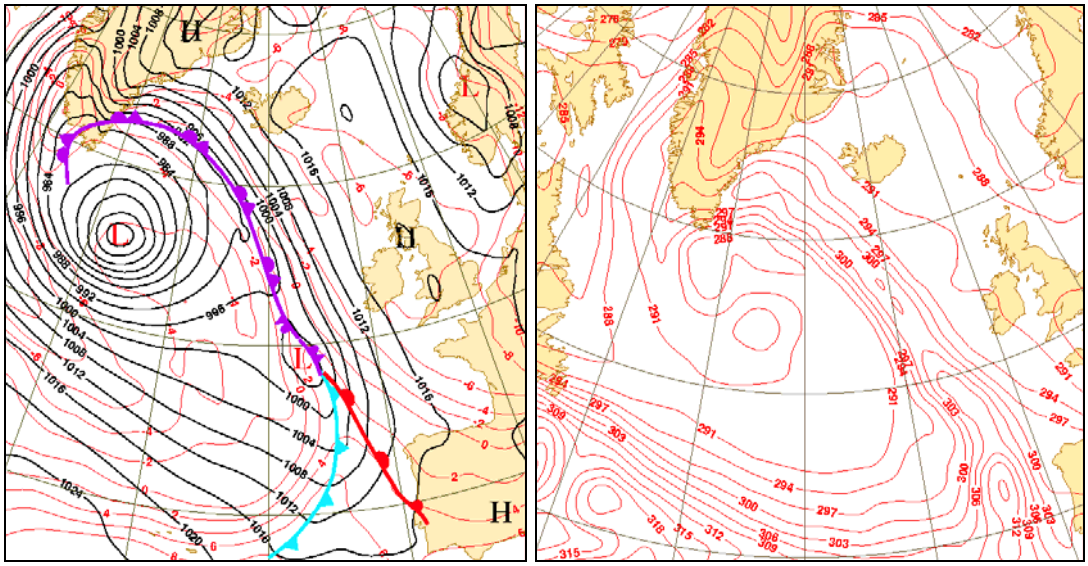

Figure 5.36. Numerical fields at 00 UTC of 05.01.2003. Left: MSLP every 4 hPa (black solid lines), 850 hPa temperature every 2 K (red thin lines) and surface frontal analysis. Right: 700 hPa equivalent potential temperature every 2 K (red thin lines).

The warm air ridge feature is well recognizable in thetae fields (850, 700 and 500 hPa) but in temperature fields it begins to be less sharp, as can be verified comparing the two fields in figure 5.36.

5.3 Non-classical development

5.3.1 Low pressure development over Mediterranean Sea 24.-25.1.2003

The low pressure development examined here occurred over central part of Mediterranean basin during the time interval 23-25.01.2003.

This development has been analyzed as occlusion in many sources, as shown in figure 5.37. Despite the general agreement among these interpretations, this development has been classified as non classical, because of its anomaly when compared to the structure of the occlusion described in the FMI guidelines. The main deviations from the classical model are:

- absence of a well recognizable warm air tongue in 850 hPa temperature
- jet stream cutting over the warm sector
- not recognizable pattern of development, i.e. no cold front catching up with the warm front and no presence of a clear warm sector shrinking and detaching upwards off the surface.

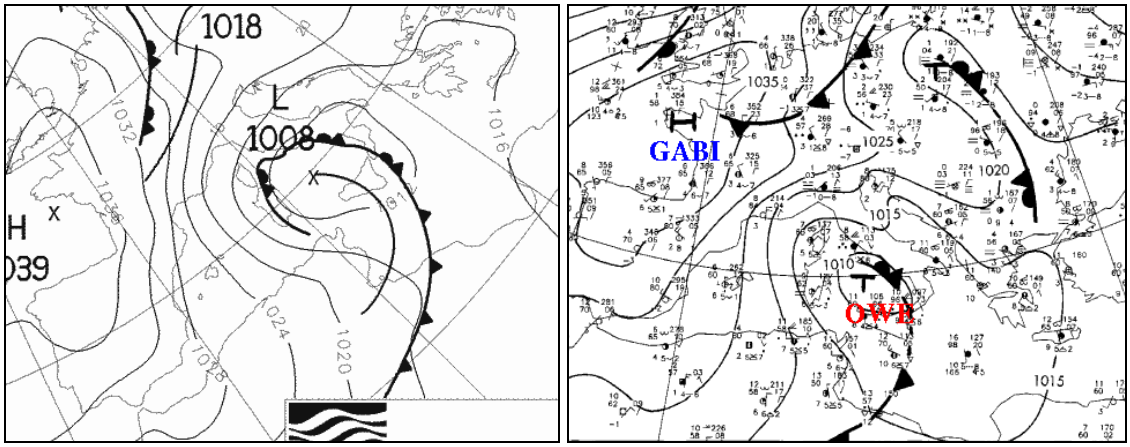

Figure 5.37. Frontal subjective analysis of the post-mature cyclone over Italian peninsula at 00 UTC of 24.1.2003 from Bracknell (left) and DWD (Deutscher Wetterdienst, right); black lines: MSLP (hPa).

After having a look at the initial stages of the development around the middle of the day 23.01.2003, we come up with the difficulty of matching low troposphere temperature gradients and upper level jet stream at 300 hPa. At 700 hPa the equivalent potential temperature field shows two main gradients, one north of the jet stream, over

Tyrrhenian Sea, and the other south of it over Northern Africa (fig. 5.38). Other fields, e.g. temperature and potential temperature, do not offer better insights into this initial phase of the development. Cloud distribution is diffuse over a large area and in principle it could match with the presence of two different frontal systems (fig. 5.39, left).

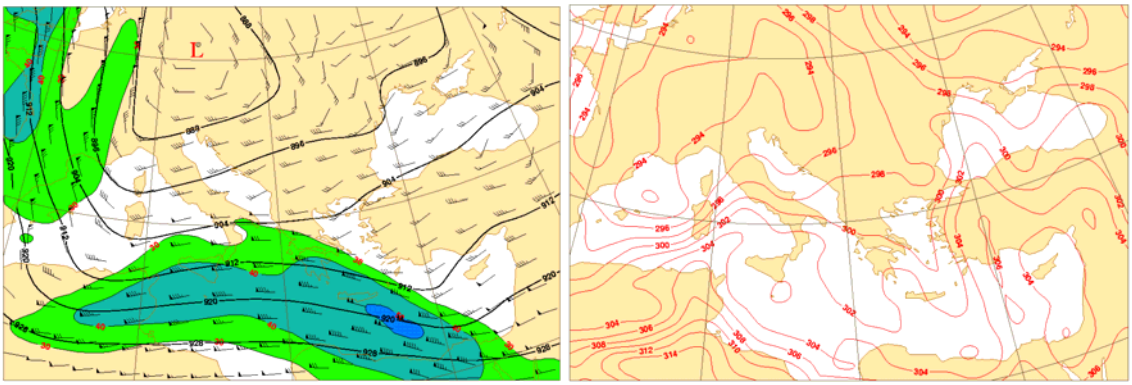

Figure 5.38. Left: 300 hPa isotaches (colored starting from 30 m/s at interval of 10 m/s), geopotential height (solid black lines) contoured every 8 dam and wind vector barbs in knots at 12 UTC of 23.01.2003. Right: 700 hPa equivalent potential temperature at the same instant contoured every 2 K.

At 18 UTC two detached structures can be still recognized, both on basis of the 700 hPa equivalent potential temperature field and the cloud distribution observed from satellite imagery (fig. 5.39, right). A comment should be made at this stage of the development: already at 12 UTC over Northern Italy there is convective cloudiness, separate from the frontal cloudiness over Central Italy. By 15 UTC the two cloud systems get closer; synop observations from the same time show the presence of heavy thunderstorms related to the northernmost convective system. At 18 UTC it is not anymore possible to distinguish the two cloud masses with the result that at a first glance the cloud's spiral-like shape reminds that of an occlusion (fig. 5.39, right), which indeed has not yet occurred by this time.

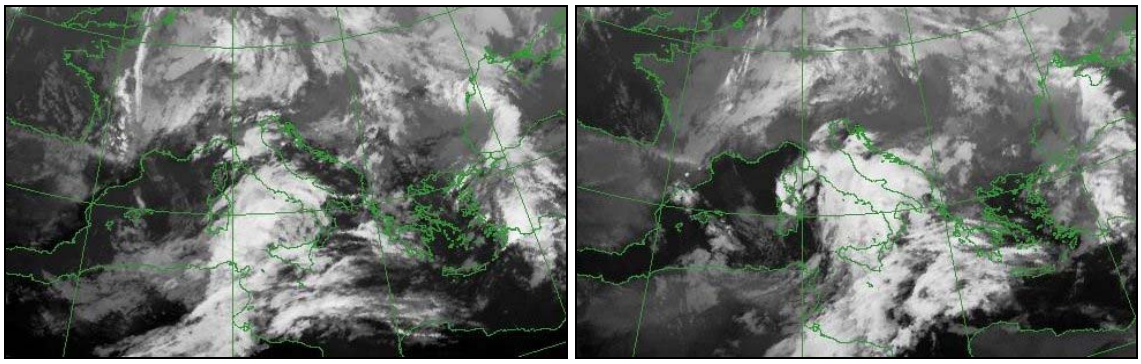

Figure 5.39. Meteosat 7 IR images at 12 UTC (left) and 18 UTC of 23.01.2003.

None of the cross sections carried out at 18 UTC supports an occlusion. The temperature advection fields at 700 and 850 hPa show a remarkable cold advection maximum over Tunisia, but there are no signs of a double system, i.e. two distinct cold advection maxima.

Still the presence of two detached frontal bands, one north and the other south of the 300 hPa jet stream, which are going to merge into one frontal system by 00 UTC of 24.01.2003, seems to be the most plausible interpretation.

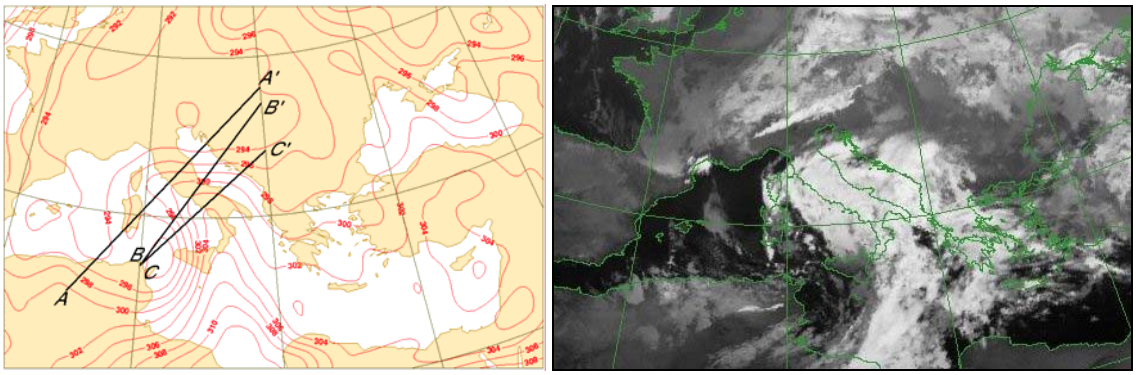

Figure 5.40. Left: 700 hPa equivalent potential temperature contoured every 2 K at 00 UTC of 24.01.2003 and vertical cross section axes. Right: Meteosat 7 IR (10.8µm) image at same instant as in left side.

Only at 00 UTC of 24.01.2003 the cloud distribution leads to a more regular pattern: the cloud distribution is now uniform (fig. 5.40, right) and also the two frontal structures have merged together, at least at lower level, yielding a well developed isentropic ridge as shown in figure 5.40(left). By this time the occlusion process has not clearly begun: the uncertainness is due to the anomaly of the process, which likely involves two different frontal structures.

Cross sections show clearly the presence of a warm sector (fig. 5.41, right), just over

southeast part of Tyrrhenian basin, in good accordance with the surface observations. On the other hand the cross section perpendicular to the northernmost segment of the axis of maximum values of the isentropes shows hints yielding a neutral-type occlusion structure (fig. 5.41, left).

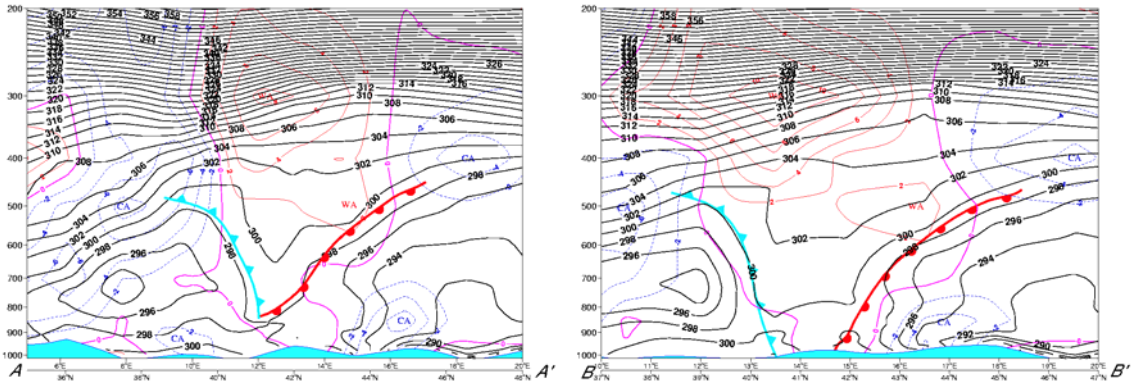

Figure 5.41. Vertical cross sections at 00 UTC of 24.01.2003. Left cross section across axis AA' and right cross axis BB' respectively as in figure 5.40(left). Solid black lines: isentropes (K); dashed blue lines: cold advection, red solid lines: warm advection and solid violet lines: value 0, contoured every 2 x 10^{-4} K s^{-1}. Frontal subjective analysis superimposed.

At 06 UTC the system exhibits a sharp warm air tongue in all temperature and potential temperature fields at several levels (fig. 5.42, upper right and lower left). The axis of the highest values of equivalent potential temperature across the warm tongue correlates exactly with the rear edge of the cloud and precipitation distributions, as shown in figure 5.43 where the axis at 700 hPa is drawn on the satellite image at 06 UTC. The occlusion process, meaning here as the formation of a well defined warm air tongue or isentropic ridge at low and middle levels, can be considered already having been begun, even if no classical frontal catch up has occurred. In figure 5.42 (upper left) a classical frontal analysis has been sketched on the basis of the surface observations and 850 hPa isentropes, despite the fact that the cyclone development does not follow a classical pattern. Also the jet stream position is not according the FMI guidelines but instead it cuts over the warm sector (fig. 5.42, lower right).

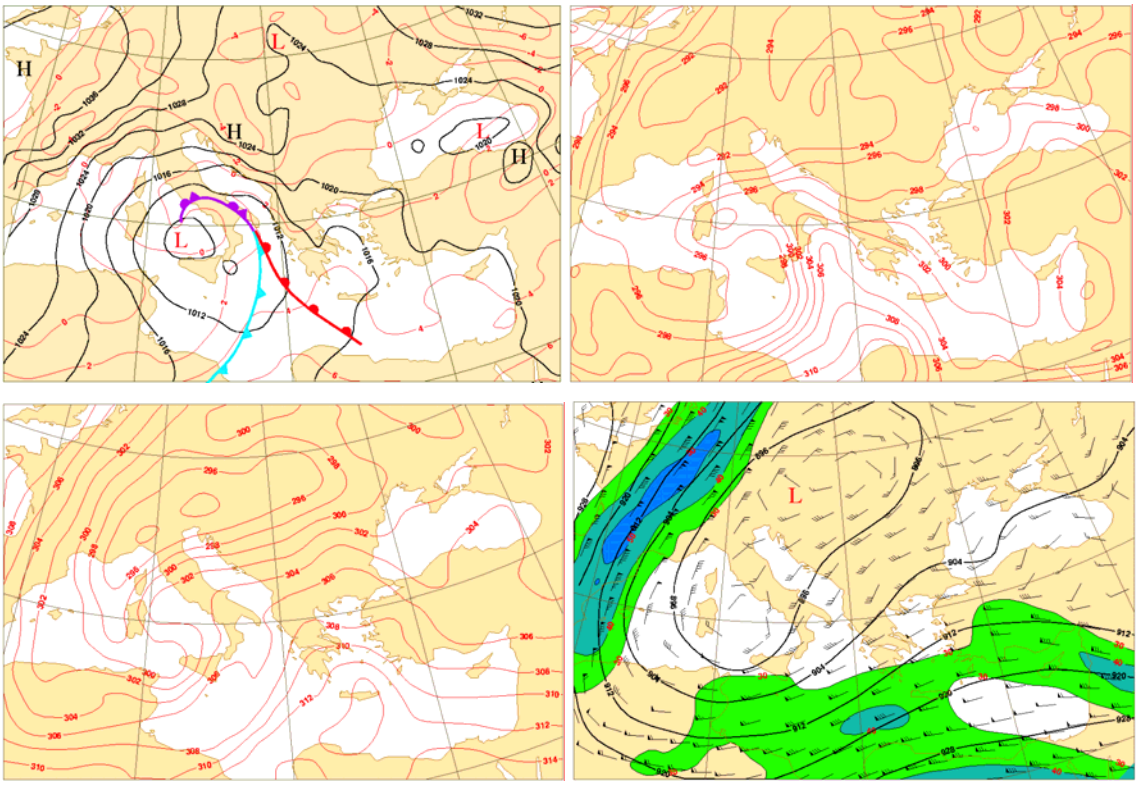

Figure 5.42. Numerical analysis fields at 06 UTC of 24.01.2003. Upper left: MSLP contoured every 4 hPa (black solid lines), 850 hPa temperature field contoured every 2 K (red thin light) and classical surface frontal analysis. Upper right: 700 hPa equivalent potential temperature contoured every 2 K. Lower left: 500 hPa equivalent potential temperature contoured every 2 K. Lower right: 300 hPa isotaches (colored starting from 30 m/s at interval of 10 m/s), geopotential height (solid black lines) contoured every 8 dam and wind vector barbs in knots.

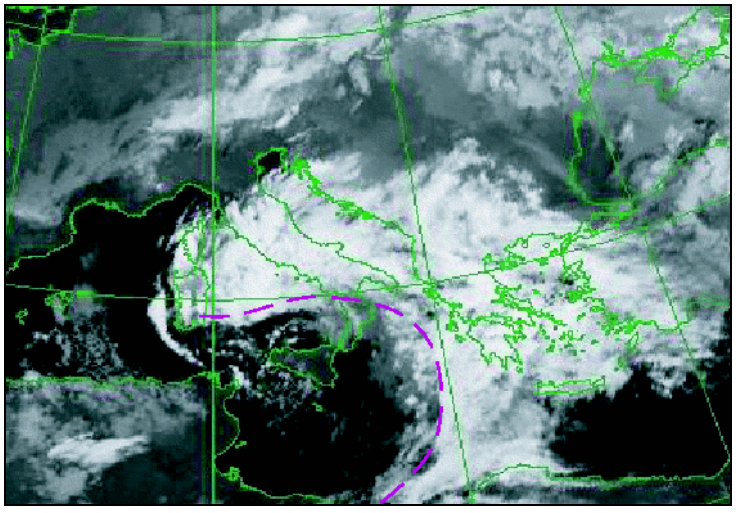

Figure 5.43. Meteosat 7 IR image at 06 UTC of 24.01.2003. The violet dashed line stands for the axis of highest equivalent potential temperature value across the isentropic ridge at 700 hPa of the same instant.

Cross sections reveal to be a good tool in the investigation, which allow deeper insights into the nature of the system, but it is often difficult to extrapolate conceptual models from them, e.g. frontal structures. The satellite image at 12 UTC (fig. 5.44, upper left)

would suggest a well developed occluded front, anyway cross sections made across the supposed occluded front show features difficult to understand in terms of classical notions: in front of the occluded front there is a remarked cold advection maximum, which might be ascribed to stagnation of the front, which indeed begins to move slowly backwards. This feature was taken into account in the cross section along the axis AA' (fig. 5.44, lower left), where the fronts are analyzed in the opposite way as it would be natural to do, i.e. in a non classical way. In the same figure the other cross section (axis CC') does not support the presence of an occluded structure as well as many other which are not shown: the frontal band seem to reach the surface and there is no clear sign of an elevated warm sector. Again classical fronts have been superimposed even if the cyclone in question is not classical: the meaning is to show how the classical concepts do not apply in this specific case.

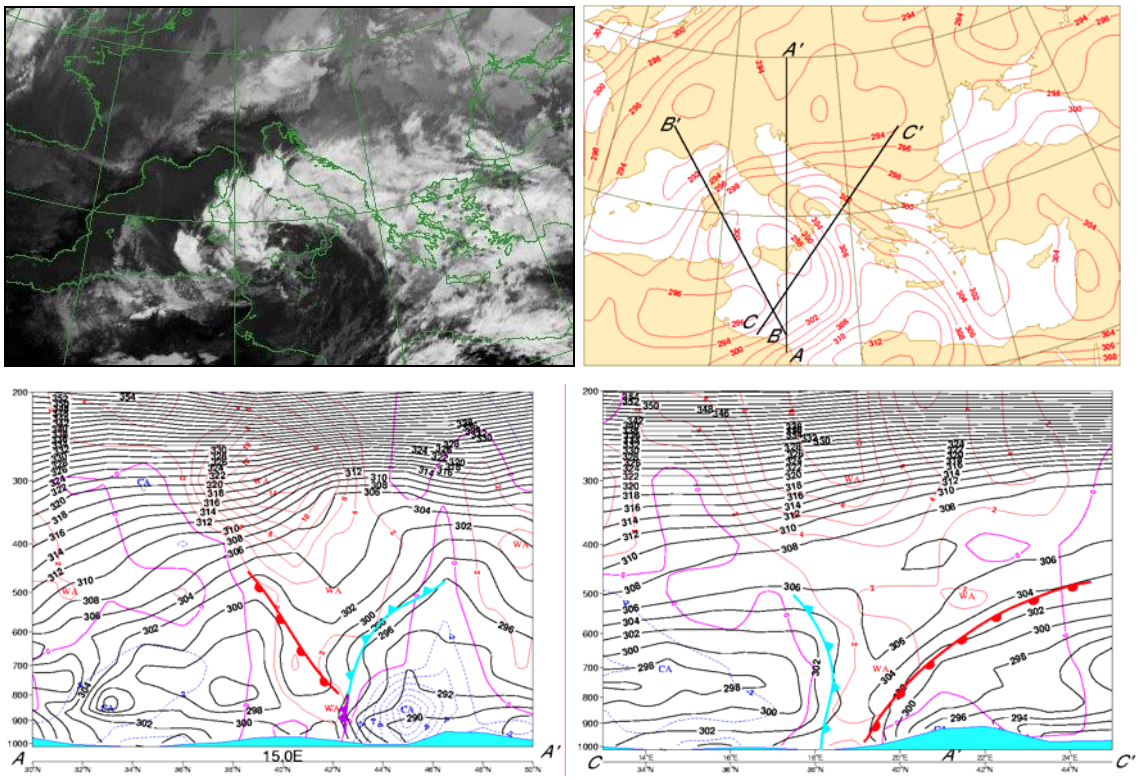

Figure 5.44. Upper: Meteosat IR(10.8μm) image over Mediterranean Sea at 12 UTC of 24.01.2003 (left) and correspondent 700 hPa isentropes contoured every 2 K with cross section axes (right). Lower: vertical cross sections at same time of upper pictures through axis AA' (left) and CC' (right); Solid black lines: isentropes (K); dashed blue lines: cold advection, red solid lines: warm advection and solid violet lines: value 0, contoured every 2 x 10^{-4} K s^{-1}.

The determination of the occlusion type does not seem proper in this case because the post-mature stage of the cyclone deviates from the classical structures. The jet stream

again does not follow any classical pattern, while the 850 hPa temperature advection field (fig. 5.45) shows cold advection in the lowest troposphere on the northeast side of the front, sign of an inversion of the direction of motion as the cold air mass is located just on that side of the front. This same feature was observed from another perspective in the vertical cross section of figure 5.44(lower left).

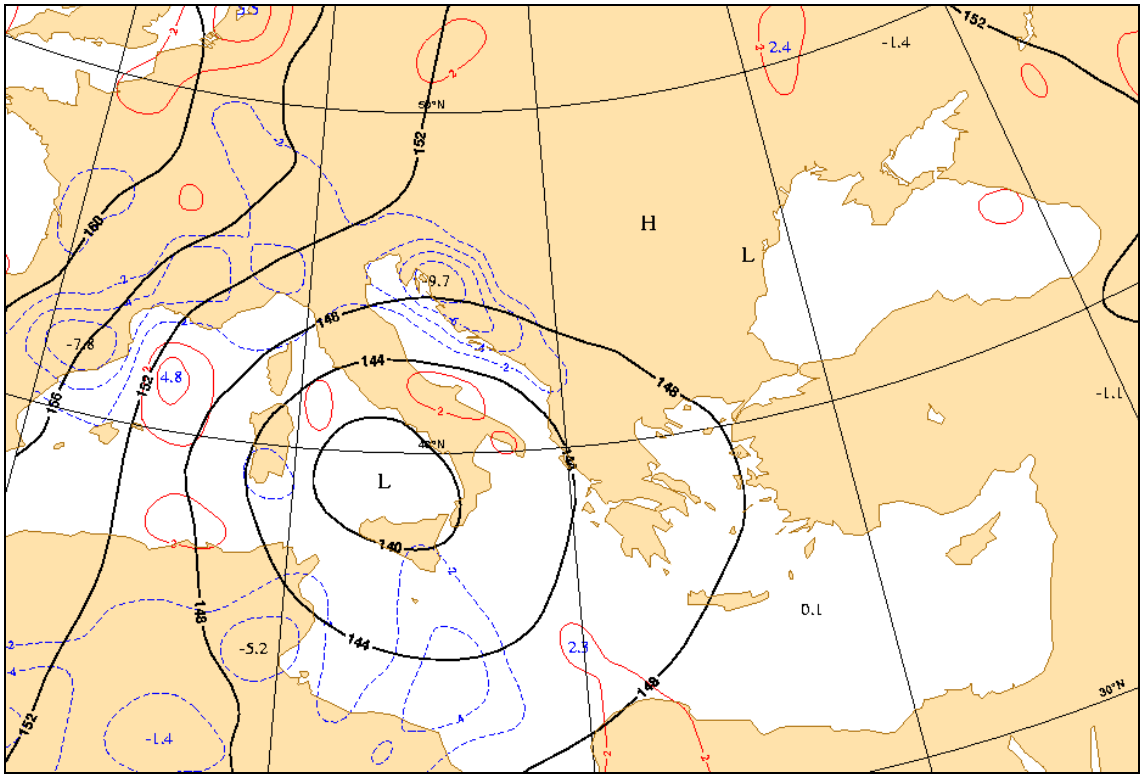

figure 5.45. 850 hPa temperature advection and geopotential field at 06 UTC of 24.01.2003; Solid black lines: geopotential height contoured every 4 dam; dashed blue lines: cold advection, red solid lines: warm advection and solid violet lines: value 0, contoured every 2 x 10^{-4} K s^{-1}

The case in question involves a backwards moving occluded front in its latest stage of life: the system has stopped and inverted its direction of motion, and the low pressure, situated over Tyrrhenian Sea, moves now slowly southeastward while filling up, so that big amounts of rain concentrate over southern parts of Italy and the Balkans.
The development does not undergo major changes later on. The front remains almost in the same place, coiling around the low and slowly breaking up into several convective systems of smaller scale.

This cyclone contains many elements which make it difficult to describe its development and structures in terms of the classical notions. In the investigation of the

cyclone the classical sign of occlusion has been used, mostly to show its inadequateness in fitting the classical structures. The only feature that makes the post-mature stage of this cyclone similar to a classical occlusion is the well developed warm tongue in the equivalent isentropic fields at 700 hPa and 500 hPa fields, even if it is not at 850 hPa so well defined, maybe because of influence of mountains.

5.4 Undetermined type occlusion over Great Britain 29.-30.11.2003

This cyclone occluding over British Isles during 29.11.2003 was classified as conflicting, which means that the cyclone exhibits throughout the development classical features, so that it can be considered as a classical occlusion, but the different parameters suggested in the FMI guidelines yield different interpretations about the occlusion type.

At first this cyclone was considered to yield more cold-type features, but after a deeper investigation using additional data and vertical cross sections the type was stated to be more like warm: the uncertainty is thus very big.

In this case study we will focus on the instant the occlusion takes place and on its structure in the earliest stage of the formation: all the material shown will thus refer to the same day of 29.11.2003.

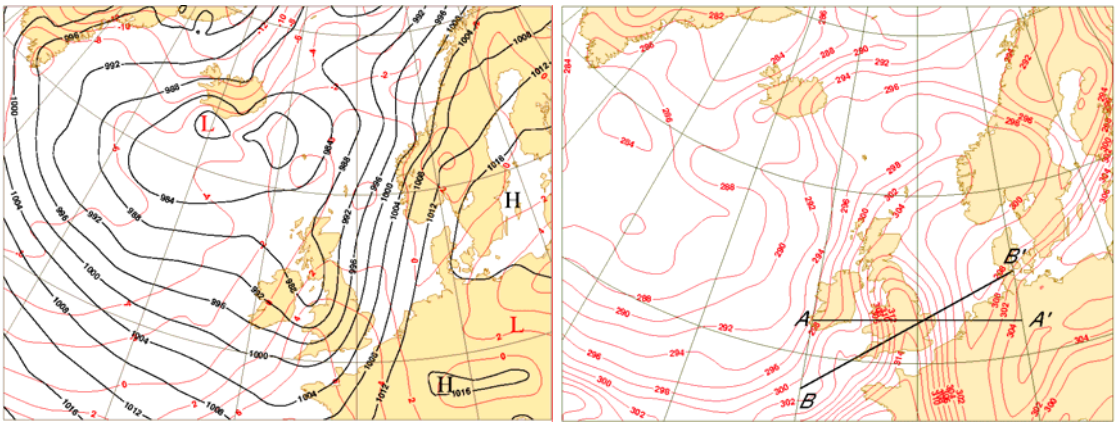

Figure 5.46. Numerical analysis fields at 12 UTC of 29.11.2003 over Western Europe. On the left MSLP (solid black lines) and 850 hPa temperature (thin red lines) contoured every 4 hPa and 2 K, respectively; on the right equivalent potential temperature contoured every 2 K (red thin lines) and position of cross sections.

At 12 UTC a sharp ridge in the equivalent isentropic field at 700 hPa, shown in figure 5.46(right) seem to lead to an occlusion structure, supported also by the satellite images

(fig. 5.49, right), while the temperature field does not necessarily yield the same conclusion (fig. 5.46, left).

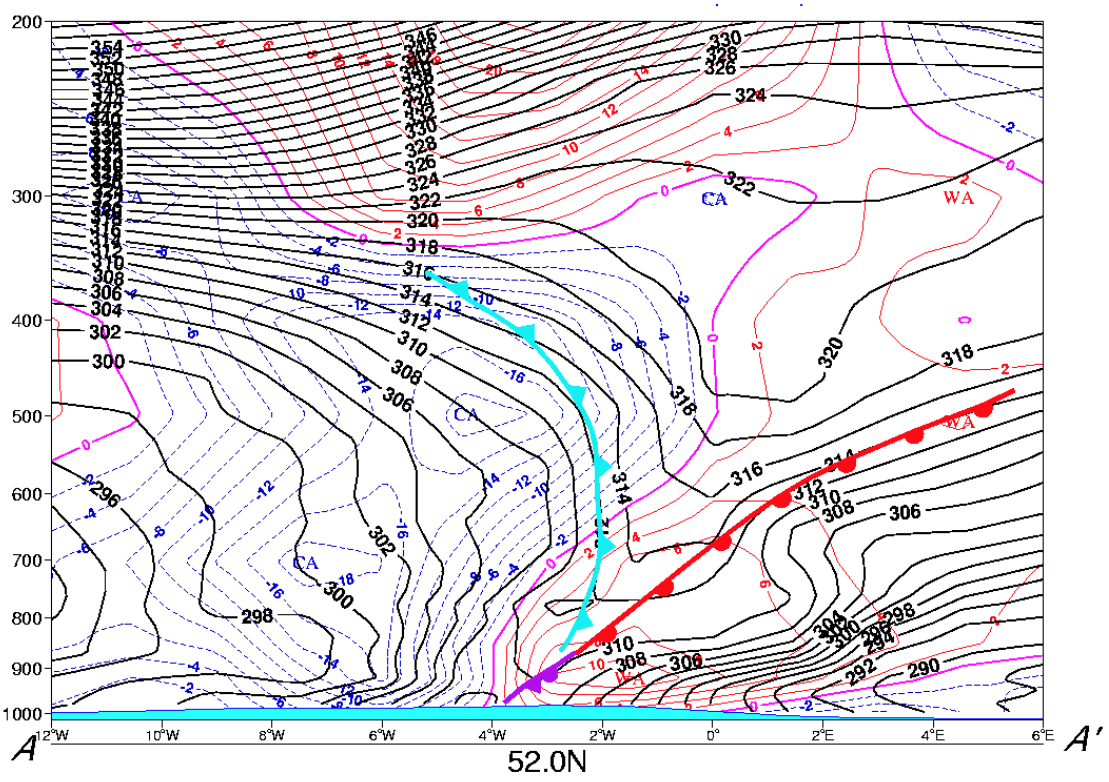

Figure 5.47. Vertical cross section at 12 UTC of 29.11.2003 along the axes AA' of figure 5.44. Solid black lines: isentropes (K); dashed blue lines: cold advection, red solid lines: warm advection and solid violet lines: value 0, contoured every 2 x 10^{-4} K s^{-1}. Subjective frontal analysis is superimposed.

Cross sections provide precious support in getting better insights into the occlusion process. At 12 UTC two vertical cross sections were made perpendicular to the axis of highest values of isentropes at 700 hPa (fig. 5.46, right). Attention must be paid in determining the right position of the fronts: it is not always straightforward because patterns can be often very different from the ideal ones. In the cross sections across axes AA' and BB', shown in figures 5.47 and 5.48, respectively, the subjective frontal analysis is superimposed: they exhibit a classical occluded vertical structure, which can be interpreted as a warm-type according to the FMI guidelines. The occluded front slopes forwards and very intense warm advection is located in front of and across it. On the other hand, the forward slope of the occluded front was evident already from the fields shown in figure 5.46, as the warm tongue at 700 hPa is ahead of the warm tongue at 850 hPa

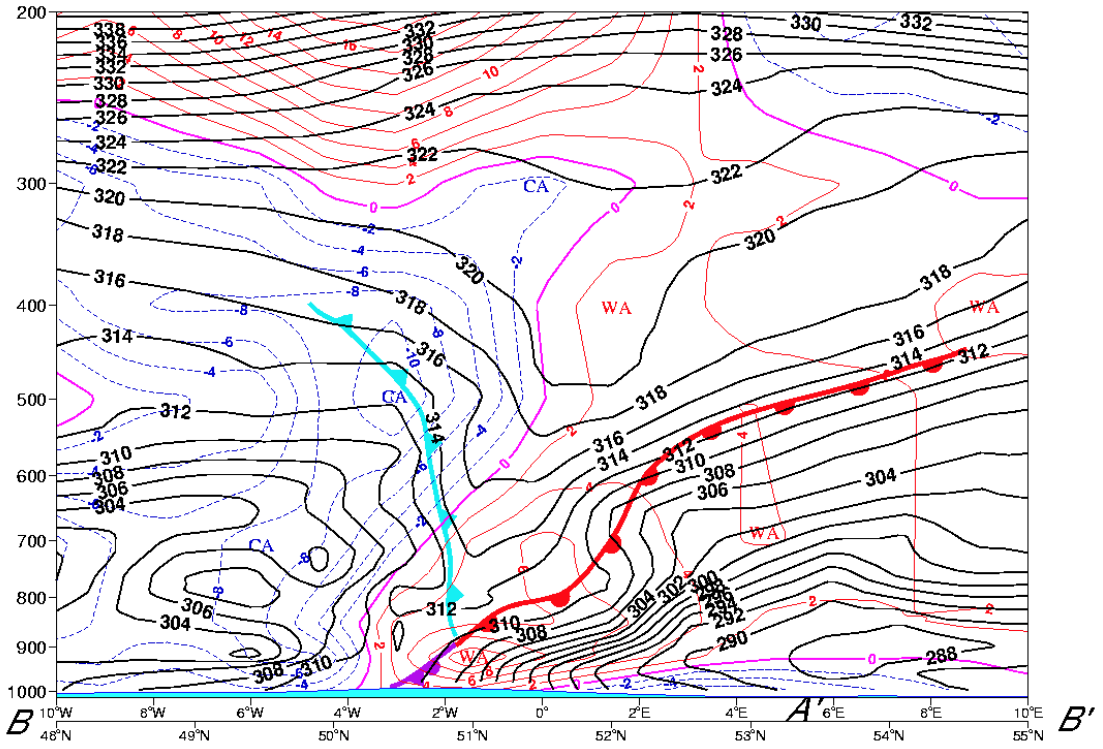

Figure 5.48. Vertical cross section at 12 UTC of 29.11.2003 along the axis BB' shown in figure 5.44. Solid black lines: isentropes (K); dashed blue lines: cold advection, red solid lines: warm advection and solid violet lines: value 0, contoured every 2 x 10^{-4} K s^{-1}. Subjective frontal analysis is superimposed.

The shape of the jet stream at 300 hPa (fig. 5.49, left) yields instead a cold-type classification: the jet streak stretches straight along the rear side of the occluded front. Also the 850 hPa temperature and the geopotential height field patterns (fig. 5.46, left) on the cold sides of the occluded front seemed to lead to a cold-type pattern, i.e. predominant cold advection on the rear side of the occluded front, which is located at 12 UTC over western part of England.

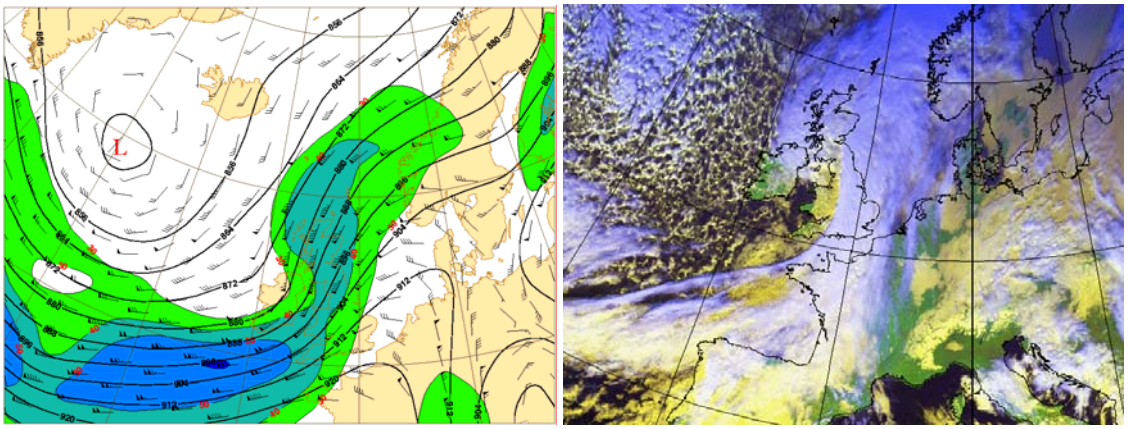

Figure 5.49. 300 hPa isotaches (colored starting from 30 m/s at interval of 10 m/s), geopotential height (solid black lines) contoured every 8 dam and wind vector barbs in knots, and Meteosat 8 RGB composite image (channels 1, 2, 10) at 12 UTC of 29.11.2003.

At 18 UTC the surface temperature distribution on both sides of the occluded front does not reveal any particular difference: arguably the land-sea distribution affects the temperatures so that is hard to say whether it grows or not after the passage of the front. The 850 hPa temperature field now turns out to be more neutral-like than cold-like (fig. 5.50); also the 850 hPa temperature advection field supports this impression because on both sides of the occluded front the strength of the advection is about the same (fig. 5.51).

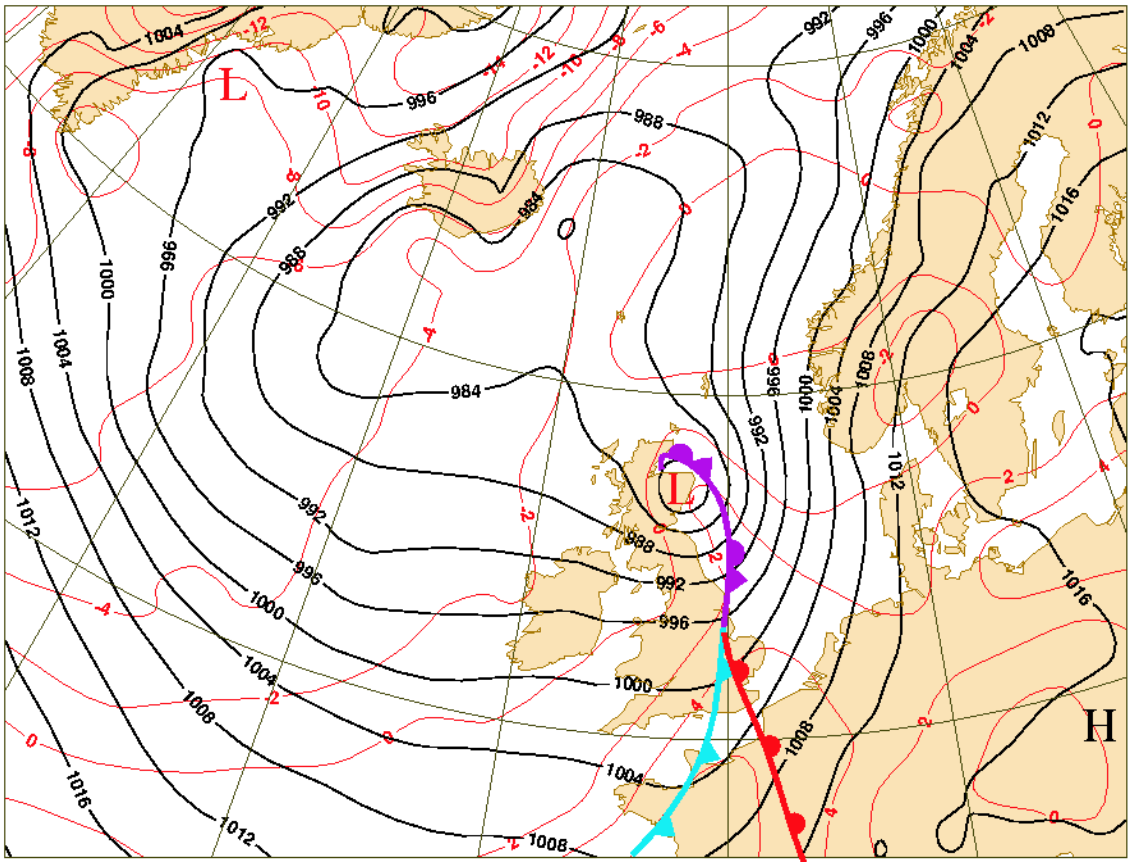

Figure 5.50. Numerical analysis fields at 18 UTC of 29.11.2003: MSLP (solid black lines) and 850 hPa temperature field (red thin lines) contoured every 4 hPa and 2 K, respectively.

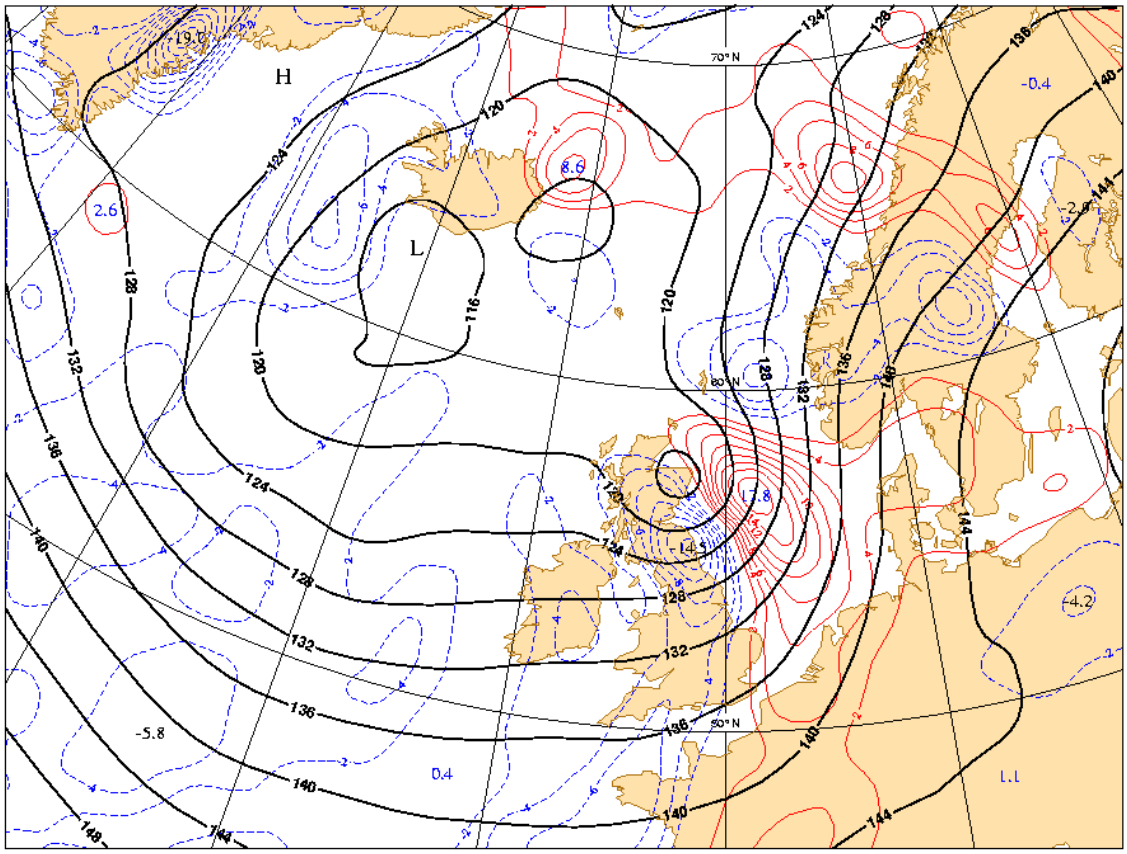

Figure 5.51. 850 hPa geopotential height and temperature advection field at 12 UTC of 29.11.2003. Solid black lines: geopotential height contoured every 4 dam; dashed blue lines: cold advection, red solid lines: warm advection and solid violet lines: value 0, contoured every 2 x 10^{-4} K s^{-1}

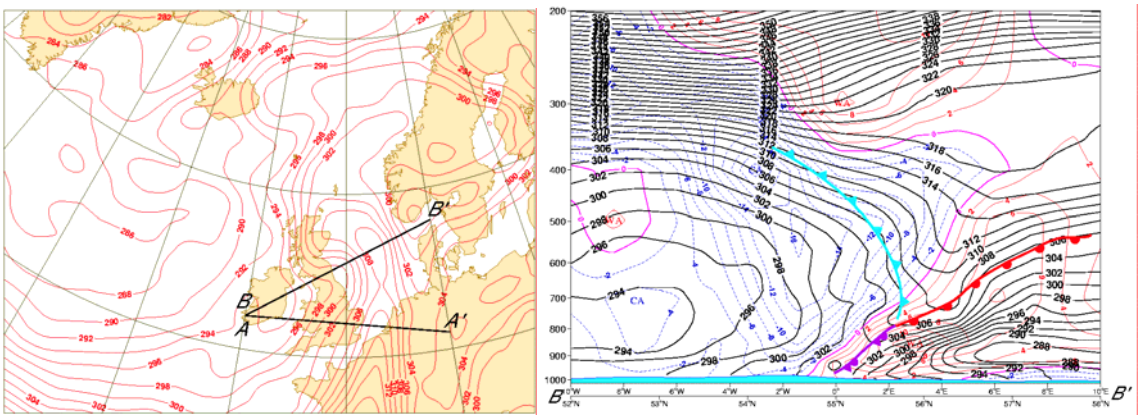

Figure 5.52. Left: 700 hPa Θ_e-field contoured every 2 K and cross vertical section axes at 18 UTC of 29.11.2003. Right: vertical cross section along axis BB'; solid black lines: isentropes contoured every 2 K; dashed blue lines: cold advection, red solid lines: warm advection and solid violet lines: value 0, contoured every 2 x 10^{-4} K s^{-1}. Subjective frontal analysis is superimposed.

Cross sections of Θ_e-field taken at 18 UTC perpendicular to the occluded front keep the warm-type structure as at 12 UTC: the occluded front tilts forward and it is a continuation of the warm front to the surface (fig. 5.52). In figure 5.53 the slope of the occluded front is examined in the light of the static stability rule of Stoelinga et al.

(2002): there is no great difference between the static stability on either side of the occluded front, even if a slightly higher stability can be qualitatively estimated on its fore side, thus supporting the forward inclination.

In figure 5.54 the potential temperature is replaced by the temperature; the occlusion structure now fits quite well the warm classical model as described in the FMI guidelines, which means that immediately behind the occluded front, in the lower part of the atmosphere, there is much warmer air than on its fore side.

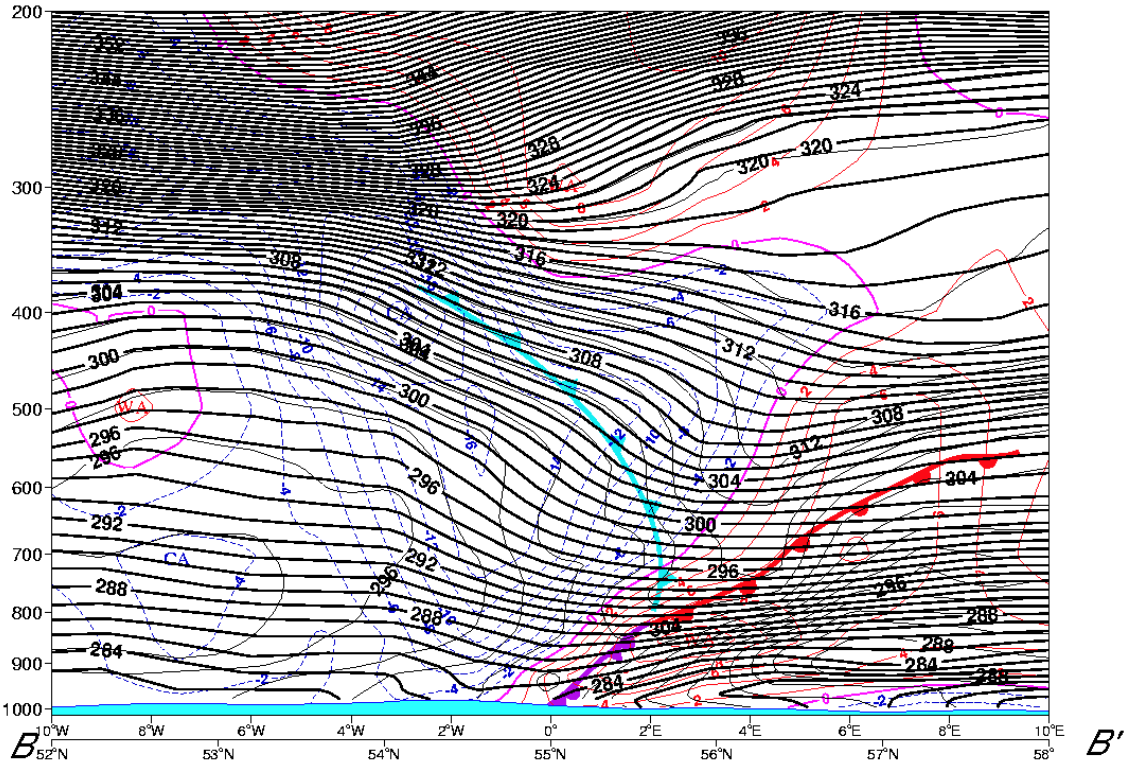

Figure 5.53. Vertical cross section across along axis BB' of fig. 5.49(left) at 18 UTC of 29.11.2003. Solid thick black lines: potential temperature (K); thin black lines: equivalent potential temperature (K); dashed blue lines: cold advection, red solid lines: warm advection and solid violet lines: value 0, contoured every 2 x 10^{-4} K s^{-1}. Frontal subjective analysis superimposed.

According to the structures exhibited in vertical cross sections the type of the occluded front can be considered without any doubts as warm. In the constant level pressure framework the determination of the type is not however so straightforward because the structures of different fields lead to different types. These argumentations thus yield an occlusion whose type is undetermined in the light of the description of the occlusion structure contained in the FMI guidelines

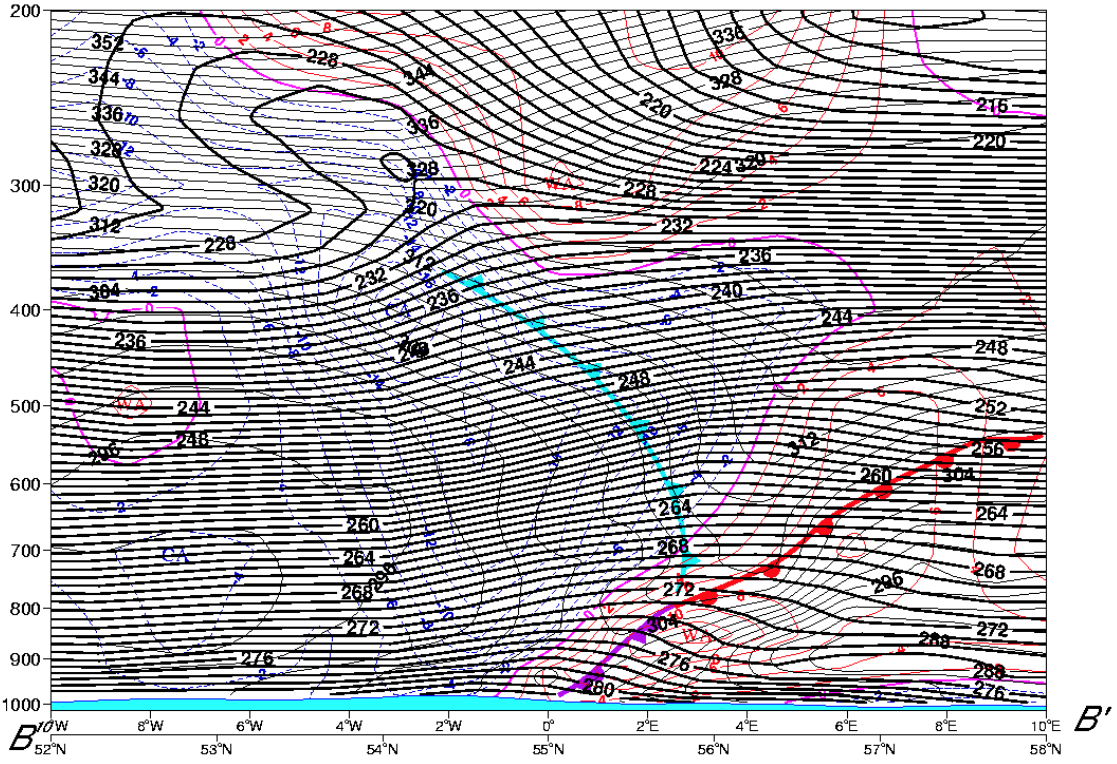

Figure 5.54. Vertical cross section across along axis BB' of fig. 5.49(left) at 18 UTC of 29.11.2003. Temperature by solid black lines (K) , otherwise legend as in figure 5.51.

.

6. CONCLUSIONS

6.1. Discussion about the features of occlusions

6.1.1. Considerations about occlusion types

In this work a very a one-year statistics about the seasonal and geographical distribution of the occlusion types has been obtained. The results offer some insights into the validity of the classical framework over areas where the basic assumptions of the classical cyclone model might not be fit.

If the easternmost part of the Atlantic Ocean and Western Europe are considered, during the cold season the air mass on the rear side of the occluded system is generally warmer than the one on the fore side, at least in the lower troposphere, because the former comes from the relatively warm ocean and the latter from the cold continent. According to the qualitative argumentation based on different air masses, which traditionally supports the division of occlusion into types within the classical framework, this would

yield the formation of warm-type occlusions. The opposite should be true during the continental warm season (summer), yielding cold-type occlusions. In this specific case that distribution of the collected data seems to support the qualitative argumentations provided by the classical model.

The distribution of types over central and western part of Northern Atlantic is not so straightforward. The simple model of two air masses is in contradiction with the observed data, because during the winter the ocean is very warm, so that the air mass coming from North America should be colder, at least in the lowest layers, and lead to the formation of cold-type occlusions; in the summer the opposite argumentation is valid. The observations show instead that warm-type cases prevail in winter and cold-type ones in summer.

The classification of occlusions on the basis of their thermal structure turns out to be too simple and seems to work only in certain regions where the basic assumptions take place.

One fundamental doubt which might arise from the earlier considerations is to what extent the temperature of the ocean surface eventually affects the air mass reasoning. One reason which might explain the disagreement between air mass reasoning and observations is that the basic assumption of the classic model, namely the existence of two distinct air masses over a relatively homogeneous surface, is not generally valid for cyclones occluding over northwestern Atlantic. In this specific case there could be a hypothetic interaction between a cold airmass from the American continent, a warm one from the ocean and an artic air mass from Northern Canada.

This same aspect is mentioned by Kurz (1998, pg. 96) who refers to the specific synoptic setup off the American eastern seaboard, called “three mass corner”, where an artic air mass eventually interacts with a quasi-stationary frontal zone between two pre-existing air masses. This interaction produces a cyclogenesis which is not a genuine classical development between two air masses, even if the thermal structure reminds of it. In these cases the occlusion type can be very hard to define on the basis of the thermal structure as the basic assumptions of the classical model do not apply anymore.

Any deeper investigation of this topic is anyway left to further studies.

6.1.2. Considerations about the intrinsic nature of occlusion types

The structures of the occluded cyclones encountered during the investigation cover such a variety of different patterns that the traditional division into three classes, according to the thermal structure as in FMI interpretation rules, barely applies in the generality.
Worth of extreme consideration is the presence of a consistent amount (23%) of classical occlusions whose type cannot be clearly assigned, because some structural features strongly lead to a certain type while others to a different type. On the other hand it has already been mentioned that also the determination of the type of imperfect occlusions bears a certain amount of uncertainty, even if it cannot be considered as conflicting.
There are therefore strong signals that suggest the need of a comprehensive revision and adjustment of the currently accepted framework which tries to classify the occluded systems on the basis of thermal structures.
The deeper investigation pursued in the case studies have shown that one reason for the poor validity of the present classification is the fact that it was based on studying constant pressure levels. Vertical cross sections have turned out to be not only a useful, but rather a necessary tool in defining the type of occlusions.

Some studies (Stoelinga & al., 2002) have arrived to the conclusion that the classical frame of occlusion is lacking firm dynamical and theoretical footing. The results obtained in this work are aligned with these same considerations: the actual framework of the occlusion is mainly based on empirical and qualitative methodologies and efforts are needed in order to create a firm theoretical background.

The statistical investigation and the case studies treated in this work have shown that the ideal thermal patterns related to the occlusion types as explained in the FMI guidelines are rather idealistic when compared to the reality. In the work it was stated that these patterns apply only to the third part of those occlusions considered classical, which highlights the weakness of the classical model in describing the observed patterns.
In several cases the configuration of the jet stream in the upper troposphere has turned out to differ from the pattern claimed in the FMI guidelines: this highlights the fact that

no dynamical argumentations are taken into account and therefore efforts should be made in order to understand the interaction among the different meteorological factors.

The case studies have also clearly shown that the type of the occlusion defined on the basis of the thermal structure does not always match with the distribution of the temperature field on the surface. In some cases the surface temperature changes anyway according to the classical model: drops after the passage of a cold occluded front and rises after a passage of a warm occluded front. In some other cases very weak correspondence is observed. Further inspections in order to understand the relation between these two features should be done. In this connection the studies of Stoelinga et al. (2002) have to be mentioned: they have shown how the typical sloping structure of different types of occluded fronts could be related to the static stability of the occluding air masses rather than to their temperatures. In the case studies of this work the static stability rule of Stoelinga et al. (2002) has yielded types of the occlusions in accordance with the type defined by means of traditional tools, when the latter are applicable.

6.1.3. Qualitative assessment of the classical occlusion model

In the statistical investigation of occlusions it was shown that non-classical occlusion tend to develop over southern and Eastern Europe, with a local higher density also over Southern Greenland, while perfect occlusions develop over northern Atlantic Ocean (fig. 4.14). This clear distribution can help highlight an intrinsic characteristic of the classical model of occlusion and help to understand why it does not seem to work over the above mentioned areas.

The classical model theory is namely based on the interaction of two well distinct air masses over a quite homogeneous (North Atlantic) sea surface, meaning the absence of synoptic scale mountain chains (Bjerknes and Solberg, 1922).

The northern Atlantic is a large maritime surface, quite homogeneous also regarding to sea surface temperatures, where distinct cold and warm airmasses meet each other without mountainous obstacles, after eventually experiencing some modifications in their lowest layers due to the interaction with the ocean waters. The Mediterranean basin is instead smaller, if compared to the north Atlantic. It has same dimensions as the cyclones and is almost completely surrounded by high mountain chains; a similar

argumentation is valid for the Black Sea, which has also mountains on the southern shore.

Several studies have shown that cyclogenesis over these areas occurs in a different way than depicted in the classical model It is called secondary cyclogenesis, and it involves the interaction with mountain chains.

On the other hand the absence of mountainous obstacles in the southern part of Mediterranean allows very warm air to flow into the basin, so that the classical scheme of two distinct air masses does not always apply over these areas, unlike the case over northern Atlantic. In some specific synoptic settings there could be the interaction of more than two airmasses, e.g. a cold and dry polar airmass from northern Europe, a warm and moist mid-latitude airmass from the ocean and a warm and dry tropical airmass from the northern part of the African continent.

A deeper analysis of the mechanism and structure of secondary cyclogenesis is beyond the scope of this work. The meaning is to accentuate that the critical areas in question do represent a very unique place for different air masses to meet, a kind of different weather basin than supposed in the classic theory. Also the presence of a local maximum of non-classical occlusions over Southern Greenland is likely due to the abrupt rising of the surface, which does deeply affect the thermal structure of occluding cyclones.

Similar conclusions have been stated in studies pursued in North America, which have stated the central part of North America as a different weather basin to that supposed in the Norwegian model, so that a comprehensive revision together with the introduction of a new conceptual model has been necessary and revealed to be a proper and convenient implementation of the existing conceptual models (Hobbs at al., 1996).

In this work we limit to stating and demonstrating the weakness of the classical model when implanted in different context than the one it was created in.

Efforts in creating new conceptual models in order to better diagnose and forecast the development of cyclones in areas or situations where the classical model exhibits difficulties are suggested for further studies.

Several cases of so called perfect occlusions have been anyway collected during the investigation and they offer handbook examples of classical developments of occlusions. The perfect occlusions discussed in detail in the case studies chapter show very clearly typical features of the classical model: depending on the type of the occlusion either of the frontal bands is forced upwards and the warm sector at the same time is detached from the surface while cold air spreads out at its place.
In the same context it has been shown how classical perfect warm occlusion can be inspected from a different point of view as a trowal, which is in fact a mere three-dimensional revision of the classical occlusion. In fact, personal communications with Canadian forecasters, have confirmed that use of the trowal in operations has nearly the same essential problems that are typical for occlusion, like for example excessive usege: in unclear synoptic situations, everything which cannot be assigned a clear interpretation becomes a trowal.

6.2. Some possibilities to enlarge the use of occlusions in operational environment

This work has demonstrated the intrinsic weaknesses of the conceptual model of occlusion and represents the proof that an urgent revision is needed in order to successfully use it in analyzing weather situations.
In the actual operational environment characterized by the strong presence of increasingly precise numerical forecasts and observations (both traditional and remote sensing) which allow the inspection of the weather systems in great detail, the conceptual model of occlusion has turned out to be inadequate as a diagnostic and prognostic tool.
A modernized conceptual model of occlusion should account for the large variety of post-mature stage of extratropical cyclones and should contain a much detailed structure of meteorological features both from a synoptic and a mesoscale point of view, not only in three-dimensional framework but also regarding their behavior and modifications with the time, thus gaining insight into the evolution of the related weather.
In this the occlusion could gain back its role as a diagnostic and forecasting tool.

The classical conceptual model of occlusion has been defined with traditional parameters. Efforts should be made in studying occlusions with new parameters and

tools, e.g. potential temperature, potential vorticity, Q-vectors and vertical cross sections, which are still not popular in the operational environment.

The case studies treated in this work have shown how useful the equivalent potential temperature field at middle levels can be in identifying well developed or dissipating occlusions or how important is the inspection of occluding cyclone by means of vertical cross sections: still in the operational routine these simple and affordable tools are disregarded.
Anyway, the successful use of the conceptual model of occlusion in operational routines requires that it undergoes a deep, modern and constructive revision.

THANKS

The completion of any significant work in one's life is cause for happiness and satisfaction. For more than three years this Master's Thesis has occupied me: I have had to balance the schedule of this work between a very animated family life and a full time job.

I would like to thank in particular my wife Teija and my children Ricardo, Nicholas and Nathalie, for supporting me with extreme patient in accomplishing this important task of my academic education as well as of my professional life.

Special thanks also to my supervisor Aulikki Lehkonen for cheering me up in those moments when the trust was abandoning me and supporting me generously with her very qualified expertise in synoptic meteorology.

Thanks also to my bosses Heikki Juntti and Kari Österberg for providing me the possibility of making this thesis partly during the working time.

Thanks to Vesa Nietosvaara for his technical assistance in retrieving and visualizing the numerical fields.

And thanks also to my parents for patiently waiting and trusting in their child's graduation.

Alessandro Chiariello

BIBLIOGRAPHY

Bjerknes, J., and H. Solberg, 1922: Life cycle of cyclones and the polar front theory of atmospheric circulation. *Geofys. Publ.,* **3**(1), 1-18

Doswell C., 1999: Some concerns about the use of conceptual models. *Personal notes available from the author's web site*: *http://www.cimms.ou.edu/~doswell/conceptual/conceptual.html*

Eliassen A., 1975: Jacob Aall Bonnevie Bjerknes, November 2, 1897—July 7, 1975. National Academy of Science, Biographical Memoirs. http://newton.nap.edu/html/biomems/jbjerknes.html

Friedman, Robert M., 1989: Appropriating the weather. Vilhelm Bjerknes and the construction of a modern meteorology. Cornwell University Press

Hartonen S., 1994: Okluusion synoptinen analyysi. Master's thesis, Helsinki University, Finland

Hobbs, P. V.; Locatelli, J. D.; Martin, J. E., 1996: A new conceptual model for cyclones generated in the lee of the Rocky Mountains. Bulletin of the American Meteorological Society, Boston, MA. **77**, 1169-1178.

Hoskins, B. J., I. Draghici and H. C. Davies, 1978: A new look at the ω-equation. Quart. J. Roy. Meteor. Soc., **106**, 707-719.

Hoskins, B. J., and N. V. West, 1979: Baroclinic waves and frontogenesis. Part II: Uniform potential vorticity jet flows—Cold and warm fronts. *J. Atmos. Sci.,* **36,** 1663–1680.

Hoskins, B. J., et al., 1985: On the use and significance of isentropic potential vorticity maps. Q. J. R. Meteorol. Soc.*,* **111,** 877-946.

Keyser, D., B. D. Schmidt, and D. G. Duffy, 1992: Quasi-geostrophic vertical motions diagnosed from along- and cross-isentrope components of the Q vector. *Mon. Wea. Rev.,* **120,** 731-741.

Kuo, Y. –H., et al.,1991: The interaction between baroclinic and diabatic processes in a numerical simulation of a rapidly intensifying extratropical marine cyclone. Mon. Wea. Rev., **119**, 368.384.

Kuo, Y. –H., et al., 1992: Thermal structure and airflow in a model simulation of an occluded marine cyclone. Mon. Wea. Rev., **120**, 2280-2297.

Kurz Manfred, 1998: Synoptic Meteorology. Training guidelines of the German Meteorological Service nr. 8, Offenbach am Main, Deutscher Wetterdienst.

Lehkonen A., et al., 2002: Synoptiset tulkintaohjeet. *Guidelines for frontal analysis in Finnish language for internal use in FMI, available from the author of this work or from FMI internal server http://edu.fmi.fi/courses.*

Locatelli, J. D., et al., 2002: Norwegian-type and cold front aloft-type cyclones east of Rocky Mountains. Weather and Forecasting, **17**, 66-82.

Martin, J. E., 2006: Mid-latitude atmospheric dynamics: a first course. John Wiley & Sons, Ltd.

Martin, J. E., 1998: The structure and evolution of a continental winter cyclone. Part I: Frontal structure and the classical occlusion process. Mon. Wea. Rev., **126,** 303–328.

Martin, J. E., 1999: Quasigeostrophic Forcing of Ascent in the Occluded Sector of Cyclones and the Trowal Airstream. Mon. Wea. Rev., **127,** 70-88.

Martin, J. E., et al., 2001: Quasigeostrophic forcing of ascent in the occluded sector of cyclones and the trowal airstream. Mon. Wea. Rev., **129**, 748-765.

Neiman, P. J., and M. A. Shapiro, 1993: The life cycle of an extratropical marine cyclone. Part I: frontal-cyclone evolution and thermodynamic air-sea interaction. Mon. Wea. Rev., **121**, 2153-2176.

Palmén, E., 1951: The aerology of extratropical disturbances. *Compendium of Meteorology.* Amer. Meteor. Soc., 599–620.

Posselt, D. J., and J. E. Martin, 2004: The effect of latent heat release on the evolution of a warm occluded thermal structure. Mon. Wea. Rev., **132**, 578-599.

Postma, K. R., 1948: The formation and the development of occluding cyclones: A study of surface-weather maps. Ph.D. Thesis, Utrecht, 57 pp.

Reed, R. J., Y.-H. Kuo, and S. Low-Nam, 1994: An adiabatic simulation of the ERICA IOP 4 storm: An example of quasi-ideal frontal cyclone development. Mon. Wea. Rev., **122**, 2688–2708.

Shapiro, M. A., and D. Keyser, 1990: Fronts, jet streams, and the tropopause. *Extratropical Cyclones: The Erik Palmén Memorial Volume,* C. W. Newton and E. O. Holopainen, Eds., Amer. Meteor. Soc., 167–191.

Schultz, D. M., Mass C. F., 1993: The occlusion process in a midlatitude cyclone over land. Mon. Wea. Rev, **121**, 918-940.

Stoelinga, M. T., et al., 2002: Warm occlusion, cold occlusion and forward-tilting cold fronts. Bull. Am. Meteorol. Soc, **83**, 709-721.

Wallace, J. M., and P. V. Hobbs, 1977: *Atmospheric Sciences: An Introductory Survey.* Academic Press, 467 pp.